# THE ESSENTIAL PHYSICS OF MEDICAL IMAGING



JERROLD T. BUSHBERG
J. ANTHONY SEIBERT
EDWIN M. LEIDHOLDT, JR.
JOHN M. BOONE

Dentsply Sirona Inc. – Exhibit 1021

# THE ESSENTIAL PHYSICS OF MEDICAL IMAGING

**JERROLD T. BUSHBERG, Ph.D.**
Associate Clinical Professor of Radiology
Technical Director of Nuclear Medicine
Director of Health Physics Programs
University of California, Davis
Sacramento, California

**J. ANTHONY SEIBERT, Ph.D.**
Associate Professor of Radiology
University of California, Davis
Sacramento, California

**EDWIN M. LEIDHOLDT, Jr., Ph.D.**
Associate Clinical Professor of Radiology
University of California, Davis
Radiation Safety Program Manager
Western Region, U.S. Department of Veterans Affairs
San Francisco, California

**JOHN M. BOONE, Ph.D.**
Associate Professor of Radiology
University of California, Davis
Sacramento, California




**Williams & Wilkins**
BALTIMORE • PHILADELPHIA • HONG KONG
LONDON • MUNICH • SYDNEY • TOKYO
A WAVERLY COMPANY



*Editor:* William M. Passano III
*Project Manager:* Victoria Rybicki Vaughn
*Copy Editor:* Mary Woodman
*Designer:* Dan Pfisterer
*Illustration Planner:* Lorraine Wrzosek

Copyright © 1994
Williams & Wilkins
428 East Preston Street
Baltimore, Maryland 21202 USA



All rights reserved. This book is protected by copyright. No part of this book may be reproduced in any form or by any means, including photocopying, or utilized by any information storage and retrieval system without written permission from the copyright owner.

Accurate indications, adverse reactions, and dosage schedules for drugs are provided in this book, but it is possible that they may change. The reader is urged to review the package information data of the manufacturers of the medications mentioned.

*Printed in the United States of America*

**Library of Congress Cataloging in Publication Data**

The Essential physics of medical imaging / Jerrold T. Bushberg . . . [et al.].
p. cm.
Includes bibliographical references and index.
ISBN 0-683-01140-5
1. Diagnostic imaging. 2. Medical physics. I. Bushberg, Jerrold T.
[DNLM: 1. Diagnostic Imaging. 2. Physics. WN 200 E78 1994]
RC78.7.D53E87 1994
616.07'54—dc20
DNLM/DLC
for Library of Congress 93-34268
CIP

94 95 96 97
2 3 4 5 6 7 8 9 10

# PROJECTION RADIOGRAPHY




Projection radiography is the imaging modality that uses a conventional x-ray tube to produce a two-dimensional image of the patient's anatomy. Radiographic images are used for a huge variety of diagnostic examinations, ranging from bone imaging to chest radiography to sinus examinations. The projection radiograph was the first imaging modality to exploit the potential of x-rays, and Roentgen himself made one of the first medical radiographic images—of his wife's hand.

## FILM-SCREEN RADIOGRAPHY

Film radiography was the first imaging modality used in radiology, and this venerable image medium remains the most widely used diagnostic tool in medicine today. Whereas screen-film radiography is sometimes overshadowed by more recent and technologically sophisticated modalities, such as CT or MRI, the radiograph is remarkably cost effective and is a valuable asset in diagnostic medicine. Recent advancements in screen and film emulsion technology have resulted in a marked improvement in radiographic image quality. In this chapter, the bread and butter modality of the radiology department is examined in detail.

Radiography is a transmission imaging technique: The radiation is emitted from inside the x-ray tube, is transmitted through the patient's body, and then reaches the detector. A fairly uniform distribution of x-rays is emitted by the x-ray tube and is incident upon the patient; the x-rays are attenuated by absorption and scattering inside the patient. These processes alter the incident x-ray distribution, producing the transmitted x-ray pattern that is imaged by the detector placed on the distal side of the patient. Radiologists quickly learn to view radiographs as a collection of patterns and signs; however, it is important to understand and perhaps remind oneself periodically that the radiographic image is the result of the physical interactions of x-rays in tissue. For a radiographic abnormality to be visible on the film, the associated trauma or pathology necessarily has to alter the physical distribution or composition of tissues in the patient. A radiograph is a *projection image,* meaning that the x-ray attenuation information concerning the three-dimensional anatomy of the pa-

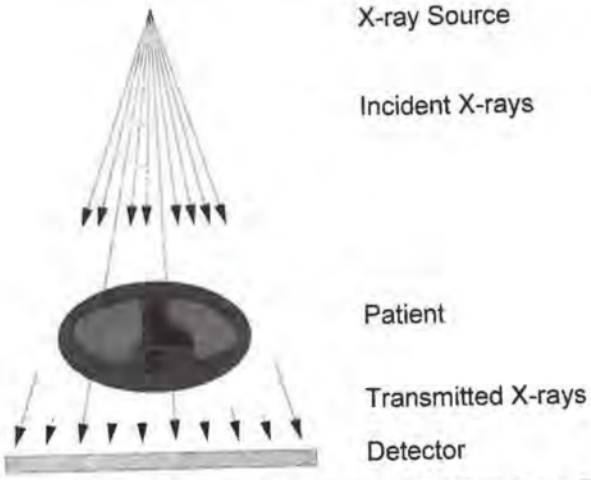



**Figure 6.1.** Radiography is a transmission projection imaging technique. The attenuation information along the straight-line paths of the x-ray photons is summed up (integrated), allowing the three-dimensional anatomy of the patient to be compressed onto a two-dimensional image. The thickness and composition of tissue that the x-ray photons transit influence the optical density of the film at each point on the film.

tient is projected onto the two dimensions of the radiograph. The optical density (OD) at a point on the film is related to the thickness and composition of the patient along a line between the focal spot to that point on the film (Fig. 6.1). Thicker structures attenuate more incident x-ray photons, resulting in fewer x-rays striking the detector and thus a lower optical density. Low values of the optical density appear white, and higher OD values are darker. The mediastinum is a relatively thick structure in the chest, and it projects as a fairly light region on a chest radiograph. The air-filled lungs, however, normally present a low-density projection of tissue, and therefore correspond to darker regions on the radiograph. Projection radiography results in a reduction of anatomical information. All the tissues that lie between a particular point on the film and the x-ray focal spot contribute to the overall film density at that point. The x-ray attenuation properties are therefore summed up (integrated) along the path of the x-ray beam. With a single film, it is difficult or impossible to determine the depth of a particular abnormal structure (without other clues). An additional radiograph, taken at a different angle through the patient (e.g., a lateral chest radiograph), is necessary to locate unambiguously a particular lesion in all three dimensions.

The radiograph is a negative image: Areas on the image that receive more exposure appear darker after the film is chemically processed. Conversely, light areas on the film correspond to regions where fewer x-ray photons struck the imaging receptor. In modern screen-film radiography, the x-rays that strike the detector act indirectly toward darkening the film. For general radiography, the film has emulsion on both the front and the back and is tightly sandwiched by two x-ray intensifying screens. The screen-film-screen sandwich (Fig. 6.2) is housed by the cas-

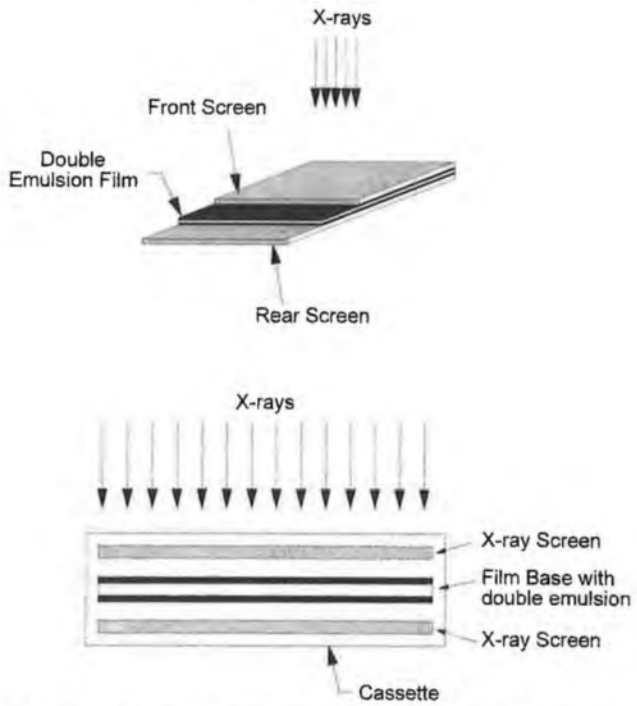



**Figure 6.2.** A dual-screen detector system uses a film base with emulsion coated on both sides. The film is sandwiched by two intensifying screens. About 50% of the x-ray photons incident on the screen-film system are absorbed primarily (~95%) by the screens. The absorption information is conveyed to the film emulsion by visible light, which is emitted in the screens as a result of x-ray interaction. The film base is usually mylar and provides a durable surface onto which the predominantly AgBr emulsion is coated. The total emulsion thickness of the AgBr is about 0.75 to 0.90 mg/cm$^2$. The adhesive layer helps bind the emulsion to the film base. The supercoating is a layer about 1- to 2-$\mu$m in thickness and helps prevent damage to the emulsion before development.

sette, which provides a light-free environment in which to transport and expose the film. The vast majority of x-rays that are absorbed by the detector sandwich are absorbed in the x-ray screen, not in the film emulsion directly. When an x-ray photon is absorbed in the screen, its energy causes excitation and ionization in the screen, which in turn cause the emission of visible light (usually green or blue) that is largely responsible for exposing the film emulsion.

The sole purpose of the x-ray screen is to increase the sensitivity of the detector system. Because the detector's sensitivity is increased, less radiation is needed to produce a readable film. Consequently, the radiation exposure to the patient is reduced. Screens also reduce the power requirements of x-ray generators and tubes. X-ray screens typically increase the sensitivity of the detector system relative to film-only detectors by about 50 times, and hence they reduce patient exposure 50-fold. This is clearly a desirable effect. One unfortunate side effect of using screens

is that the noise visible in the image (the quantum mottle) increases because fewer photons are used in the formation of the image. Another negative consequence of the intensifying screen is a loss of resolution. The light generated in the screen by x-ray interaction diffuses toward the film emulsion over a finite thickness of screen material. As the light diffuses, it spreads out. The initial x-ray signal becomes blurred, because of the spread of the resulting light emission in the screen, which results in a loss of spatial resolution in the image. Screens epitomize the classic compromise between resolution and sensitivity, inherent to virtually all imaging systems. With intensifying screens, sensitivity is gained but resolution is compromised. The need for a screen to act as an intermediary in the image formation process can be thought of in more graphic terms: Consider that in radiography, the x-ray generator is designed to generate x-ray photons with enough energy to penetrate 30–40 cm of tissue. When the photons penetrate the patient, a film emulsion that is no more than 10-$\mu$m thick is expected to absorb most of these x-ray photons. Because a film emulsion must be composed of silver-halide (mostly AgBr, with some AgI), there is little flexibility to provide for better attenuation properties. By introducing an x-ray screen or two to the detector system, and thereby exposing the film emulsion *indirectly,* there is much greater flexibility to design detector systems with excellent x-ray absorption properties.

### The Cassette

Screen-film systems are housed inside a cassette. The cassette itself is primarily responsible for "keeping the dark in." The screens are permanently mounted inside the cassette. Cassettes are designed to keep the screens in tight contact with the film, and this is usually accomplished by using compressible foam backing to mount the screens to the cassette. Many cassettes are hinged on one side and open up much like a book. The film is loaded into the cassette in the darkroom, and when the cassette is closed, the screens contact the film at the hinged side first, and the zone of screen-film contact spreads toward the latch side of the cassette. The foam is compressed in the process, and air that may otherwise be trapped between the screen and film is forced out.

Many modern radiology departments use daylight loading systems. This means that the cassettes are loaded in film-loaders outside of the darkroom and are unloaded in a mechanism that feeds the film right into a processor. Daylight systems improve departmental efficiency because the technologists do not have to go in and out of a darkroom frequently. Some daylight systems unload the exposed film, send the film to the processor, and reload fresh film into the cassette, all in one stop for the technologist. Daylight systems place special demands on the cassettes, because they must be automatically opened and closed by a mechanical device and not human hands. In some daylight systems, the cassette does not open, but the film is essentially injected into a slot on the end of the cassette. Systems that cause excess friction between the film and the screens

must address the problem of static electricity charging, and this often requires a supercoating on the film with antistatic properties.

X-ray cassettes are not ambidextrous; even dual-screen, dual-emulsion systems are designed with a front and a back. The front side of the cassette is often made from material that attenuates very little of the x-rays, such as carbon fiber. This is especially true in mammographic cassettes, where the energy of the x-ray beam is low and the absorption in the cassette can be high if improperly designed. Also, the backs of many cassettes have layers of lead in them. Because of the high atomic number of lead (Pb), x-ray absorption is much more likely than scattering, and therefore the Pb layer reduces the amount of backscatter that will strike the screen-film system.

### X-ray Intensifying Screens

Thick screens absorb more x-rays than thin screens. The thickness of a screen is measured in units of phosphor mass per unit area, $mg/cm^2$. Typical x-ray cassettes contain two screens with about 60 $mg/cm^2$ of phosphor per screen, for a total of 184 grams of phosphor per $35 \times 43$ cm ($14 \times 17$ in) cassette. Whereas it is always desirable to absorb as many x-ray photons as possible, thicker screens also can degrade the spatial resolution of the image (Fig. 6.3). Thicker screens result in a greater distance between the point where the visible light is emitted in the screen and the film emulsion. Because the visible light is emitted from the x-ray interaction site uniformly in all directions (isotropically), it spreads out as it travels greater distances. Consequently, thicker screens result in greater

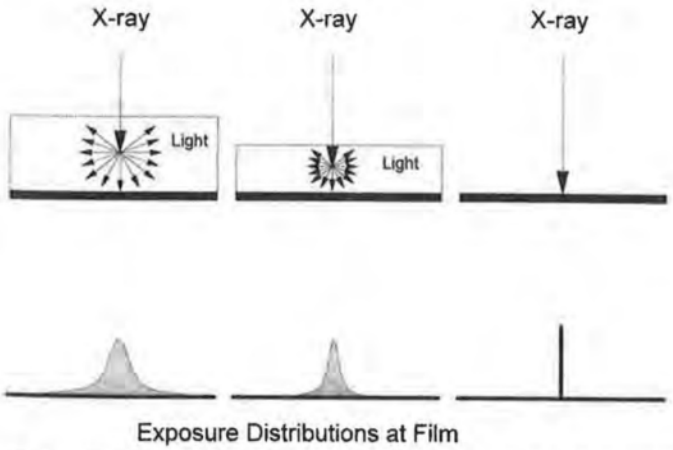



**Figure 6.3.** Thicker screens absorb a higher fraction of the x-rays incident upon them, but the light emitted in the screen can travel further and spread out more. This results in blurring, and a loss of spatial resolution. Thinner screens have a lower quantum detection efficiency but have better resolution properties. Direct film offers excellent resolution, but the lack of x-ray absorption efficiency requires excessive radiation dose to the patient.

**Table 6.1**
**The Quantum Detection Efficiency of Various Screen Film Systems**

| Screen | Composition | Thickness ($mg/cm^2$) | QDE (%) | | |
|---|---|---|---|---|---|
| | | | 60 kV Extremity | 80 kV Chest | 120 kV Chest |
| Hi-Plus | $CaWO_4$ | 120 | 53.2 | 42.0 | 26.3 |
| Quanta III | LaOBr:Tm | 108 | 60.0 | 53.2 | 33.2 |
| Lanex Regular | $Gd_2O_2S$:Tb | 130 | 54.3 | 52.6 | 39.5 |
| Trimax 12 | $Gd_2O_2S$:Tb | 165 | 60.8 | 59.3 | 46.5 |

blurring of the x-ray absorption information. Resolution is just one important imaging property that is significantly affected by the presence of an x-ray screen.

The noise in a radiographic image is intrinsically related to the number of x-ray photons that contribute toward producing the image. Increasing the number of photons lowers the relative noise. Because intensifying screens allow radiographs to be produced with substantially fewer x-ray photons, they always increase image noise relative to direct film as a detector. However, all modern radiographic images are produced with screens. A screen-film system produces the image in two steps: (1) the absorption of x-rays in the screen, and (2) the transfer of information concerning the absorption events to the film emulsion via the light emitted from the screen. The first step involves the x-ray *quantum detection efficiency* (QDE), also called the quantum efficiency. The QDE is the fraction of x-ray photons absorbed by the screen. Typical QDEs are listed in Table 6.1. The QDE depends on the kV of the x-ray beam, the composition and thickness of the tissue the beam must pass through, and on the thickness and composition of the screen phosphor. The second step required to produce an image is to transfer information concerning the x-ray absorption to the film emulsion. This step is performed by the light emitted in the screen which is absorbed by the film emulsion. The efficiency of this step involves the *conversion efficiency*. The overall efficiency is the product of the detection efficiency and the conversion efficiency.

X-ray photons that pass through the patient, but also pass through the screen-film detector, do not contribute to the image formation process; they are wasted. Only the x-ray photons that are absorbed in the detector can contribute to the image. Therefore, it is the number of absorbed x-ray quanta in the detector, and not the number of photons that are incident on the detector, that matter. Noise calculations always make use of the number of absorbed photons, which is the product of the QDE and the number of photons incident upon the screen.

The overall efficiency of a screen-film system is usually expressed by the *speed* of the system. So-called *Par* speed systems are usually assigned an arbitrary speed of 100 by each film manufacturer. *Faster systems have higher numbers,* and screen-film system speeds of 50, 200, 400, and 600 are in common usage in radiology. Other speeds can be found commercially as well. Faster systems are more efficient at converting x-ray expo-

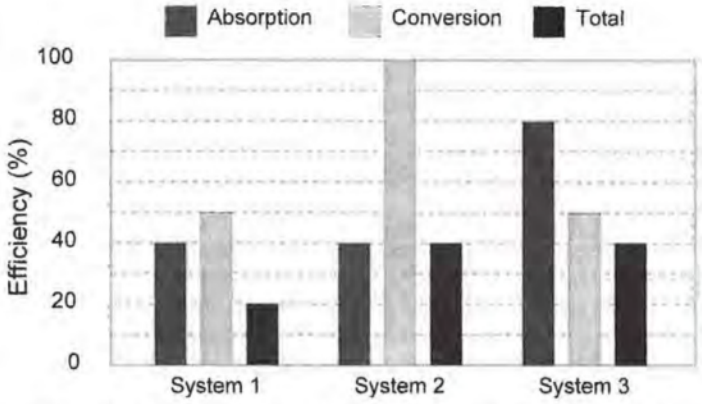



**Figure 6.4.** The quantum detection efficiency (QDE), conversion efficiency, and total efficiency for three hypothetical screen-film systems. Systems 2 and 3 are twice the speed of system 1. System 2 achieved this by doubling the conversion efficiency. System 2 will therefore use half the absorbed photons as Systems 1 and 3 to achieve proper film darkening, resulting in an increase in quantum noise. System 3 doubled its speed by doubling the QDE, and therefore uses the same number of absorbed photons as system 1, but at half the dose to the patient. The screen in system 3 may be thicker, however, compromising resolution.

sure to optical density, and thus they require less radiation and usually are noisier. The speed of a screen-film system can be manipulated in two ways, by changing either the QDE or the conversion efficiency. Figure 6.4 shows that the total efficiency of system 1 is 20%, and this is a consequence of a 40% x-ray absorption efficiency and a 50% conversion efficiency ($0.4 \times 0.5 = 0.2$). Systems 2 and 3 are both twice the speed of System 1, because their total efficiencies are both 40%. This essentially means that Systems 2 and 3 require half the incident radiation of System 1, to get the same amount of film darkening. *Remember that it is film-darkening that is generally held constant in radiography.* System 2 achieved the increase in speed by doubling the conversion efficiency, whereas in System 3 the absorption efficiency was doubled. By doubling the absorption efficiency, System 3 absorbs the same number of photons as the slower System 1 but requires half the patient dose. This means that for System 3 the noise will not increase, relative to System 1, even though the speed did increase. However, because the conversion efficiency was doubled in System 2, to get the same film darkening as the other two systems, half as many x-ray photons will be absorbed. Thus, System 2 will be noisier than the other two. Noise is not the only consideration in screen-film systems, however. If the increase in absorption efficiency of System 3 was achieved by making the screen thicker, this system will probably have poorer resolution than system 1, because of the blurring phenomenon discussed earlier. The various trade-offs in screen-film systems are often optimized for given applications (e.g., chest radiography or mammography) using a computer analysis of all the pertinent parameters (and their consequences) taken together. Other issues, such as the x-ray spectrum used, the scatter properties at play, and the physical char-

acteristics of the subject contrast (soft tissue or bone), also must be considered.

The thickness of the screen is not the only parameter that affects quantum absorption; the composition of the screen is, also, very important. Up until the early 1970s, calcium tungstate ($CaWO_4$) was the phosphor most commonly used in screens. It was then recognized that rare-earth phosphors have excellent characteristics for x-ray screens. Rare earth screens made from gadolinium oxysulfide ($Gd_2O_2S$:X), yttrium oxysulfide ($Y_2O_2S$:X) (The X is a dopant atom), lanthanum oxybromide (LaOBr), and others have higher conversion efficiencies than $CaWO_4$. In addition, because of the energies of their K-edges relative to typical x-ray spectra used in radiography, rare earth phosphors also have better quantum detection efficiencies than $CaWO_4$. By replacing $CaWO_4$ with a rare-earth phosphor, the screen itself can be made thinner but still retain the same x-ray detection efficiency. This means that for the same speed, rare-earth screens have better resolutions than $CaWO_4$ screens. Alternately, rare-earth screens with similar resolutions as $CaWO_4$ are faster but not noisier. Rare-earth screens have higher QDEs and higher conversion efficiencies. The relative quantum detection efficiencies for several phosphors and for film are shown in Figure 6.5, for x-ray spectra generated at different kVs. A 10-cm patient thickness and 120 mg/cm$^2$ total screen thickness were used in the calculations for Figure 6.5. The QDE improvement of the rare-earth phosphors over $CaWO_4$ is substantial. The detection efficiencies of the screens are more than an order of magnitude greater than film by itself.

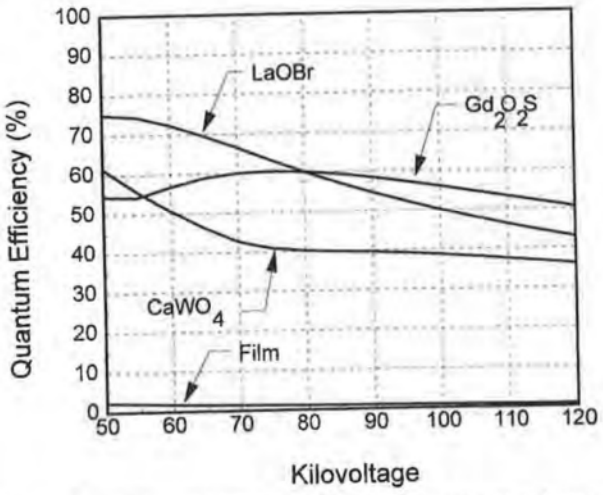



**Figure 6.5.** The quantum detection efficiency (or QDE) for several common x-ray phosphors and film, as a function of the kV of the x-ray spectrum. The vast improvement of the screens over film is obvious. The rare earth phosphors, LaOBr and $Gd_2O_2S$, both have significantly better QDEs than the conventional $CaWO_4$ screen. These data were calculated using polyenergetic x-ray spectra, a 10-cm patient thickness, and 120 mg/cm$^2$ of screen material.

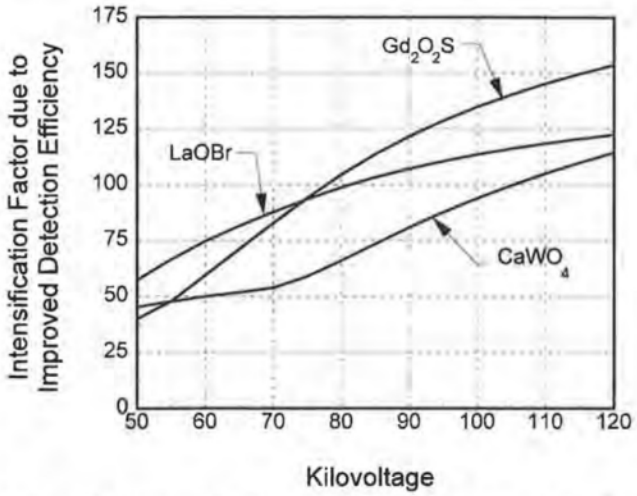



**Figure 6.6.** The intensification factor of several screens relative to film, accounting only for the improvement in quantum detection efficiency in the screen phosphor over film by itself as a detector. Conversion efficiencies are affected by screen design and intrinsic phosphor properties and would cause the total intensification factor to change up or down.

The *intensification factor* refers to the increase in speed that a screen provides, over a film-only detector. Intensification factors depend on both the quantum efficiency and the conversion efficiency of the screen. The intensification factors for the quantum efficiency component are illustrated in Figure 6.6. Here, the comparison was made using 120 mg/cm$^2$ total screen thickness and a typical AgBr total thickness of 0.8 mg/cm$^2$. By manipulating properties that affect the conversion efficiency, the intensification factors in Figure 6.6 can be adjusted up or down to get a specific screen-film speed.

## Radiographic Film

X-ray film is remarkable because of its ability to perform several important functions—it is a detector, a display device, and an archival medium. Unexposed film consists of a mylar base, with emulsions on one or both sides. A supercoating protects the emulsion from being scratched during handling. Supercoatings are sometimes designed to reduce static electricity buildup, which can result in often beautiful but problematic static artifacts. Static can be a very difficult problem in some geographical regions, especially during the winter when the air is very dry.

One of the purposes of the film emulsion as a detector is to absorb the light emitted by the screen. The absorption of light in the photographic emulsion causes a photochemical reaction. In the exposed emulsion, a latent image is stored but is not yet visible until the film is developed. Development is a process that results in silver being chemically

reduced. The amount of silver reduced is related to the amount of photochemical reaction that has occurred in the emulsion, which is a function of the light exposure. For dual emulsion film, it is important that the light intended to expose the emulsion on one side does not cross over and expose the emulsion on the other side. Because the film base is quite thick, light that crosses over to the opposite emulsion is very blurred, and this causes a loss of resolution as well as a loss of image contrast.

As a display device, film is almost unsurpassed. With the advent of mylar as a film base, x-ray film is rugged and portable. The transparent film base used in radiology allows the images to be viewed by letting the light from a viewbox be transmitted through the film. Transmission viewing has much greater fidelity than viewing light that is reflected off of the film, which is how most photographs are viewed. The optical density (OD) of film describes the amount of light transmitted through the film base and developed emulsion at a given location on the film (6.1). If the film transmits a certain fraction (T, the *transmittance*) of the light shone upon it, then the OD will be:

$$OD = -\text{Log}(T) = \text{Log}(1/T) \qquad (6.1)$$

The relationship expressed above is identical to that between the hydrogen ion concentration and the pH, familiar to all physicians. For a $[H+]$ of $10^{-7}$, the pH is 7. Similarly, for a transmittance of $10^{-3}$, the OD is 3. Examples of the conversion between transmittance and OD are given in Table 6.2.

X-ray film typically used in radiology has a slight tint to the mylar base (often this is a blue tint, which is considered more appealing), so that unexposed film has an OD of about 0.13 after development. Heavily exposed film can yield ODs of about 3.0 to 3.5 in radiography. This means that the total range of light transmission from x-ray films viewed on the viewbox can run as high as 75% (at 0.13 OD) to as low as 0.03% (at 3.5 OD). This is a very wide dynamic range, and is the principal reason why film in radiology is viewed using light transmitted through it rather than light reflected off of it. The dynamic range using reflected light is about 10 times lower. A large dynamic range allows subtle differences in contrast to be visible. For example, on a chest radiograph the OD is low in the diaphragm and mediastinum but is high in the lung fields. A wide dynamic range affords subtle contrasts to be detectable in both areas. Actually, an even wider dynamic range would be useful, as discussed later.

**Table 6.2**
**The Relationship Between Transmission and Optical Density**

| Transmission | Optical Density | Comment |
|---|---|---|
| 1.000 | 0.0 | 100% Transmission |
| 0.741 | 0.13 | Typical base + fog |
| 0.100 | 1.0 | Good exposure |
| 0.010 | 2.0 | Lung field on chest film |
| 0.001 | 3.0 | Very dark; need a hot lamp |
| 0.0003 | 3.5 | Maximal darkness in medical radiography |

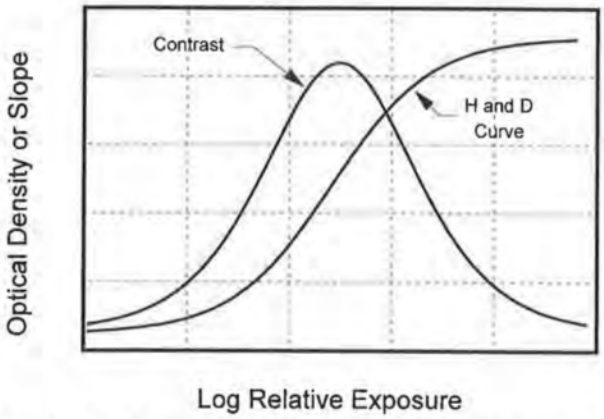



**Figure 6.7.** Film has a nonlinear response to exposure, and consequently the slope of the H and D curve changes as a function of exposure. The contrast of the film, is equal to the slope of the characteristic curve at each point. The middle of the exposure region renders the most contrast, whereas in underexposed and overexposed regions of the film, the contrast is reduced.

X-ray film gets darker with increased exposure, but different film types will vary with regard to how rapidly the OD changes as a function of exposure. A plot of this relationship is called the film's *characteristic curve* (also known as the "H & D curve," after Hurter and Driffield who first investigated these relationships). Different features of characteristic curves are shown in Figure 6.7. There are two important characteristics about film that are evident on the characteristic curve: (1) the relative speed is related to the lateral position along the exposure axis. Faster screen-film systems (Film A in Figure 6.8) have characteristic curves to the left of slower screen-film systems (Film B), because faster films require less radiation exposure to produce similar film darkening. (2) The contrast of the film is equal to the slope of the characteristic curve at a given point. Films with steeper characteristic curves have higher contrast (Films A and B have higher contrast than Film C.). Because the characteristic curves of most screen-film systems are nonlinear, the slope of the curve changes (and therefore so does the contrast) depending on the level of exposure. The shape of a typical H and D curve results in the contrast of the film being highest at medium exposures, with reduced contrast at lower and higher film densities. Figure 6.7 illustrates the strong dependence of the contrast in the film image on exposure—a fact that underscores the importance of producing properly exposed radiographs.

Contrast is often a desirable trait, and when the slope of the characteristic curve is greater than 1, the subject contrast is enhanced by the film contrast. The subject contrast is the contrast intrinsic in the patient and depends on the x-ray attenuation properties of the patient and on the kV of the x-ray spectrum used. Most radiographic films have a film contrast of about 3. Therefore, the film contrast serves to amplify the subject contrast. There are problems associated with high-contrast film, however, because the dynamic range of acceptable exposures is reduced

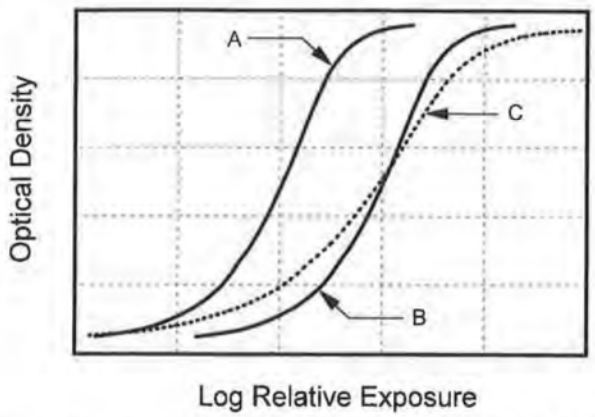



**Figure 6.8.** Characteristic curves for three different screen-film systems. Curve A and B are identical in shape, but curve B demonstrates that more exposure is required to achieve the same film darkening as Curve A; Film B is therefore slower than A. Lateral shifts of the H and D curve indicate a different sensitivity or speed. The slope of the curves are proportional to the *contrast* of the film, and steeper curves yield more contrast. Films A and B have more contrast than Film C.

as the contrast increases. In radiology, the term dynamic range is also called *latitude*. Although transmission viewing of the film improves the dynamic range of the film compared to reflective viewing, dynamic range is still quite limited. In examinations where there is a large variation in the x-ray exposure striking the detector, such as in chest radiography, wide latitude (lower contrast) screen-film systems are required. If a high-contrast system is used for chest radiography, the lungs will be too dark and the mediastinum will be too light. In bone radiology, where the subject contrast is not as great as in the chest, high-contrast films are preferred. High dynamic range, wide latitude (or just "latitude") films are more forgiving but produce "grayer" or "flatter" looking images.

Figure 6.9. illustrates other terms relating to the characteristic curve. The useful density range of the film is about 0.25 to 2.0 OD. The shape of the characteristic curve therefore governs the latitude of the film. If the slope of the curve in Figure 6.9 were steeper, the latitude would be reduced. The contrast characteristics of the film are related to the absolute grain size and the distribution of grain sizes that are present in the film emulsion. In general, high-contrast emulsions have a fairly uniform distribution of small grains, and lower contrast emulsions have larger grains and a wider distribution of grain sizes.

The low exposure side of the H and D curve is called the toe, and the high exposure side is called the shoulder. If a piece of film is developed without being exposed, the resulting OD is attributable to the "base + fog." The film base is not completely transparent and, in fact, often contains blue tints to give a more pleasing appearance to the film. Without the blue tint, the emulsion can leave the film with subtle but unpleasant hues of brown or orange. "Fog" refers to unintentional exposure of the film, which increases the background OD. Sources of fog

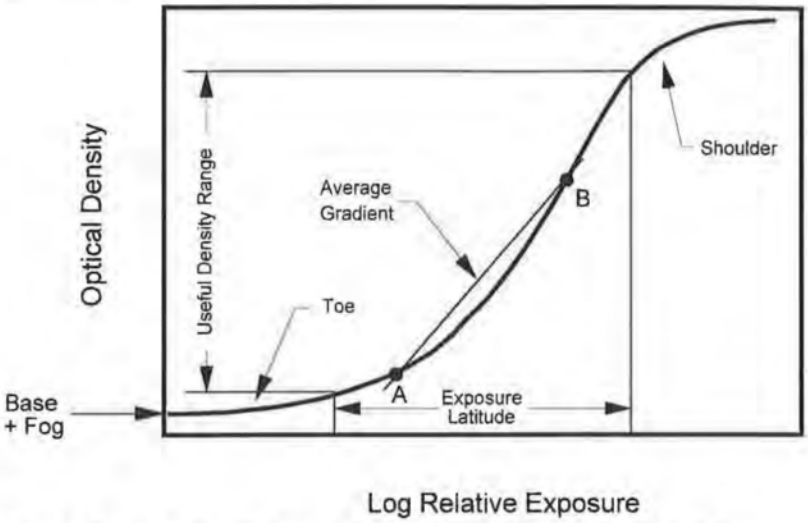



**Figure 6.9.** The nuances of the characteristic curve. The exposure could be from visible light, or from the light emitted by a screen when exposed by x-rays. The lower exposure region is called the toe, and the higher exposure region is called the shoulder. The center portion of the H and D curve is usually the steepest and renders the best contrast. The average gradient is defined between two points on the curve, point A and B. The useful density range is reflected onto the exposure axis by the characteristic curve; steeper curves (more contrast) therefore result in less exposure latitude, and flatter curves (less contrast) have more exposure latitude.

include heat exposure, light leaks from improperly maintained darkrooms, and the penetration of x-rays from adjacent radiographic rooms into the darkroom where film is stored. The "base + fog" levels for film are typically between 0.11 and 0.17 OD. The *average gradient* is simply the slope of the characteristic curve between two defined points, points A and B in Figure 6.9. Typically, point A is where the film density is 0.25 + base + fog (in OD units), and the OD at point B is 2.0 + base + fog. The average gradient is a single measure of the contrast of a particular film system:

$$\text{Average Gradient} = [OD_B - OD_A] / [\text{Log}(E_B) - \text{Log}(E_A)] \qquad (6.2)$$

where $OD_A = 0.25 + \text{base} + \text{fog}$ and $OD_B = 2.0 + \text{base} + \text{fog}$.

The speed of screen-film systems is usually a relative term used by each film manufacturer, where so-called Par speed systems are given an arbitrary speed rating of 100. Although loose comparisons can be made between different vendors' speeds, significant variation can occur. A more uniform definition of screen-film speed is given in inverse exposure units. *Absolute system speed* is defined as the inverse of the number of roentgens ($1\ R = 2.58 \times 10^{-4}$ C/kG) of exposure needed to achieve a film density of 1.0 + base + fog:

$$\text{Absolute Speed } (R^{-1}) = 1 \,/\, (\text{Exposure in R to yield an OD of } [1.0 + \text{base} + \text{fog}]) \qquad (6.3)$$

Typically, the values for absolute exposure are on the order of 0.002 R, corresponding to a speed of 500 $R^{-1}$. If the x-ray exposure needed to expose a slower screen-film system is large enough that increased x-ray exposure times are needed, then the potential for motion artifacts is increased. This is one reason why modern screen-film systems for angiography are usually fast, 400–800 speed.

As an archival medium, modern x-ray film can be stored for decades without significant degradation. Cellulose nitrate was used early in the century but was flammable and eventually was replaced with cellulose triacetate. With the plastics revolution of the 1960s, polyesters such as mylar became the standard for film base. Mylar does not yellow or curl, and so the film quality remains excellent over time.

### Screen-Film Systems

Dual-screen, dual-emulsion systems are commonly used in general radiographic procedures such as chest, abdominal, and head radiography. By sandwiching screens on either side of the film, each screen can be kept relatively thin, and using two screens substantially improves the absorption of x-rays. When high-resolution, fine detail visualization is needed as in hand radiography or mammography, single-screen, single-emulsion screen-film systems are used. The absorption of x-rays in the screen is exponential (rapidly at first, then more slowly), and this means that more x-rays are absorbed in the x-ray tube side of the screen, where the x-rays enter. Because of this, single-screen, single-emulsion systems are oriented with the single screen on the back side of the cassette. In this orientation, the x-ray photons incident upon the cassette pass through the film, then strike the screen. Because more of the light emitted in the screen comes from the side of the screen which is in close contact to the emulsion, it diffuses a shorter distance (on average) and the resolution loss is not as severe (Fig. 6.10). Some dual-screen, dual-emulsion systems are asymmetric, meaning that the screens on either side are different—either a different thickness, a different phosphor composition, or both. For asymmetric systems, the thinner screen is closest to the x-ray tube and thicker screen is in the back of the cassette.

If a film with an OD of 1.0 is placed on top of another film with an OD of 1.2, the OD measured through both films would be 2.2. In other words, OD units add. In the case of dual-emulsion films, the OD from one side of the film adds to that on the other side of the film, yielding the total OD for that film. If dual-emulsion film is observed at an angle other than straight on, then the images that were formed on the top and bottom emulsions will become slightly misregistered with respect to one another, causing a reduction in resolution. This is called *parallax*. To achieve high ODs and wide latitude with a single-emulsion film, the single emulsion has to be thicker. For modern double-emulsion films, the total thickness of AgBr is about 0.75 to 0.90 $mg/cm^2$. Single-emulsion films contain about 80% of this, or 0.60 to 0.70 $mg/cm^2$, but of course this is coated only on one side of the film base.

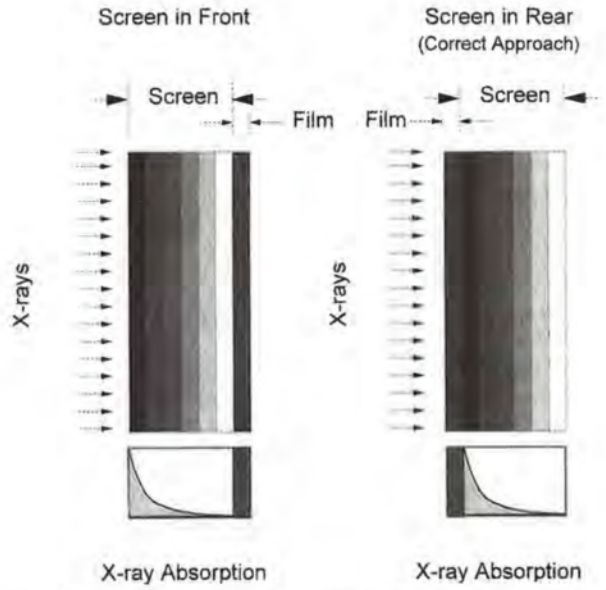



**Figure 6.10.** Single-screen exposure. The absorption of x-rays in an intensifying screen is an exponential function of depth in the screen. This means that most of the x-rays are absorbed on the side of the screen where they enter. A single-screen, single-emulsion system makes use of this fact to improve the resolution of the screen-film system. By positioning the film in front of the screen, the light emitted by the screen due to x-ray interactions travels (on average) a shorter distance before striking the film emulsion. Better spatial resolution results.

A characteristic curve for film can be measured by exposing the film to visible light (not x-rays) without a screen. Hence, the abscissa ($x$ axis) on the characteristic curve can be the logarithm of the relative visible light exposure. A *sensitometer* is a device that exposes film to a range of visible light intensities and is commonly used in processor quality assurance programs. A *densitometer* is used to measure OD. A characteristic curve for the screen-film system can also be produced by exposing the film in a cassette with screens by using x-ray radiation. In principle, the characteristic curves for light exposure and x-ray exposure will be quite similar. This is because the intensifying screen is a very linear system; the visible light output of the screen is a very linear function of the radiation exposure to the screen. (This is true only for a constant x-ray beam quality.) The relative *shape* of the characteristic curve is determined almost solely by the film's characteristics. When the H and D curve is measured using x-rays and a screen, the curve's *position* with respect to the abscissa (log relative exposure) can vary depending on the properties of the screen. The screen characteristics will affect the lateral position of the characteristic curve (the speed), but the shape (the curvature and the slope) of the characteristic curve is primarily a result of properties of the film. It is best to evaluate characteristic curves for a

given screen-film system by using x-ray exposure, because this information yields the absolute speed of the system in inverse roentgens, as well as the shape of the curve. A technique of 70 kV is usually used for characteristic curve measurement.

Different phosphor materials used in screens have different wavelengths of optical emission. $CaWO_4$ screens emit a continuous distribution of blue light. Rare earth phosphors, in general, emit a series of line spectra whose position depends not only on the phosphor (e.g., $Y_2O_2S$, $Gd_2O_2S$, $YTaO_4$) but also on the dopant used. For example, $Gd_2O_2S$:Eu emits predominantly at 624 nm (red), but $Gd_2O_2S$:Pr emits mainly around 514 nm. The spectra for these two phosphors is shown in Figure 6.11. The wavelength of the screen emission is an important consideration in designing a film to be used in conjunction with that screen. The film emulsion, AgBr (and some AgI), is naturally sensitive to ultraviolet wavelengths (around 300 nm). If sensitivity to longer wavelengths is necessary, sensitizing dyes are added to the emulsion. Emulsions sensitized to green wavelengths are called *orthochromatic,* whereas emulsions sensitive to the entire visible spectrum (e.g., photographic films) are called *panchromatic.* Red safelights in darkrooms can cause film fogging with some orthochromatic and all panchromatic films.

The light generated in the screen by x-ray interaction diffuses through the screen, and some of the light will escape the screen and expose the film emulsion. If for some reason a space were to exist between the screen and the film, then the diffusion distance of the visible light would be increased and more blurring would occur. This is why very close screen-film contact is important. If the cassette is damaged such that the

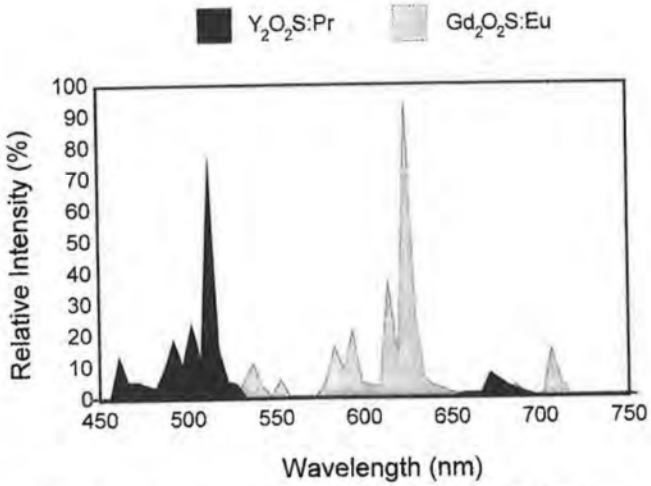



**Figure 6.11.** The optical emission of $Gd_2O_2S$:Eu and $Y_2O_2S$:Pr. The spectra emitted from most rare-earth screens have discrete line components to them, whereas the emission from conventional $CaWO_4$ screens are a continuous blue spectrum. The spectral properties of the screen need to be matched to the spectral absorption properties of the film emulsion.

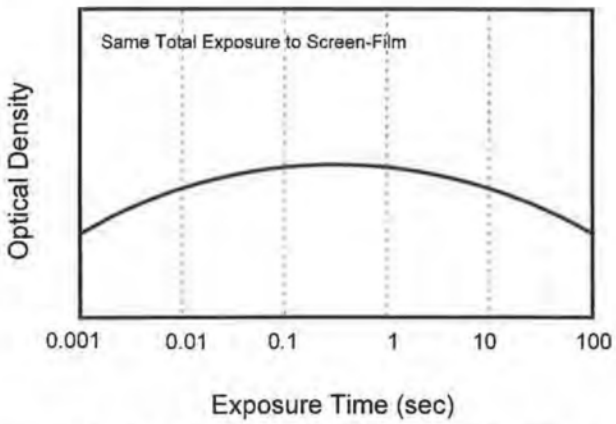



**Figure 6.12.** Reciprocity law failure. The total exposure at each point on the curve is identical, only the time to make the exposure is varied. The reciprocity law states that the resulting optical densities should all be identical, regardless of the time required to make the exposure. The curvature in the graph illustrates the breakdown of the reciprocity law, particularly at very short and very long exposure times. This curvature is referred to as the *reciprocity law failure* and is a characteristic of screen-film systems.

compressible foam backing no longer presses the screen against the film, air spaces can occur that will cause screen-film contact artifacts on the image, which have the appearance of regionally blurred areas. If dirt grains get into a cassette, they can not only scratch the screen surface but also force a gap between the screen and the film, causing a screen-film contact artifact on the image.

The relationship between optical density and exposure is usually independent on exposure rate, and this observation is known as the *reciprocity law*. The intensifying screen drastically increases the rate at which film is exposed (compared to direct x-ray exposure), and reciprocity law failure has been observed with screen-film systems (Fig. 6.12).

## PHOTOSTIMULABLE PHOSPHOR SYSTEMS

There is a special class of x-ray phosphors that, when struck by x-rays, trap a fraction of the x-ray energy imparted to the phosphor in a quasi-stable state within the crystalline lattice of the phosphor. The energy absorbed during x-ray exposure is re-emitted some time later, by exposing the phosphor to another energy source, such as light or heat. This phenomenon is called *photoluminescence* when light causes the emission of trapped energy, or *thermoluminescence* when heat is used. Thermoluminescent substances (e.g., lithium fluoride) are the basis for thermoluminescent dosimeters (TLDs), discussed in Chapter 16. There are many photoluminescent substances—zinc sulfide, alkalihalide, natural diamond, silicon, and some oxidized compounds. The energy storage properties of these phosphors can be used to record an image using x-rays. The latent x-ray image can then be read from the *storage phosphor* at a

later time using a scanning laser beam to stimulate the emission of the stored energy. The phosphor that is used in radiography is barium fluorohalide, doped with europium as an activator. These phosphors are also known as *photostimulable phosphors.*

### Mechanism

The photostimulable phosphors (PSPs) used in radiography are mixtures of $BaFI:Eu^{+2}$, $BaFCl:Eu^{+2}$ and $BaFBr:Eu^{+2}$. Because iodine, chlorine and bromine are halides, the PSPs are also referred to as barium fluorohalides. When x-rays interact with the molecules of the phosphor, valence electrons are excited to the conduction band and become trapped in higher energy metastable states. An energy diagram is shown in Figure 6.13. During the ionization of the phosphor molecules that occurs under x-ray exposure, the $Eu^{+2}$ ions are oxidized to $Eu^{+3}$ (creating so-called *electron holes*), and the released electrons are trapped by halogen vacancies in the crystalline lattice. This trapped energy can remain in the phosphor for days to weeks and is slowly released because of thermal processes. The trapped energy can be released much more rapidly by stimulating the phosphor with visible light. The visible light is absorbed by the *color center* created by the trapped electron, producing secondary excitation that excites the trapped electrons back into the conduction band. Once in the conduction band, the electrons are free to migrate to

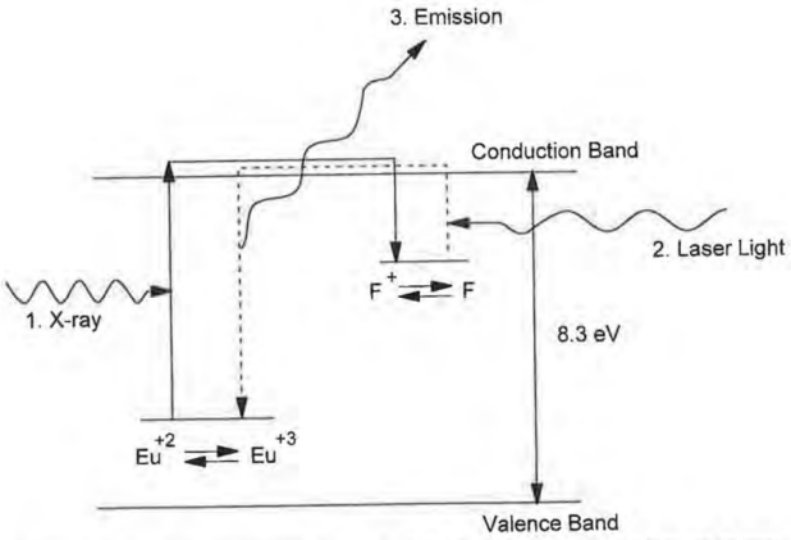



**Figure 6.13.** The mechanics of how a photostimulable phosphor is thought to work. *1.* The europium (dopant) atoms are ionized by exposure to x-rays, and the electrons are freed to travel to the conduction band. Once in the conduction band, the electrons are free to travel to a so-called F-center, where they are trapped in a metastable state. It is here where the x-ray absorption information is stored. 2. When the read-out laser scans the imaging plate, the laser light stimulates the electrons trapped in the F-centers up to the conduction band, where they are free to migrate to the europium atoms, causing $Eu^{+3}$ to return to the $Eu^{+2}$ state. This transition results in the emission of light that can be measured electronically.

the $Eu^{+3}$ ions, causing the emission of light as the trivalent ion goes back to the divalent state. Because the light that is emitted is of a different color than the light used to stimulate the phosphor, the emitted light is isolated with a color filter and detected using a photomultiplier tube (PMT). The emitted light intensity is proportional to the amount of x-rays that were absorbed locally in the phosphor.

### Equipment

Photostimulable phosphors are used for x-ray imaging by forming them into screens, similar to an intensifying screen. The PSP screens or *imaging plates* are placed in an enclosure (a cassette) and are exposed to x-rays just like a screen-film cassette is. The cassette is then placed into a read-out unit. The read-out unit provides a function similar to that of film processing, but it uses a completely different mechanism because no film is involved in the detection process. A schematic of the read-out system is shown in Figure 6.14. Inside the read-out system the exposed imaging plate is automatically removed from the cassette that houses it and is placed on a translational stage that can be moved along the $y$ axis of the image plate under computer control. A helium neon laser beam is reflected off of a rotating mirror and scans the imaging plate in the $x$ axis of the image, stimulating the photoluminescent emission from the imaging plate at the very small location where the laser energy is focused.

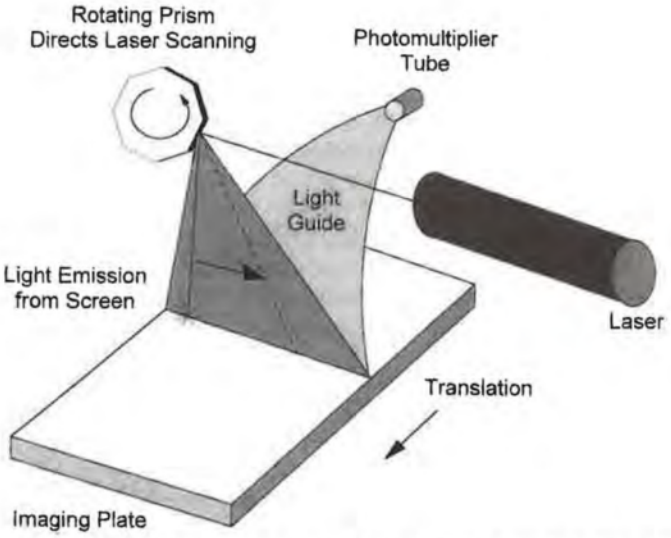



**Figure 6.14.** The read-out system for the photostimulable phosphor plates uses a long axis translation of the imaging plate. The plate is read out in the short axis by a scanning laser beam. The beam is scanned using a multi-sided rotating prism, which causes repetitive scanning of the laser on the plate using only rotary motion. The light that is emitted due to the laser excitation is collected using a light guide and is detected using a photomultiplier tube and associated electronics. The final electrical signal is digitized, thereby assigning a gray scale value to that $(x,y)$ point that is being excited on the plate.

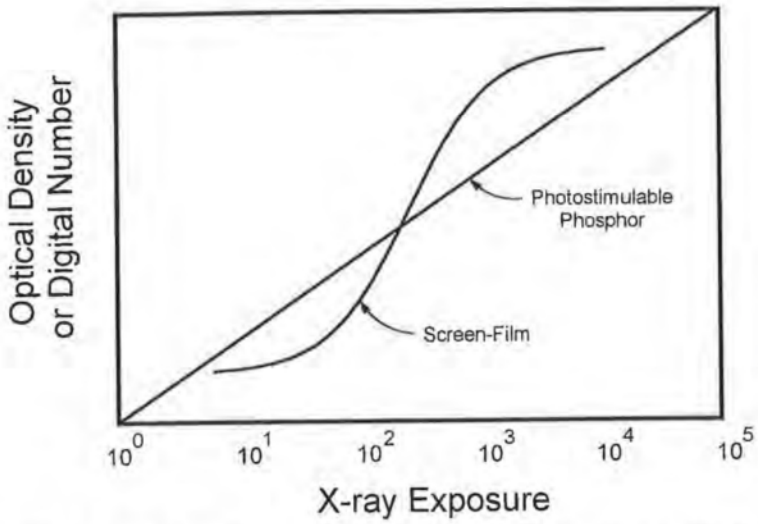



**Figure 6.15.** The dynamic range of photostimulable phosphor systems is wider than the dynamic range of film. This gives PSP systems much broader exposure latitude than screen-film systems. This broad latitude is achieved through the use of sensitive electronic components and by the use of a pre-scan technique, which is in effect, a type of automatic gain control.

The angle of the mirror determines the *x*-position, and the position of the translational stage determines the *y*-position on the image. The amount of energy emitted by the imaging plate is detected electronically at each image location, and the electronic signal is digitized to a gray scale value, which is positioned at the (*x*,*y*) pixel in the digital image.

Because of the high sensitivity of the electronics and their intrinsic linearity, the dynamic range of the digital image that is recorded from the imaging plate is superior to that of film. Figure 6.15 illustrates the characteristic curves of screen-film and photostimulable phosphor systems. Because of certain pre-scan operations that are performed before the initial read-out of the imaging plate, the electronics apply what is effectively an automatic gain control during the acquisition of the photostimulated image. This means that underexposed images are recorded with equal "brightness" as overexposed images. This is the most highly touted attribute of photostimulable phosphor systems; rarely does an image need to be retaken because of incorrect exposure.

The formation of the radiographic image using PSP systems is completely digital. Surprisingly, the standard clinical system sold by many manufacturers (but licensed from Fuji, who holds patents on the technology) has only analog film output. Coupled to the read-out system is a laser imager, which produces a film copy of the digital image for radiologist evaluation. The digital data is then thrown away in some systems. Upgrades to the basic system allow for a computer interface, which facilitates the archival and electronic transmission of the digital image data.

There are limitations to PSP technology. The barium fluorohalide phosphor does not have the same x-ray absorption capabilities of the rare-earth intensifying screens used for screen-film radiography. Consequently, the quantum detection efficiency of PSP systems is inferior to screen-film systems. This means that for the same dose to the patient, there will be more quantum noise in the image. Furthermore, because the image is digital and uses fairly large pixels (~0.2 mm for chest radiography), the spatial resolution of the images cannot approach that of film. For the 0.2-mm pixels used in PSP systems for chest radiography, the Nyquist limit is 2.5 line pairs/mm. For screen-film systems commonly used in chest radiography, 7 line pairs/mm resolution or better is achievable. Because of this limitation in spatial resolution, PSP systems used for chest radiography have been shown to be inferior in the assessment of small anatomical details such as pneumothoraces.

### Digital Radiography

There are certain intrinsic advantages to having the image data resident on a computer rather than on an analog piece of film. There are disadvantages as well. One of the advantages of digital images is that an infinite number of copies can be made with no degradation in image quality. Digital images can be electronically conveyed to referral centers such as the ICU or to the on-call radiologist at home. The transmission of images to remote sites is called *teleradiology*. For local transmission of digital images around the hospital and the imaging center, the term *Picture Archiving and Communication Systems* (PACS) has been in common usage. Although the electronic storage (archiving) of digital images in principle makes it easy for the radiologist to call up the past images of the patient, there are pragmatic issues that compromise this ability. These issues include the cost associated with keeping huge amounts of data on-line and instantly accessible on the computer system, the relatively poor quality of images displayed on computer monitors compared to film, and the fair amount of animosity that radiologists have for computer keyboards.

Digital images are of course available to the computer for processing and evaluation. Research in computer-aided diagnosis (CAD) for chest radiography and mammography in particular has resulted in substantial advances. For very specific types of evaluation, computer-aided diagnosis has been shown to be comparable to human performance. When combined with the radiologist's input, CAD programs have been shown to improve diagnostic performance substantially, essentially by contributing another set of "eyes" to the task. In effect, CAD can provide a free second opinion. It is only a matter of time before this research becomes a clinically available tool, outside university medical centers.

## SCATTERED RADIATION IN PROJECTION RADIOGRAPHY

Scattered radiation can play havoc with a radiographic image. Without defensive measures, scattered x-ray photons can contribute very significantly to the exposure of the image. In screen-film radiography, scattered

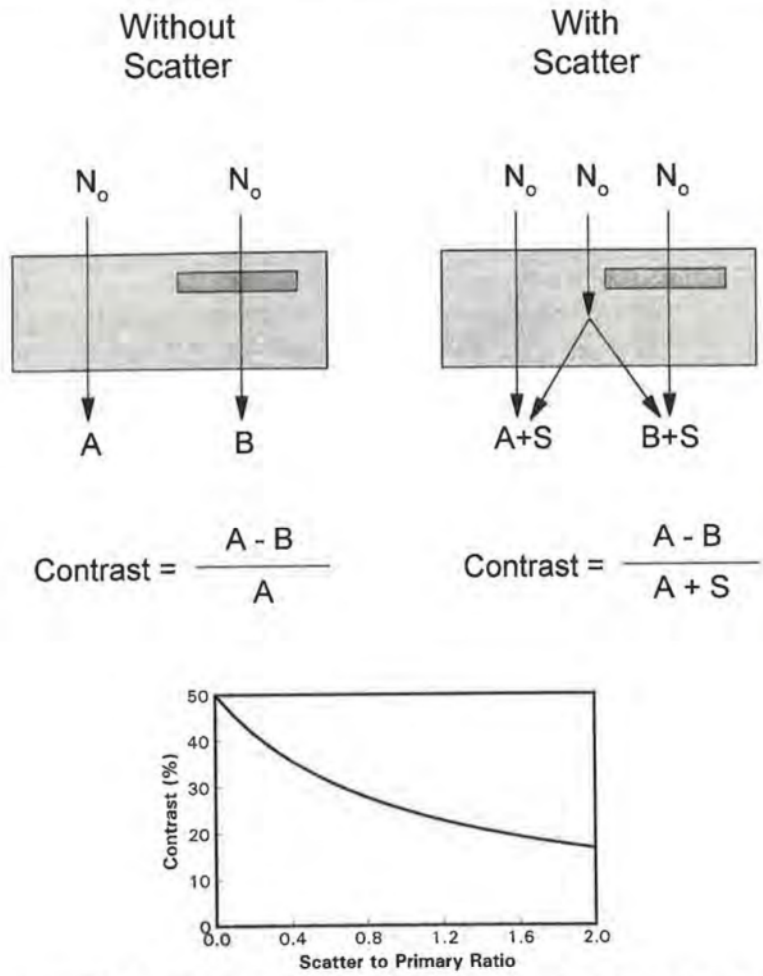



**Figure 6.16.** Subject contrast without the degrading influence of scatter (left) and the influence of scattered rays (right). The contribution of scatter (*S*) to the A and B regions is approximately the same, and so it has no effect on the numerator, because $(A+S)-(B+S)=(A-B)$. Because scatter contributes to the denominator $(A+S)$, the contrast goes down as the amount of scatter (the value of *S*) goes up. The graph at the bottom of the figures illustrates an object that has 50% contrast with no scatter. As the SPR (the ratio of *S* to *A*) increases, the contrast is degraded significantly. At a scatter to primary ratio of 1.0, the contrast is half of what it should be (25% instead of 50%).

radiation causes a reduction of contrast in the image. The reasons for this are illustrated in Figure 6.16. In projection radiography, a three-dimensional object (the patient) is imaged onto a two-dimensional planar image. The density on a radiographic image at a given point on the film is related to the attenuation characteristics of the patient along a line between that point on the image and the source of the x-rays (the x-ray tube). The main premise of this projection of the three-dimensional anatomy onto the two-dimensional image plane is that *x-rays travel in straight*

*lines*. Scattered radiation violates this central requirement of projection imaging, because the scattering event effectively causes the redirection of the x-ray energy. When a scattered x-ray photon strikes the imaging receptor and is recorded, that information is not related to the attenuation characteristics in the patient between that point on the image and the focal spot.

Scattered radiation contributes an almost constant background fog level to the film image. For digital images, where contrast can be arbitrarily increased by using windowing and leveling techniques, the main effect of scattered radiation is to increase the noise in the image. For quantitative imaging applications, such as digital subtraction angiography and dual energy radiography, scattered radiation causes inaccuracies in transmission measurements and therefore reduces the performance of the techniques.

As a diagnostic x-ray beam penetrates a patient, three types of x-ray interactions can occur: photoelectric absorption; Rayleigh scattering; and Compton scattering. Of these, two are scattering events; however, Rayleigh scattering does not occur with much prevalence in the clinical radiography setting (except in mammography). The probability of Compton scattering relative to the probability of photoelectric absorption is very dependent on the energy of the x-ray photon. However, in diagnostic radiography, the x-ray beam contains a wide spectrum of x-ray energies. Consequently, the strong energy dependence that would occur if monoenergetic x-ray beams were available is highly diminished because of the fact that a wide energy range of photons are used.

The amount of scattered radiation energy can be expressed relative to the amount of primary radiation energy deposited at the same point in the image. This ratio, called the *scatter to primary ratio* (SPR), is illustrated in Figure 6.17. The SPR increases with thicker patient anatomy and

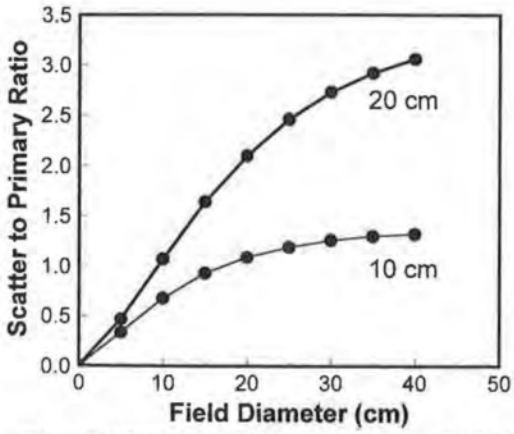



**Figure 6.17.** The relationship between the scatter to primary ratio, field size (diameter of a circular field), and the thickness of the object. These values are for a 100 kV x-ray beam, and a water equivalent object. The SPR values are determined at the center of the field of view. Scatter increases with increasing thickness and increasing field size.

larger field sizes. Even though the scatter increases with increased x-ray energy, so does the amount of transmitted primary radiation, and therefore the SPR only increases by a few percent as the kVp is increased from 80 to 120, for example.

How significant is scattered radiation? For fields of view typical in the abdomen and for large patients, the SPR can be as high as 4 or greater. An SPR of 4 implies that only 20% of the photons contributes to the image information; the other 80% of the energy that is detected is useless scattered information. From these numbers, it is clear that scattered radiation can be a very large problem if steps are not taken to limit its effect on the image.

### Methods to Reduce Scattered Radiation

In radiography, the main defenses against scattered radiation are aggressive field collimation, the antiscatter grid, and the use of an air gap. The use of air gaps has limitations and will be discussed later. Collimation of the x-ray field to the minimal size necessary to image the anatomy of interest is a simple way to reduce the amount of scattered radiation that is generated. As shown in Figure 6.17, the amount of scattered radiation that emanates from the patient on the side of the detector increases with thicker patients and with large fields of view. In effect, the *volume* of tissue that is irradiated by the primary beam largely determines the amount of scatter that is generated. Because the patient cannot be made thinner (except in mammography by compression), reducing the field area is the only realistic measure that can be used to reduce the amount of scattered radiation that is generated in the patient. Of course, the x-ray field cannot be limited too much without the risk of missing diagnostically important information on the image. Therefore, the antiscatter grid becomes necessary in most circumstances.

The radiographic grid is composed of a series of very small parallel bars of highly attenuating material (Pb or tantalum). Most grids are linear, but grids in which the grid strips run in two directions are also available (crossed-grids). The spaces between the highly attenuating grid strips are filled with low attenuating material: cardboard, aluminum, or wood. The antiscatter grid is positioned between the patient (the source of the scattered radiation) and the detector. The channels in the grid that are formed by the spaces between the grid bars are tall and thin in cross-section (Fig. 6.18), and the long axis is pointed toward the x-ray source. The spaces between the grid bars act like tiny collimators. Primary radiation, by definition, always emanated from the patient in straight lines from the focal spot. Because the grid spaces are aligned with the focal spot, a large fraction of the primary x-ray photons can pass through the grid spaces. Scattered radiation does not exit the patient aligned with the focal spot but rather has a broad angular distribution. This means that scattered x-ray photons strike the grid in a direction nonparallel to the grid spaces, on average, and therefore scattered x-rays have a higher probability of striking the grid bars and being absorbed. A grid is only effective if it absorbs a higher percentage of scattered x-rays than primary x-rays. The

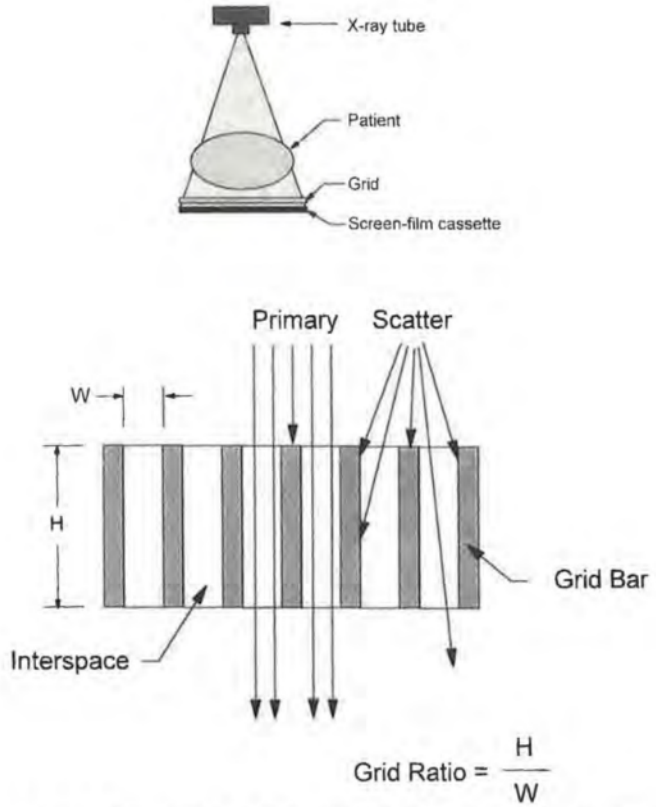



**Figure 6.18.** A cross-section of an antiscatter grid. The grid ratio is the ratio of the height to the width of the low attenuating spaces between the grid bars. Because the interspaces are aimed at the focal spot, the primary rays have a very good chance of passing through the grid and striking the detector. Scattered rays are emitted by the object with a wide distribution of angles. Consequently, they have less of a chance of passing through the grid and striking the detector.

ratio of the primary transmission to the scatter transmission of a grid is called the *selectivity*. Because the scattered radiation that is emitted by the patient is dependent on the thickness of the patient, the field of view, and to a lesser extent on the x-ray spectrum used, the selectivity and other measures of grid performance depend on the measurement conditions.

It is interesting to compare antiscatter strategies between radionuclide imaging and radiography. In nuclear medicine studies, the radionuclide is distributed throughout a volume in the patient, and therefore the gamma rays to be imaged do not emanate from a point source. This means that a scatter grid would not be effective, because grids rely on geometrical assumptions requiring a point source. Instead, radionuclide imaging uses monoenergetic gamma ray emitters and relies on the energy resolving capabilities of the scintillation camera. Scatter is rejected

on the basis of its reduced photon energy, relative to the monoenergetic emission energy of the isotope (140 keV for Tc-99m). Energy discrimination cannot be used in radiography, because the x-ray source is polyenergetic and because the photon flux is much too large to detect and characterize each photon's energy.

## Grid Characteristics and Performance

There are many terms that have been used to describe the properties of an antiscatter grid. These include the primary transmission factor, scatter transmission factor, the selectivity, the Bucky factor, the grid ratio, the grid strip density, the lead content, and the contrast improvement factor. These terms and their definitions are listed in Table 6.3. Of these terms, two are relevant in the routine radiography setting—the Bucky factor and the grid ratio.

A radiograph that is produced without the use of a grid will require a certain radiographic technique (kV and mAS). When a grid is used to produce an image of the same object at the same kV, both the primary and scattered radiation striking the detector will be reduced by the grid. Therefore, to produce the same level of film darkening, the mAS will have to be *increased* when the grid is used. The amount of increase that is needed when a grid is used is called the *Bucky factor*. Because the mAS (at a given kV) is proportional to the exposure incident on the detector, the Bucky factor is also a measure of the ratio in incident exposure to the patient, with and without the grid. The Bucky factors for realistic grids used in radiography range between 2 and 5. Because grids are virtually always used in radiography (except in portable radiography), the knowledge of the Bucky factor for a certain grid is not necessary. Rather, the Bucky factor is a good indicator of the increase in radiation dose that the patient receives when a grid is used. To improve the contrast in the image by reducing the effects of scattered radiation, an in-

**Table 6.3**
**Parameters That Characterize Antiscatter Grid Performance**

| Parameter | Definition |
|---|---|
| Bucky factor | Increase in incident exposure when a grid is used. |
| Selectivity | The relative transmission of the primary radiation divided by the relative transmission of the scattered transmission. |
| Grid ratio | The height of the grid bars divided by the width of the interspace material. |
| Primary transmission | The fraction of primary radiation that penetrates the grid. |
| Scatter transmission | The fraction of scattered radiation that penetrates the grid. |
| Contrast improvement ratio | The improvement in contrast when a grid is used. Equal to the ratio of the contrast with a grid over the contrast without a grid. |
| Lead content | Mass of Pb per unit area ($mg/cm^2$). |

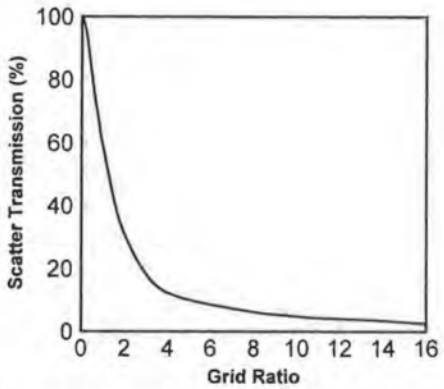



**Figure 6.19.** The scatter transmission as a function of the grid ratio of the antiscatter grid. Practical linear grids used in radiography (outside of mammography) range from about 8:1 to 12:1. After 12:1, the benefit of higher grid ratios become less apparent and the propensity for the higher grid ratio grids to cause artifacts increases.

crease in patient dose on the order of 2 to 5 times is required. This is not a trivial increase in radiation exposure.

The *grid ratio* is a characteristic of an antiscatter grid. The grid ratio is the ratio of the height to the width of the spaces between the Pb strips in the grid (Fig. 6.18). As the grid ratio increases, the collimating capabilities of the grid slits also increases. Therefore, increasing the grid ratio also increases the scatter rejection properties of the grid, up to a point. The scatter transmission of the grid as a function of its grid ratio is shown in Figure 6.19. Although high grid ratios such as 16:1 have some improvement in scatter rejection capabilities over a 12:1 grid, high grid ratio grids also are more prone to grid-induced artifacts. The range of grid ratios that are used in radiography, outside mammography, is from about 8:1 to 12:1.

### Grid Artifacts

Grids can produce artifacts when improperly aligned. Because there is plenty of opportunity for a grid to be positioned incorrectly in a busy imaging facility, the radiologist should be aware of the potential for grid artifacts. The artifacts caused by improper alignment of a grid are the consequence of the grid being oriented or positioning incorrectly *with respect to the x-ray tube focal spot.* Common examples of grid misalignment are illustrated in Figure 6.20.

Grid artifacts can occur that are not a consequence of misalignment. The manufacturing capabilities with respect to grids have improved substantially over the years, and now grids are made with grid strips so small that they are hardly noticeable on the film. Modern grids have very small interspace widths and grid bar widths. Consequently, it takes only a little mechanical abuse to cause physical distortion in the alignment of the grid bars in the grid. Dropping, bending or crushing a grid can cause deformation of the grid bar alignment that can be noticeable on the im-

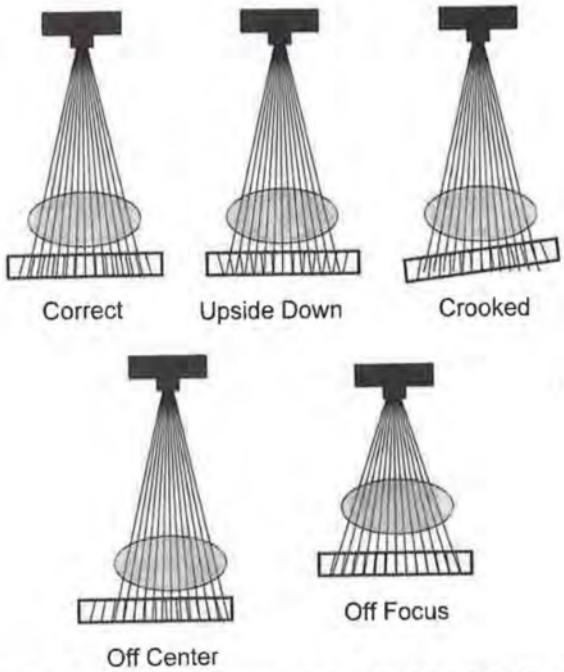



**Figure 6.20.** Some of the situations that can lead to grid cut-off artifacts.

age. These effects are usually subtle and are usually obscured by the image of the overlaying patient anatomy. However, if a grid is imaged by itself, the artifacts in the physical construction and integrity of the grid can be seen. Radiographing a grid by itself is therefore a common quality assurance measure that should be performed on grids on a routine (but infrequent) basis.

Stationary grids cast a radiographic shadow of the grid bars that is usually too fine to become a problem in general radiographic studies, because the number of grid strips can range from 30 to 40 strips per centimeter. However, the high frequency line pattern caused by a stationary grid can become a problem when the radiographic image is being *sampled*. For example, when radiographs are digitized at sufficient resolution, the sampling imposed during the digitization can combine with the high-frequency grid pattern and produce a Moiré pattern. The Moiré pattern is the effect of aliasing between the digital sampling and the image of the grid bars. This can be a problem when film is digitized by a laser digitizer, or with photostimulable phosphor systems that are scanned during the read-out process. Scatter grids are also used routinely over the image intensifier for fluoroscopy. The grid bars should be aligned so that they are perpendicular to the horizontal scanning direction of the video camera, or Moiré patterns can be generated on the fluoroscopic images. These image artifacts are better resolved at higher exposure lev-

els, and therefore can impact the quality of digital subtraction angiography or photospot studies.

### Moving Grids

The grid bars of an antiscatter grid can be removed from the image by inducing motion blurring of the grid bars themselves. This is done by moving the grid in a direction perpendicular to the alignment of the grid bars. Such a system is called a Bucky grid, after its inventor (circa 1921). Most radiographic rooms have a Bucky tray under the table, into which the screen-film cassette slips. This tray holds the x-ray cassette just below the moving grid. The grid motion is initiated when the x-ray tube prestart button is engaged, just before x-ray exposure.

### Air Gaps

The use of an air gap between the patient and the detector system can be an effective alternative to using an antiscatter grid. Because the source of the scattered radiation is the patient, moving the detector away from this source reduces the scatter exposure received by the detector. The reduction in the primary exposure to the detector of course also decreases, but not as much as the reduction in scattered exposure (Fig. 6.21). The limitation to using an air gap to reduce the detected scattered radiation is that an air gap also imposes additional magnification of the object. Magnification has several unfortunate consequences; it exacerbates the resolution degradation caused by a finite focal spot and reduces

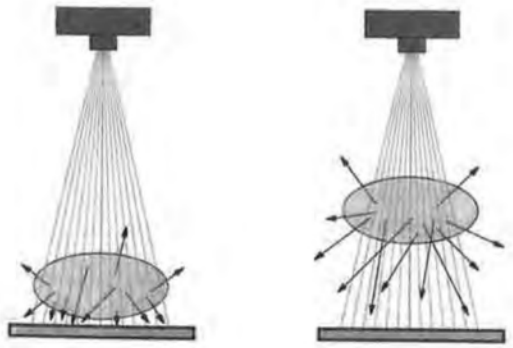



**Figure 6.21.** By separating the object and the detector with an air gap, the amount of scattered radiation that reaches the detector will be reduced. Air gaps have good potential for scatter cleanup; however, they are limited in use because the introduction of an air gap causes an increase in the magnification of the object. Increased magnification exacerbates resolution losses due to focal spot blurring (unless a very small, limited output, focal spot is used). Higher magnification also results in a smaller effective field of view in the patient, and so less anatomy is covered on a given size of film.

the amount of anatomy that can be imaged onto a given size of x-ray film. These issues tend to limit the use of the air gap technique for scatter reduction.

## SUMMARY

Projection radiography is the mainstay of the radiology department and has withstood the test of time for a century. Although today's screen-film systems represent a highly refined state of the art, technological advances will continue to improve the capabilities of this mature but vital imaging modality. Digital image detectors have made slow but steady progress in establishing a niche in projection radiography. The photostimulable phosphor systems described above and other types of digital imaging systems will continue to gain a market share in x-ray imaging. The high-resolution images and the cost effectiveness of planar radiography makes this imaging modality one of the most useful diagnostic tools in medical diagnosis.

# FLUOROSCOPY




## GENERAL PRINCIPLES

Fluoroscopy is an imaging procedure that allows live x-ray viewing of the patient. It is used in radiology for two principal reasons: real-time imaging and for aligning the patient with respect to the imaging system for filming. Modern fluoroscopic systems use image intensifiers and closed-circuit TV systems, as shown in Figure 7.1. Fluoroscopic systems have undergone significant technological advancements in recent years. Image intensifiers (IIs) have increased in size, from the early 6-inch systems to 16-inch systems available today. It is now possible to view an entire abdomen with large field-of-view (FOV) IIs. TV camera electronics are vastly superior to earlier systems, and further improvements are iminent as a result of the development of high definition TV (HDTV) for broadcast television.

Fluoroscopy and radiography both use x-ray radiation to penetrate the anatomy, but there are differences. Fluoroscopic examinations can require several hours, with a total beam-on time upwards of an hour. During the study, when the beam is on, the patient is being irradiated. To keep the radiation dose to the patient from becoming a health hazard in itself, the *exposure rate* in fluoroscopy is several orders of magnitude lower than that in radiography. An example will illustrate this point. In radiography, it is desirable to acquire the image in as short a period of time as is possible to prevent motion blurring. For a radiographic exposure at a given kV (quality), the product of the x-ray tube current (the "mA") and the time (in seconds) determines the amount (quantity) of x-rays emitted from the tube. The mA × time (in seconds) is commonly referred to as the mAS. A typical abdominal technique (250 speed system) for a medium-built adult male is 75 kV, 600 mA and 0.1 sec (60 mAS), and this would result in about 1.0 roentgen (R) of entrance exposure to the patient. If 600 mA were used for 10 minutes of fluoroscopy, the entrance exposure would be about 5900 R and would result in serious radiation injury to the patient. (In reality, the x-ray tube would fail even with a small fraction of such an exposure.) A fluoroscopic examination of this man may require around 3 mA (1/200th the radiographic

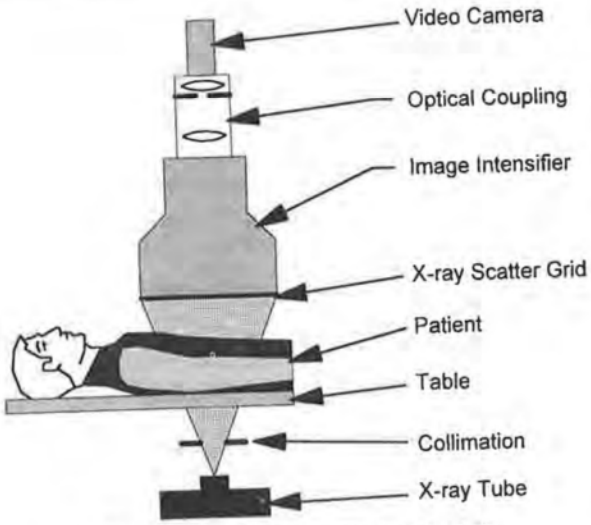



**Figure 7.1.** The fluoroscopic imaging chain

mA), and 10 minutes of fluoroscopy would result in about 30 R to the patient. The *exposure rate* in fluoroscopy is much less than in radiography, but the *total x-ray exposure* is usually a lot more because of the amount of time the fluoroscopic beam is on. The exposure rate in fluoroscopy is about 200 times lower than in radiography, and typically 30 images are produced every second. These facts tell us something already about fluoroscopic images and about the detector system. Relatively few x-ray photons are used in forming a single fluoroscopic image; consequently, fluoroscopic images are statistically inferior to radiographic images. In the comparison mentioned above, the radiographic image would be formed with 600 times more photons than the fluoroscopic image. The fluoroscopic system must produce an image bright enough for the radiologist to see but cannot use a lot of x-ray photons. Therefore, fluoroscopic systems must have a very high gain. In terms of absolute speed, fluoroscopic systems have speeds around 600,000 $R^{-1}$, corresponding to fluoroscopic exposure rates of 50 $\mu$R/second to the II and frame rates of 30 frames/second. Radiographic screen-film systems, by comparison, use *absolute* speeds on the order of 1000 $R^{-1}$.

The modern fluoroscopic imaging system (Fig. 7.1) consists of an x-ray system capable of continuous low mA output, an II, a video camera, and a tandem lens apparatus. Other components are often found attached to this basic system for added flexibility. Systems with x-ray tubes over the patient and IIs under the patient are also common. The collimator that limits the size of the x-ray beam is automatically adjusted to the proper field of view. When the source-to-detector distance is changed, as it often is when panning over anatomical regions of variable patient thickness, the collimator opens or closes to accommodate the differing

height of the II. The x-ray generator requires additional circuitry to operate in fluoroscopic mode. In many systems, a three-phase radiographic system may have single-phase fluoroscopic circuitry. The low mA used in fluoroscopy tends to smooth out the single-phase waveform via the capacitive influence of the cables. Additional electronics, known as the automatic brightness control, also distinguishes a radiographic/fluoroscopic x-ray generator from a generator designed only for radiography.

The fluoroscopic system accommodates a wide variety of modification and is the central component in many modalities, such as photospot imaging, spot film acquisition, digital subtraction angiography, endoscopic examination (e.g., bronchoscopy), lithotripsy, and cine-radiography. The R/F room (pronounced "R and F room") is also the most expensive system in the hospital for generating x-ray projection images. Unlike with screen-film radiography, CT, or MRI, the *radiologist* is the person who most frequently operates the fluoroscopic machinery. It is important to understand how these systems function and what parameters influence image quality to perform fluoroscopic examinations with expertise and confidence.

## REAL-TIME IMAGING

Dynamic studies require a real-time imaging device capable of displaying a sequence of events with enough temporal resolution (images per second) to determine a diagnosis. Temporal resolution is improved by acquiring images at a faster rate. A barium swallow is one example of a dynamic study, where the peristaltic movement of the esophagus is monitored as the patient swallows a liquid barium solution. Because the peristaltic motion in the esophagus occurs within a short time frame, a series of cut film images would not convey the temporal information necessary to determine normal esophageal function. The live display of the x-ray image made possible by fluoroscopic equipment does provide excellent temporal resolution. Dynamic studies are usually recorded on video tape recorders for playback and interpretation. In cardiology, cine film is commonly used for recording cardiac images. Cine cameras are attached to the II and record what is essentially high exposure rate fluoroscopy onto film at rates of up to 120 images per second.

## POSITIONING

Most fluoroscopic studies fall under the positioning category. In gastrointestinal and angiographic studies, fluoroscopy is used for guiding barium through the GI tract or catheters through the vascular system. In both situations, there is the intention of identifying diagnostic views for radiographic film acquisition. The radiographic application strongly influences the type of fluoroscopic equipment that is needed. Although smaller facilities may use one fluoroscopic system for a wide cross-section of procedures, larger hospitals have fluoroscopic suites dedicated to specific applications, such as GI/GU, cystography, peripheral vascular, cardiac, and neurovascular examinations.

## FLUOROSCOPIC EQUIPMENT

### Image Intensifier

The image intensifier is the cornerstone of modern fluoroscopy systems. Image intensifiers used in radiology convert the x-ray signal incident upon them in to visible light images. X-ray IIs are very similar in their design to night vision goggles used in night-time military activities. Night vision goggles amplify the sparse night-time ambient light to produce a bright image for the wearer. An x-ray II has an additional stage in front, where x-rays are converted to visible light, which is then amplified for the viewer.

Before IIs were invented in the 1950s, fluoroscopy was performed by viewing the live image produced when x-rays, transmitted through the patient, struck a thick intensifying screen. The room had to be completely dark so the faint glow of the screen could be seen, and the radiologist also needed to be dark-adapted. The pragmatic difficulties of dark adapting (which takes about 20 minutes), and of working in the dark led to the development of the II. With the old-fashioned screen-based fluoroscopy, a so-called *quantum sink* occurred between the x-ray absorption event and the radiologist's eye, resulting in wasted radiation dose to the patient. Of course, screen-based fluoroscopy was practiced in an era when the concerns about radiation dose to patient and radiologist were widely unappreciated. The notion of the quantum sink was discussed in Chapter 5 and is also mentioned later in this chapter.

### Anatomy of an Image Intensifier

A modern II is shown in Figure 7.2. There are four principal components of an II: (1) a vacuum bottle to keep the air out, (2) an input layer that converts the x-ray signal to electrons, (3) electronic lenses that focus the electrons, and (4) an output phosphor that converts the energy of the electrons bombarding it into visible light.

Although the job of keeping the air out and the vacuum in may appear rudimentary, the vacuum bottle in a modern II embodies significant

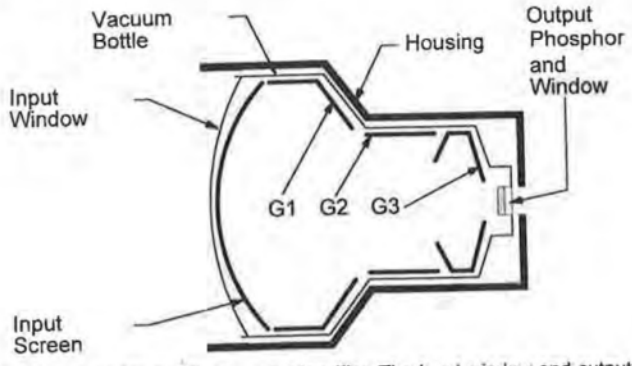



**Figure 7.2.** A diagram of the image intensifier. The input window and output window are part of the vacuum bottle. In newer IIs, the input window is metallic. The G1, G2 and G3 electrodes are part of the electronic focusing system.

technical development. It is the vacuum bottle that limits the size of the II. The input window of a large FOV (35 cm) II supports over a ton of force, from the air pressure pushing against it. The vacuum bottle is the cell membrane of the II; it is designed to regulate what passes in and out of its volume. In addition, as with the cell membrane, if its integrity is compromised, the system's viability ceases. Indeed, it is the breakdown of the vacuum inside the II that ultimately limits its lifetime—an important consideration given its high cost.

The input layer of the II consists of four different layers, as shown in Figure 7.3. The first layer is the input window, a thin (1-mm) aluminum (Al) window that is part of the vacuum bottle. The input window keeps the air out of the II, and its curvature is designed to withstand the force of the air pressing against it. The second layer that the x-ray beam strikes is the substrate layer, which is strong enough to support the phosphor and photocathode layers but thin enough to allow a very high percentage of the x-rays to pass through it. The substrate, commonly 0.5 mm of aluminum, is also the first layer in the electronic lens system. The input screen is the first component in the electronic lens system, and its curvature is crucial to accurate electronic focusing. Because the curvatures for optimally supporting the air pressure and for proper electronic focusing are different, the input window is not used as the substrate for the input phosphor.

After passing through the 1.0-mm thick Al input window and the 0.5-mm Al substrate, the x-rays strike the input phosphor, whose function is to absorb the x-rays and convert their energy into visible light. The input phosphor in an II serves the same purpose as the intensifying screen in screen-film radiographic systems. It also is subject to the same, classic compromise. It must be thick enough to absorb the majority of the incident x-rays, but thin enough not to degrade the spatial resolution of the system significantly. IIs offer a high vacuum environment that an x-ray cassette cannot, and therefore unique phosphor technology can be used. Virtually all modern IIs use cesium iodide (CsI) for the input phosphor. CsI could not be used in intensifying screens because it is very hygroscopic and would break down rapidly without the protection of the air-free, moisture-free environment of a vacuum. CsI has the unique property of forming in long, needle-like crystals, which are literally grown right onto the support layer (Fig. 7.4). The long, thin needles of CsI function as light pipes, channelling the visible light emitted within them by x-ray interaction toward the photocathode with minimal spreading. As a result, the CsI input phosphor can be quite thick but still maintain high resolution. The K-edges of cesium (36 keV) and iodine (33 keV) are well positioned with respect to the x-ray spectrum, and this fact helps contribute to a high x-ray absorption efficiency. The CsI crystals are approximately 400 $\mu$m tall and 5 $\mu$m in diameter. The needles form by vacuum evaporation of CsI onto the substrate, in a process that combines an artisan's know-how with high technology. For a 60-keV x-ray photon absorbed in the phosphor, approximately 3000 light photons (at about 420 nm wavelength) are emitted.

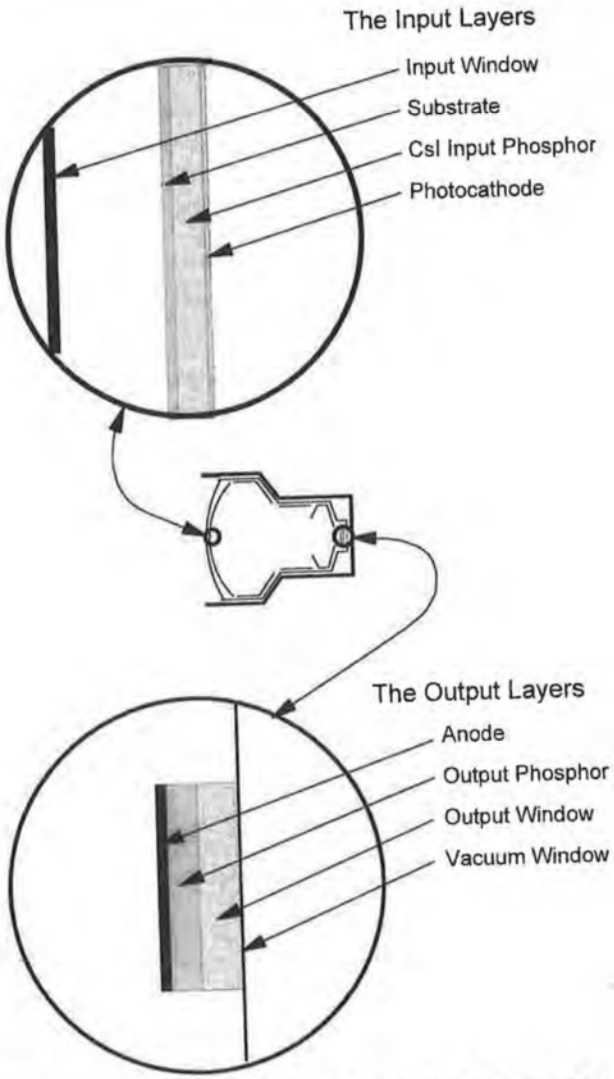



**Figure 7.3.** A diagram of the input and output layers in an II. INPUT: The input window is curved to optimally withstand the vacuum pressure, which for a large field of view II can be over a ton of force. The substrate/input phosphor/photocathode layers are curved to allow the best focusing of electrons. OUTPUT: The output layer consists of the anode, the output phosphor, and the output window.

The photocathode is a thin layer of antimony and alkali metals (such as $Sb_2S_3$) that releases electrons when struck by visible light. With a 10–20% conversion efficiency, approximately 400 electrons are released from the photocathode for each 60-keV x-ray photon absorbed in the phosphor.

The G1, G2, and G3 electrodes in Figure 7.2, along with the input screen substrate (the cathode) and the anode near the output phosphor

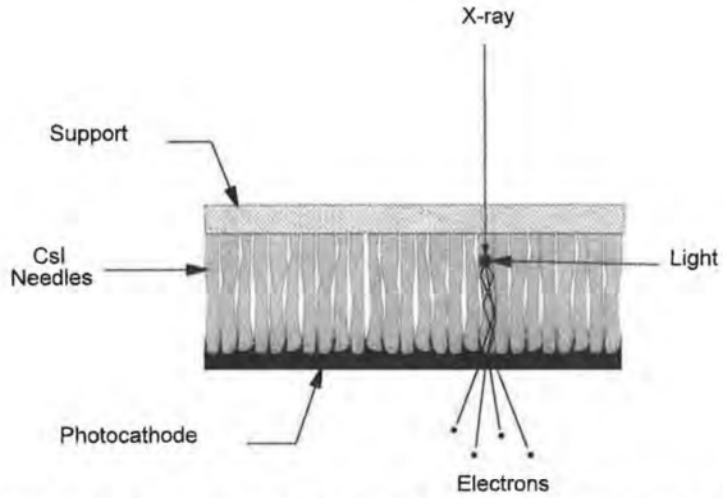



**Figure 7.4.** The energy conversion steps at the input phosphor. X-rays pass through the input window and substrate and are primarily absorbed by the input phosphor, which for modern IIs is CsI. The needle-like structure of the CsI phosphor acts to channel the light emitted within the needle to the photocathode with minimal lateral diffusion, preserving resolution. The photocathode emits electrons when struck by light photons.

comprise the pentode electronic lens system. The electronic lens system focuses the electrons that are emitted from the photocathode, and accelerates them to the output phosphor by a large electric potential of 25–35 kV. The operating potential within an II is similar to that used in producing x-rays in a mammographic system. The electrons are released from the photocathode with very little kinetic energy, but under the influence of the electric field they are accelerated toward the anode. The output phosphor is small (2.5 cm in diameter) relative to the input phosphor (23–35 cm in diameter), and hence the electron flux is highly amplified in the focusing process. To maintain an equal path length between all points on the input phosphor and the output phosphor, the input phosphor/photocathode layer must be curved. The amount of curvature is a function of the FOV and length of the II. To keep the length of the II to a minimum, greater curvature is needed, although this compromise results in unavoidable *pincushion distortion* of the image.

The output phosphor most widely used is P20, a zinc cadmium sulfide compound doped with silver. The emission spectrum of P20 is maximal around 530 nm (green light). Green light is toward the middle of the visible spectrum and is well matched to the sensitivity of many video camera target materials. The phosphor particles are very small (1–2 $\mu$m), and the output phosphor is quite thin (4–8 $\mu$m), to preserve high spatial resolution. There is a very thin (0.2-$\mu$m) coating of aluminum on the vacuum side of the P20 phosphor, which is electrically conductive to carry away the electrons once they deposit their energy in the phosphor. Each electron causes the emission of approximately 1000 light photons on the window side of the output phosphor.

The image is highly minified at the output phosphor, because a 23- to 35-cm diameter image (at the input phosphor) is mapped onto a circle with perhaps a 2.5-cm diameter (1-inch). To preserve a resolution of 5 line pairs per mm at the input plane, the output phosphor must deliver resolution in excess of 70 lp/mm. Put differently, a 100-$\mu$m resolution cell at the input plane maps to a 7-$\mu$m resolution cell at the output plane. This is why a very fine grain phosphor is required at the output phosphor. Because the granularity of the output phosphor can limit the overall resolution of an II, some exotic and expensive IIs are built with 5-cm diameter (2-inch) output phosphors to overcome this limitation and therefore deliver very high resolution.

The last stage in the II that the image signal passes through is the output window. The window is part of the vacuum bottle, and must be transparent to the emission of light from the output phosphor. The output phosphor is often coated right onto the output window. The glass output window can be the source of image problems, if not properly designed. A fraction of the light emitted from the output phosphor is reflected in the glass window, and is re-emitted as scattered light. This optical light scattering can lead to a reduction in image contrast and is called *veiling glare*. Some manufacturers have used fiber optic (light pipe) output windows that reduce veiling glare appreciably. The newest technology in output windows is a thick clear glass window. The thickness of the window (about 14 mm) requires internally reflected light to come in contact with one of the sides of the window, which are coated to scavenge the scattered light.

## Characteristics of an Image Intensifier

The function of the x-ray II is to convert an x-ray flux into a minified light image. There are several characteristics that describe how well the II performs its function. These parameters are useful in specifying the capabilities of the II and are also useful in troubleshooting IIs when they are not performing adequately.

### Conversion Factor

The conversion factor is a measurement of the gain of an II. The input to the II is an exposure rate, measured in mR/sec. The output of the II is luminance, measured in candela per meter squared. The conversion factor of an II is the light output per unit input:

$$\text{Conversion Factor} = (\text{light out of II [in Cd/m}^2\text{]}) \,/\, (\text{exposure rate into II [in mR/sec]}) \qquad (7.1)$$

In the units given above (Cd-sec/mR-m$^2$), the conversion factor of a new II ranges from 100 to 200. The conversion factor degrades with time and ultimately can lead to the need for replacement. In standard fluoroscopy, a conversion factor of 200 is entirely too great to be useful, and the gain is reduced, in effect, by throwing away some of the light emitted by the II. This will be discussed later.

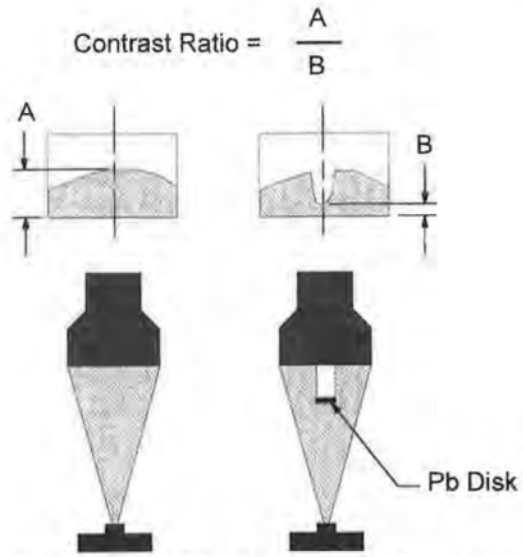


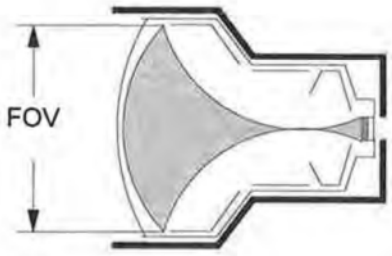

**Figure 7.5.** The contrast ratio (CR). The light output of the II is measured at a point near the center of the window, with nothing in the x-ray field. The value *A* results. A Pb disk is placed in the center of the field, and a value *B* is measured as the light output at the point corresponding to the center of the disk. The CR would be infinite for a perfect system (because $B \rightarrow 0$), but with real systems the CR runs between 15 and 30.

### Field of View / Magnification Modes

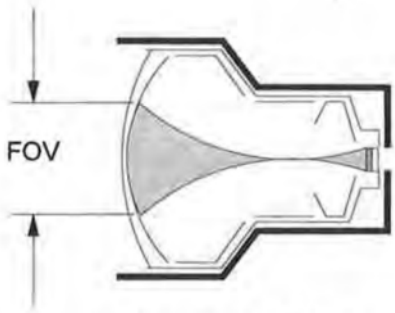
The field of view (FOV) is a specification of the size of the input phosphor of the II. The most common diameter of an II is 23 cm (9 inch); however, larger 30-cm (12-inch), 35-cm (14-inch), and even 40-cm (16-inch) IIs are available (at much higher cost). Large FOV IIs are very useful for examinations in which a large area of the patient's anatomy needs to be viewed, for instance in lower GI studies. A large FOV II allows more of the anatomy to be imaged simultaneously, resulting in less panning and potentially shorter studies. However, often it is necessary to focus in and magnify a selected region of the patient's anatomy. This can be accomplished on most IIs by changing the electric field in the electronic lens system so that a smaller region of the input phosphor is projected to the output phosphor (Fig. 7.6). The magnification mode is selected by pushing a button, and IIs with dual mode or trimode magnification are common. For instance, a trimode 23-cm (9-inch) II usually comes with 12- and 18-cm (5- and 7-inch) modes.

### Detected Quantum Efficiency

The detected quantum efficiency (DQE) is a parameter that relates the statistical quality of the signal at the output of the imaging system to the statistical quality of the x-ray signal incident on the imaging system. A DQE of 100% would be indicative of a perfect imaging system in terms of its noise performance. If the imaging system adds no additional noise




Normal Operation




Magnification Mode

**Figure 7.6.** Magnification with an II is achieved by applying different voltages to the electronic lens system. In magnification mode, only the electrons emitted from a smaller diameter circle are focused onto the output phosphor. Because a smaller portion of the image is blown up to the full output window, this results in a magnified image of the object.

to the signal, then the DQE will equal the absorption efficiency, also know as the quantum detection efficiency (QDE). In real imaging systems, where some additional noise is always present, the DQE will be from 50% to 80% of the QDE.

The DQE is a function of the x-ray spectrum used to measure it, but there is an attempt to standardize the measurement of this parameter. To reduce the variability caused by different x-ray spectra, a monoenergetic isotopic source, Am-241, which emits a 57.5-keV gamma ray, is used. Detectors with DQE values between 60% and 80% are commonly available. The advantages of a high DQE are lower noise images at the same exposure rate, or lower exposure rates for the same noise levels.

### Modulation Transfer Function and Limiting Spatial Resolution

The *spatial resolution* of the II is best described by a *modulation transfer function* (MTF) curve, which is a plot of the ability of the imaging system to display object contrast as a function of the size of the object. MTFs for fluoroscopic systems will be discussed in more detail below.

For convenience, the limiting resolution of the II may suffice. The limiting resolution is the highest spatial frequency on the MTF where the contrast transfer is still visible. The limiting resolution of modern IIs ranges between 4 and 5 lp/mm in 23-cm mode. Higher magnification modes (smaller fields of view) are capable of limiting resolutions up to 7 lp/mm. The limiting resolution is easily measured by imaging a line pair phantom using the system. This technique is subjective but is the most practical way of determining the resolution of IIs in the clinical setting.

## Artifacts Associated with an Image Intensifier

### Veiling Glare

*Veiling glare* is mainly the consequence of light scatter in the output window of the II. The scattered light, just like scattered radiation, adds to the background signal and reduces the contrast in the image. Veiling glare can be reduced by purchasing IIs with advanced output window designs. For a given II, not much can be done about the presence of veiling glare. The contrast ratio is a good way to quantify the magnitude of the problem.

### Pincushion Distortion

*Pincushion distortion* is a form of spatial distortion that warps the appearance of the image. It is a consequence of projecting the image formed on a curved input phosphor to a flat output phosphor. Pincushion distortion results in slightly higher magnification of the input image toward the edge of the image. The amount of pincushion distortion is usually determined by imaging a grid or screen with regular rectangular spacing. This is shown in Figure 7.7.

### Vignetting

The brightness as measured at the output phosphor will vary from the center to the periphery of the image, even when a homogeneous x-ray field is incident upon the II. The brightness will be the greatest toward the center of the image and will fall off at the edges. One source of

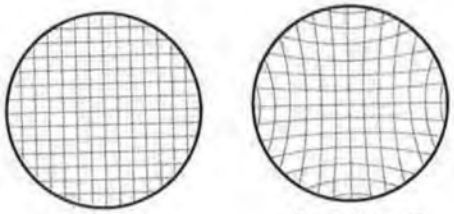



**Figure 7.7.** Pincushion distortion results because the input phosphor is curved but the output phosphor is flat. This results in a warped image, which bends straight lines inward. The pincushion distortion is exaggerated in the figure. Pincushion distortion is reduced when magnification modes are used.

vignetting is a consequence of pincushion distortion. With pincushion distortion, the image is magnified to a greater extent toward the periphery. This means the minifying, electron-concentrating effect of the electron optics is reduced at the periphery, causing less brightness there. Vignetting also occurs in the optical coupling between the II and recording devices, because of scattered light effects.

#### S Distortion

The *S distortion* is a spatial warping of the image along an S-shaped axis through the image. This type of distortion is usually subtle, if present, and can be obscured by the more obvious pincushion distortion. S distortion is the result of stray magnetic fields. On fluoroscopic systems capable of rotation, the S distortion can change its position or its severity because of the change in orientation of the earth's magnetic field relative to the II when the II is moved. Whenever electrons are accelerated, especially through large distances as in an II, their trajectories can be disturbed by a magnetic field.

### Optical Coupling

#### Distribution Mechanism

The connection between the II and the closed-circuit TV camera requires a pair of optical lenses for focusing the light emitted by the output phosphor onto the TV camera target. For simple fluoroscopy systems, the optical coupling between II and the TV camera consists of a light-tight enclosure with two permanently mounted lenses. A light-limiting diaphragm (aperture) between the lenses is also required. For fluoroscopic systems that have additional imaging capabilities, often a light distribution mechanism is required. The optical distributor (Fig. 7.8) has several ports to provide a mounting area for an accessory device. An optical distributor usually consists of a prism or mirror that can be moved inside the light-tight housing and that serves to momentarily redirect the optical image toward a spot film camera, a cine camera, or some other imaging accessory. The mirror in some optical distributors is only partially silvered, and therefore reflects only a portion of the light in one direction and the remainder passes through the mirror. This is called a *beam splitter*. Beam splitters allow two recording devices to operate simultaneously. Beam splitters have the advantage of distributing the light without requiring the expense of a motor driven moving part. The various types of imaging systems that can be mounted on the optical distributor will be discussed later.

#### Aperture Effect on Dose Rate and Image Noise

The light-limiting aperture in the optical coupling has a very important influence on the fluoroscopic image quality. IIs are very efficient at converting the incident x-ray flux into light; they have very high gains, which are not readily adjustable. If there were no way to reduce the light output of the II, only a very low exposure rate could be used because higher

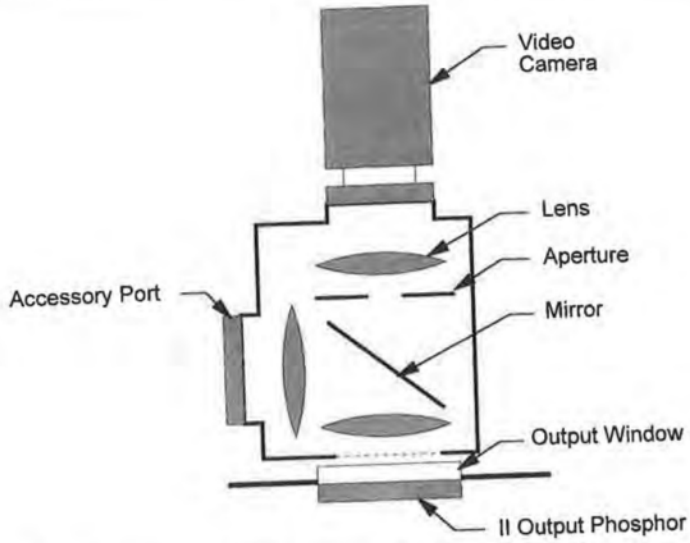



**Figure 7.8.** The light-tight optical distributor. The mirror can flip into the light path to momentarily redirect the light output from the II to an imaging device mounted onto the accessory port. Sometimes, partially silvered mirrors are used, called beam splitters, and send the light output from the II to two different ports simultaneously.

exposure rates would result in images too bright to be handled by the TV camera. With very low exposure rates, so few x-ray photons would be used in forming the fluoroscopic image that they would be unusable. The aperture, which is positioned between the two lenses, cuts down the amount of light between the II and TV camera, and thereby reduces the gain of the system. This means that more x-ray photons (a higher exposure rate) can be used. The aperture can be easily adjusted, similar to those used on the 35-mm cameras used in photography. The ease of adjustment of the aperture makes it a simple matter to change the speed of the system and thus the statistical quality of the image. The compromise in this situation is that of radiation exposure to the patient versus image quality. A wide open aperture (a low f-stop number such as f/1.2) will allow much of the light through the lenses, resulting in low exposure rates (and low dose rates), but the fluoroscopic image will be noisy. A small aperture (an f-stop number such as f/11) will drastically reduce the amount of light reaching the TV camera, requiring a higher exposure rate (high dose rate) but will render a fluoroscopic image with less apparent noise. The f numbers are proportional to the aperture diameters, but the light that corresponds to the f number is proportional to the aperture area. Consequently, changing from f/11 to f/1.2 will increase the optical gain by a factor of $(11/1.2)^2 = 84$.

### Video Cameras

Modern fluoroscopy systems use a closed-circuit TV system for viewing the output of the II. Viewing the output of the II directly requires an

additional mirror/optics viewing port. Instead, a video camera mounted to the optical distributor receives the optical image from the II. The image is transmitted to a video monitor, also called a *cathode ray tube* (CRT), for viewing by the radiologist.

There are advantages and disadvantages of using a closed-circuit TV system. The disadvantage of the TV chain, aside from its additional cost, is that the resolution of the TV system over the imaged FOV is significantly lower than that of the II: TV is the weak link in the imaging chain when it comes to spatial resolution. In most radiological procedures, the fluoroscopic image viewed from the video monitor is used for positioning; diagnostic images are acquired on film or spot film. Used in this manner, the resolution constraints of the TV do not affect the quality of the diagnosis.

The advantages of TV are numerous. The TV monitor is stationary, even when the II is moved. Therefore, the radiologist can focus her gaze on the stationary monitor, even while panning the II. The monitor is much larger than the output phosphor of the II, and therefore can be viewed from a considerable distance. Numerous monitors can simultaneously display the fluoroscopic image, allowing personnel at various stations in the room to observe the study. This is important in any teaching environment, and is in fact helpful whenever several people are involved in a study. The TV signal can easily be recorded by using a video tape recorder. Also, by displaying the image away from its source at the output phosphor of the II, the radiologist does not need to crowd the II and can perform the study at arm's length, reducing his or her radiation exposure.

The television system consists of a TV camera, the TV monitor, and associated electronics called a *camera control unit* (CCU). A television camera converts a two-dimensional image into a voltage-versus-time signal for transmission along the video cable. The TV monitor receives the one-dimensional signal from the video cable and converts it back into a two-dimensional picture. Inside the TV camera, there is a photoconductive target that is scanned in raster fashion (Fig. 7.9) by a beam of electrons. In bright areas of the image, the target is more conductive (less resistance), and in dark areas of the image, the target is less conductive (more resistance). When a tiny area of the target is scanned by the electron beam, the number of electrons that pass through the target to a signal collection plate depends on the conductivity in that tiny area. The video signal at any point in the image is therefore governed by the amount of light striking that location. The current (flow rate of electrons) reaching the signal plate is converted to voltage (an electric potential) by subsequent electronics. In this manner, the two-dimensional pattern of light striking the TV camera target is converted to a one-dimensional voltage-versus-time signal.

The voltage-versus-time video signal is converted back into a picture in the TV monitor. The TV monitor is a vacuum chamber in which a scanning electron beam strikes a phosphor that is coated onto the display screen. The amount of electrons in the scanning beam (beam current) determines the brightness of the displayed picture at any given point in

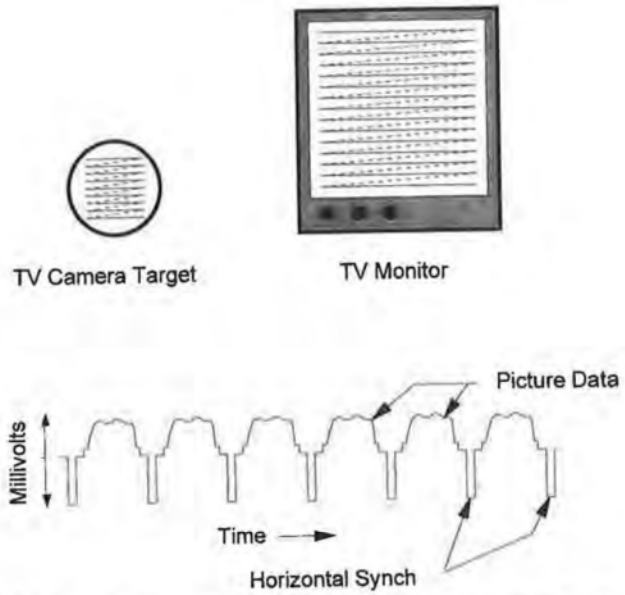



**Figure 7.9.** Video signal. An electron beam scans a raster pattern on the TV camera target. The video signal is generated where the voltage signal at a given location is proportional to the amount of light shining onto the TV camera target at that location. This is transmitted in a one-dimensional voltage-versus-time video signal to the TV monitor, where the video signal is converted into a two-dimensional light image by an electron beam scanning a phosphor in the TV monitor. The raster scanning pattern is synchronized between the camera and the monitor by synch pulses in the video signal (horizontal synch pulse are shown in the video signal).

the image. The electron beam current is modulated by the video signal voltage, and therefore the light striking the TV camera target is recreated on the TV monitor.

The rectilinear scan is composed of a number of individual scan vertical lines, and the number of TV lines that is used will clearly influence the resolution of the TV system. The lines are, by convention, scanned horizontally, and the standard TV signal used in North America uses a total of 525 lines (Fig. 7.10). The vertical resolution (top to bottom) of the TV image is governed by the number of scan lines. The TV image is produced horizontally along each line by the scanning motion of the electron beam. The resolution in the horizontal direction of the TV image is influenced by how rapidly the television electronics can generate (in the camera) and respond to (in the monitor and associated electronics) a change in the video signal voltage. If low quality, slow electronics are used, the brightness along each scan line will change slowly, and the spatial resolution in the horizontal direction will be poor. Conversely, fast electronics will produce high horizontal resolution. In the vernacular of electronics, the speed of the electronics is called the *bandwidth*. Higher bandwidth systems are faster and produce images with better horizontal resolution than lower bandwidth systems.

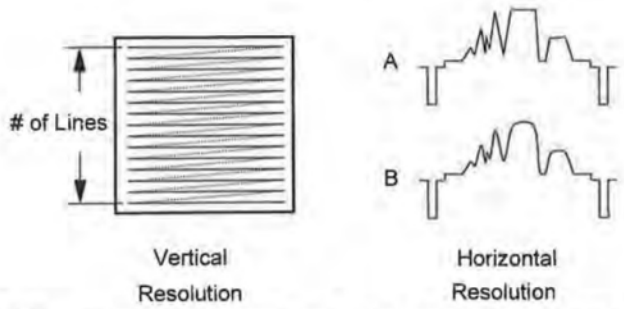



**Figure 7.10.** The resolution in the vertical direction of the image depends on the number of usable lines the TV system utilizes. For 525 line TV systems, some lines are not utilized because of the retrace time and other factors, thus resulting in only about 340 useful TV lines. The limiting vertical resolution is easily calculated as the number of line pairs (there are 170 line pairs in 340 lines) divided by the diameter of the FOV (measured in mm). The horizontal resolution depends on the bandwidth of the electronics in the camera. For systems with high bandwidth, the signal responds quickly to different light intensities across the TV camera target, resulting in a sharp image (**A**). If slow electronics limit the response of the signal (low bandwidth), the edges in particular are rounded off resulting in lower resolution, blurred images (**B**).

The RS-170 standard used for closed circuit black-and-white television in North America uses 30 images ("frames") per second. The frames are produced using an interlaced scan, which means that each frame is transmitted in two halves ("fields"). Because each frame requires ⅓₀ of a second, the two fields that comprise one frame each require ⅙₀th of a second. The odd TV lines (the odd field) are produced in ⅙₀th second, and the even lines (the even field) are produced in the next ⅙₀th second. The TV signal uses interlaced scanning to avoid image flicker. If a sequence of television or cinematography images is displayed too slowly, the human eye will detect a choppy sequence of images instead of a smooth transition from one frame to the next. The frame rate necessary to avoid the perception of flicker is about 45–50 frames per second. Because the image is updated every ⅙₀th of a second in interlaced scanning, flicker is not apparent. This trickery allows the image to be updated 60 times per second but requires only the bandwidth to convey 30 frames of new information per second. Interlaced scanning is an expedient forced by the slower bandwidth electronics that were available when television was being developed. With interlaced scanning, a problem arises when there is a bright horizontal structure in the image. In some cases, the bright line in the image will only occur (for example) in the odd field, and not in the even. In this case, the horizontal line will turn on and off 30 times per second, i.e., at a rate lower than the flicker threshold. Newer noninterlaced TV signals are much preferred over interlaced scanning for this reason. Noninterlaced scan formats are also called *progressive scan* in radiology. Noninterlaced scanning is used in most personal computer displays, which are essentially closed-circuit TV systems where computer memory replaces the video camera.

Television was developed before the invention of the electronic transistor. The electronics revolution of the past decades has made possible

vast improvements in television technology; however, to deliver these improvements the characteristics of the TV signal need to be changed. In broadcast television, changing the TV signal would make hundreds of millions of TVs obsolete in North America alone. However, for closed-circuit TV systems like those used in fluoroscopy, newer TV technology can be used. In North America, a 1023 line ("high line rate") standard has emerged, and newer fluoroscopy systems often use this technology (usually an option when buying new fluoroscopic systems). Some equipment vendors use their own custom standards, but it is difficult to find accessories such as video tape recorders and additional TV monitors for nonstandard TV formats.

Television cameras are available with a variety of different photoconductors as targets, and the target material will affect the camera's imaging performance. The venerable vidicon uses an antimony trisulfide ($Sb_2S_3$) target material. The photoelectrical characteristics of $Sb_2S_3$ result in a fair amount of *image lag,* which means that each new TV image actually contains residual image information from the last several frames. Lag is good and bad. When there is rapid motion in the sequence of images, lag tends to smear bright objects across the image. A rapidly moving bright spot on the image will leave a trail behind it, much like a comet. Thus, in applications where a rapid sequence of change occurs, lag is detrimental. For a slowly moving sequence of events, however, lag acts to smooth the quantum noise in the image. Less noise is apparent with laggy cameras, and this can be a true benefit in fluoroscopy, where the images are inherently noisy. TV cameras with targets made of lead oxide (PbO) are called *plumbicons,* and this material has low-lag characteristics. Plumbicons are often used as the video source in digital subtraction angiography, because in this application lag is detrimental. There is a wide selection of TV target materials available in addition to $Sb_2S_3$ and PbO.

There have been recent advancements in TV camera technology, where instead of scanning electron beams that sweep a photoconductive target, the target itself is composed of a large array of discrete light-sensitive elements. These *charge coupled device* (CCD) cameras are essentially computer chips with a large array (e.g., $512 \times 512$) of photosensitive pixels. The image is not formed by a scanning electron beam but rather by reading out each of the pixels in a manner not unlike how a computer reads its internal memory. CCD cameras are extremely rugged and are the principal technology presently used in home video cameras. They are not influenced by magnetic fields as conventional television cameras can be. CCD technology will undoubtedly impact fluoroscopic imaging systems in the near future. Because CCD cameras have very low lag properties, other means of producing lag may be necessary to achieve low noise fluoroscopic images. Lag can be produced with digital images by a computer, or by using phosphors in the TV monitor which have long persistence.

Television technology is presently experiencing rapid development, as many companies and countries are vying to develop high definition

television (HDTV) systems for broadcast television. Fluoroscopic TV systems may ultimately benefit from these developments.

### Automatic Brightness Control

The exposure rate in modern fluoroscopic systems is controlled automatically. The purpose of the *automatic brightness control* (ABC) is to keep the brightness of the image constant at the monitor. It does this by regulating the x-ray exposure rate incident on the input phosphor of the II; the goal of the ABC is to keep the luminance at the output phosphor relatively constant. When the II is panned from a thin to a thick region of the patient, the thicker region attenuates more of the x-rays, so fewer x-rays strike the II. The system senses the reduction in light output from the II and sends a signal to the x-ray generator to increase either the mA, the kV, or both. What tells the generator to increase or decrease the exposure rate? Fluoroscopic systems use one of two methods for sensing the light output from the II. Some systems use a light-sensitive device called a *photodiode,* which is permanently positioned near the output window of the II. Other systems use the signal generated by the video camera as a measure of the light output of the II. The video signal is summed up in a circular region in the center of the image. The size of the integration circle can be adjusted by the service personnel. Whichever technique is used, the amplitude of this signal is conveyed electrically to the generator and is used to regulate the mA or kV supplied to the x-ray tube.

The fluoroscopic ABC circuitry in the x-ray generator is capable of changing the mA and the kV. Any particular generator changes the mA and the kV in a predetermined sequence; however, this sequence varies with different brands of generators. When the kV increases, the subject contrast decreases because of the physics governing x-ray absorption. Therefore, to maintain high contrast, the mA is often increased when imaging conditions call for an increase in the number of photons striking the II. The mA can be increased only so far, and once this point is reached, the system will then increase the kV to increase the penetration of x-rays through the patient. Increasing the mA first, and the kV second, will result in high contrast images with more dose to the patient. If the kV is driven first, and mA second, the contrast will suffer but the dose to the patient will be reduced. Some systems drive the mA and the kV together. A few older fluoroscopic systems may be found with only manual controls for the mA and kV. Manual override of the ABC system is available in many systems. The manual overide feature can be helpful in some imaging situations.

## FLUOROSCOPIC EQUIPMENT SUMMARY

The fluoroscopic imaging system plays a very important role in the radiology department. Knowing the physical characteristics of fluoroscopic systems is important to radiologists, because they are the individuals who use them. The fluoroscopic image is generated by a series of subcom-

ponents, and the term *imaging chain* is descriptive of the II/TV camera system. There are two principal configurations that a fluoroscopic system can assume. For GI work, the R/F room consists of a large table that can be rotated from horizontal to vertical to put the patient in a head-down or head-up position. The II can be either over or under the table. The table has large cowlings under it, hiding the x-ray tube or the II. The table usually will have a Bucky tray in it, to be used with an overhead x-ray tube, mounted on a ceiling crane. A spot film device or photospot camera often accompanies this table configuration. In the angiographic setting, the table does not rotate but rather floats. The fluoroscopic system is typically mounted on a C-arm or U-arm apparatus, which can be rotated and skewed, and these motions provide considerable flexibility in providing standard and oblique projections.

The fluoroscopic imaging chain allows the adjustment of the exposure rate used in producing images, by manipulation of the aperture in the optical stage between the II and TV camera. This flexibility does not exist for screen-film radiography, where the speed of the detector system is fixed. In this respect, the II/TV system can illustrate the trade-offs between quantum noise and patient dose. Ten minutes with a block of Lucite as an object, and access to the aperture control on the fluoroscopic system, would provide the radiologist-in-training a valuable lesson in quantum noise.

Continuous, low mA fluoroscopic systems acquire images at 30 frames per second, and so the acquisition time for each image is 33 msec. For some applications, 33 msec is long enough to cause significant blurring of the images caused by patient motion. Instead of a low-mA continuous operation, pulsed fluoroscopic systems pulse the x-ray tube in synchrony with the TV camera acquisition. Images are presented at 30 frames per second, but the acquisition time per image is perhaps 5 ms, and motion blurring is far less of a problem. The human visual system has some lag to it. This means that when fluoroscopic images are displayed live, about 6 images (0.2-sec lag $\times$ 30 frames/sec) are integrated by the human eye. Therefore, the image quality of live fluoroscopic images is improved by the effect of a sliding average of the last 6 images displayed. The eye perceives the contribution of all the radiation used in the last 6 images and increases the effective signal-to-noise performance by about 2.5 ($\sqrt{6}$). The live display of cine film has the same result. This is why the noise in a freeze-frame image looks worse than in the live display of an imaging sequence.

Figure 7.11. illustrates the resolution of the various components of the fluoroscopic system. Also shown are the MTFs of the various stages of the system. The resolution of the poorest component in the imaging chain dominates the resolution of the system as a whole. In this sense, the imaging chain suffers the resolution of the weakest link in the chain.

The maximal exposure rate to the patient permitted in the United States is governed by Federal regulations, under the auspices of the Center for Devices and Radiological Health, a branch of the Food and Drug Administration. The maximal legal entrance exposure rate for normal fluoroscopy to the patient is 10 R/min. This regulation applies to fluoro-

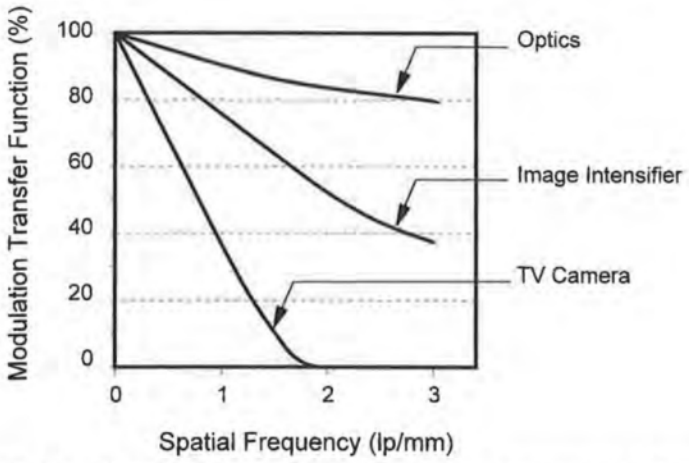



**Figure 7.11.** Modulation Transfer Function (MTF) of several components in fluoroscopy. The MTF for a 525-line TV system with a 23-cm FOV II is shown. For the fluoroscopic image viewed on the monitor, the TV system is the resolution-limiting subcomponent in the imaging chain. Diagnostic images acquired through cine film or photospot film do not use the TV system, and therefore enjoy the full resolution of the II.

scopic equipment manufacturers. Most state health departments have identical regulations that are imposed on hospitals and private offices. Typical entrance exposure rates for fluoroscopic imaging are about 1.5 R/min for thin (10-cm) body parts and 3–5 R/min for the average patient. Heavy patients will require 8–10 R/min. Fluoroscopic examinations are the largest contributor of medical radiation exposure to the U.S. population, far exceeding the exposure due to radiography or computed tomography.

## QUANTUM SINK

A signal such as a fluoroscopic image passes through many stages in its formation. The stage where the fewest number of information carriers is used will be the weakest point in terms of the noise. In fluoroscopy, there are numerous stages in which the signal passes. The x-rays are absorbed, and their energy is converted to light (input phosphor), to electrons (photocathode), back to light (output phosphor), back into electrons (TV camera), and then back into light again (TV monitor). The number of quanta (discrete information carriers) used at each stage in the signal can be illustrated diagrammatically (Fig. 7.12). The *quantum sink* is the point in the imaging chain where the fewest number of quanta are used to convey the signal.

A design goal for all medical imaging devices that use x-rays is that the system have the quantum sink at the stage where the x-rays are absorbed in the detector. If a quantum sink occurs after the x-ray detection stage, the noise in the system will not be dictated by the number of x-rays used in forming the image, but by the noise in some component (the stage where the quantum sink occurs) in the imaging system. This

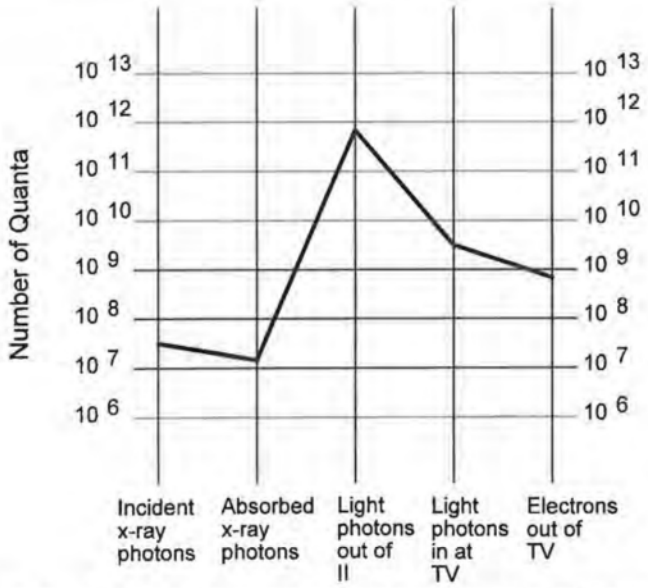



**Figure 7.12.** A quantum sink diagram for fluoroscopy representing an exposure rate of 50 $\mu$R/s at the input surface of the II. Higher exposure rates would simply shift the curve up. The quantum sink occurs at the point where the least number of information carriers conveys the image signal. For image intensified fluoroscopy, this occurs at the absorption of the x-ray quanta.

implies that detected x-ray quanta are being wasted, and the patient is receiving radiation exposure that does not contribute to the image quality. Because ionizing radiation has a small but finite risk of causing cancer, wasting exposure because of poor equipment design is considered inappropriate and unethical.

## OTHER IMAGE INTENSIFIER BASED IMAGING SYSTEMS

### Photospot Cameras

A photospot camera can be used to generate film images, taken from the output of the II. The most common formats are 100-mm cut film, or 105-mm roll film. Spot film cameras are convenient; if the radiologist wants to archive an image during the fluoroscopic examination, he or she simply steps on a floor pedal. The mirror in the optical distributor swings into the optical path, redirecting light rays toward the spot film camera. The x-ray generator produces a radiographic pulse of x-rays, and the image is recorded on film. The film is advanced and stored in a take-up magazine. Photospot images are made directly from the output phosphor of the II, through lenses, and therefore enjoy the full resolution of the II systems, unencumbered by the video system. The speed of the photospot images is determined by the aperture setting on the photospot camera

itself. An entrance exposure to the II of 75 to 100 $\mu$R/frame is typically required for an II operating with a 23-cm (9-inch) FOV.

### Digital Photospot

Digital photospot cameras are high-resolution, slow-scan TV cameras in which the TV signal is digitized and stored in computer memory. The contents of the computer memory can be instantly displayed on a TV monitor, and therefore can be viewed without the time delay caused by film processing required in conventional photospot acquisition. Digital photospot cameras are typically 1023 line TV cameras. The TV target is exposed by the light emitted from the II, produced from a short radiographic pulse of x-rays, in the same manner and with the same exposure that conventional photospot images are acquired. The TV target is scanned by the electron beam slowly (often using four conventional frame times, for a total of 0.133 seconds), easing the bandwidth restrictions of the camera electronics. An analog-to-digital convertor converts the voltage signal into a series of digital numbers stored in computer memory, and the contents of the computer memory can be displayed on the TV monitor. Hardcopy images can be produced using multiformat cameras (or laser imagers), which are commonly used to produce film images from computerized sources such as CT, MRI, and DSA. Although the spatial resolution is less than a 100-mm film, the rapid display and image processing capabilities enable a flexibility that is worth the slightly inferior spatial resolution.

### Spot-Film Devices

A spot-film device is an apparatus that attaches to the front end of the II and can automatically acquire images on a radiographic screen-film cassette by a simple press of a button. There is a small control panel on the attachment, which enables the radiologist to acquire a radiographic image using the spot-film device. The spot-film device has a transport mechanism which, when an image is called for, moves a screen-film cassette from a parked position to a position directly in front of the II. Newer systems automatically collimate to a variety of formats. For example, one 30-cm $\times$ 30-cm cassette can be exposed with four different 15-cm $\times$ 15-cm radiographic images. Although quite heavy and cumbersome, spot-film devices are convenient when large FOV images are routinely required as in GI studies. The spot-film device allows the acquisition of radiographic screen film images. The fluoroscopic system participates in the positioning for the radiograph, but the II is not used to acquire the image. Because screen-film systems deliver substantially more spatial resolution that an II, there is an important distinction between photospot cameras, which do use the II, and spot-film devices, which do not.

### Cine-Radiography

A cine camera attaches to a port on the optical distributor of an II and can record a very rapid sequence of images on 35-mm film. Cine is used frequently in cardiac studies, where a very high frame rate is needed to

capture the rapid motion of the heart. The frame rates of cine cameras run from 30 frames/sec to 120 frames/sec or higher. Cine radiography uses very short radiographic pulses, and therefore special generators are needed. The x-ray tube loading is usually quite high, and so large anode, high heat capacity x-ray tubes usually accompany the other necessary cine hardware. An entrance exposure to the input phosphor of approximately 10 to 15 $\mu$R/frame (23-cm diameter) is used for cine-radiography studies.

# ADJUNCTS TO RADIOGRAPHIC IMAGING




## STEREO RADIOGRAPHY

Stereo radiography is sometimes used to enhance the radiologist's perception of the three-dimensional anatomy of the patient. Before computers were commonplace, stereo pairs of radiographs were manually acquired, and either the radiologist learned to look at the stereo pair "cross-eyed," or viewed the stereo images with a stereoscopic viewer. The widespread historical interest in stereo radiography was perhaps a result of the widespread interest in stereo photography in the early decades of the century. Stereo photography was popular in the 1930s, and stereo pictures of such famous scenery as Yellowstone National Park could be purchased and viewed using inexpensive stereo viewers. Stereo radiography came of age in an era when the risks of ionizing radiation were not fully understood. Of course, the two views required for stereo radiography essentially doubled the radiation dose to the patient.

Although the fanfare surrounding stereo radiography has subsided, there remains a small but committed group of radiologists who still routinely use stereo radiography. The applications for stereo radiography include cranial, chest, knee, and spinal radiography. Stereo radiography was in fairly common usage up until the early 1960s in many parts of the country. Tomographic techniques, such as CT, ultrasound, and MRI, have reduced the need for stereo, because the three-dimensional anatomy can be studied slice by slice with these techniques.

### Depth Perception, Monocular Clues

Humans are visual animals, and depth perception is something that most humans experience as part of life. Individuals without the use of one eye, however, have to adapt to modern living without the benefit of true depth perception. Instead, these individuals rely on other visual clues that are monocular in nature but omnipresent in the human experience. Indeed, monocular signs yield considerable information to all two-eyed creatures. Monocular visual clues include shadowing, which gives three-dimensional relief more vivid texture. On dull, cloudy days it is much more difficult to ski on moguls (mounds in the snow), where the flat lighting

eliminates shadows and makes visualization of the uneven terrain difficult. Objects that are more distant look smaller. Automobile mirrors that minify objects are often labeled with warnings to this effect so the unwary driver does not misjudge distances. Closer objects block out ones that are further away. The net on a basketball hoop serves as foreground for a ball passing through the hoop, but as background for an "air-ball." The basketball net increases the accuracy of judging whether the basketball has passed through the hoop. Haze or smoke in the air provides a sense of foreground for distance objects. Although haze is relatively transparent, it becomes less so as the light path between the object and the viewer increases in length. There are also motion clues to depth perception. In a moving automobile, closer objects pass by the window much faster than objects that are further away. These are all examples of monocular clues that contribute to depth perception. Monocular clues are as important as binocular clues. The success of television, a strictly monocular medium, is testimony to the importance of monocular clues in our interpretation of the visual surroundings.

### Binocular Clues

Binocular visual clues are realized when two slightly different, discrepant images are viewed simultaneously with each eye. Nature hints at the importance of binocular vision in terms of survival. It is difficult to think of any animal that has just one eye, although some animals have limited overlap in their visual fields (e.g., whales, pigeons). The image seen by each eye is slightly different because the spacing between the eyes causes *parallax*, a change in observational position that provides a new line of sight (Webster). If you hold two fingers up at an angle to your face, and close each eye alternately, the apparent spacing between fingers changes between the two fingers. This is of course due to parallax. The brain uses the parallax between *discrepant images* to create a three-dimensional impression of the scene, in a process we routinely experience.

### Making Stereo Pairs

Stereo imagery is acquired using either two imaging systems simultaneously or by shifting a single imaging system laterally. The rule of thumb for acquiring stereoscopic views is that the x-ray tube shift should be about 10% of the source-to-image distance (SID) between views. For typical 100-cm SIDs, the tube shift would be about 10 cm. This amount of shift translates to an angular shift of 5.7° between images. The amount of shift has little to do with the spacing between one's eyes. The amount of parallax between the images as presented to each eye changes with the distance from which the object is viewed, and consequently we are able to compensate easily for a wide variety of parallax angles. As objects get very far away, the angular shift afforded by eye separation becomes very small and the stereo effect is lost. To increase stereo clues at a distance, aerial stereo imagery (used in making topographic maps) is acquired with very large (hundreds of meters) separation between stereo pairs.

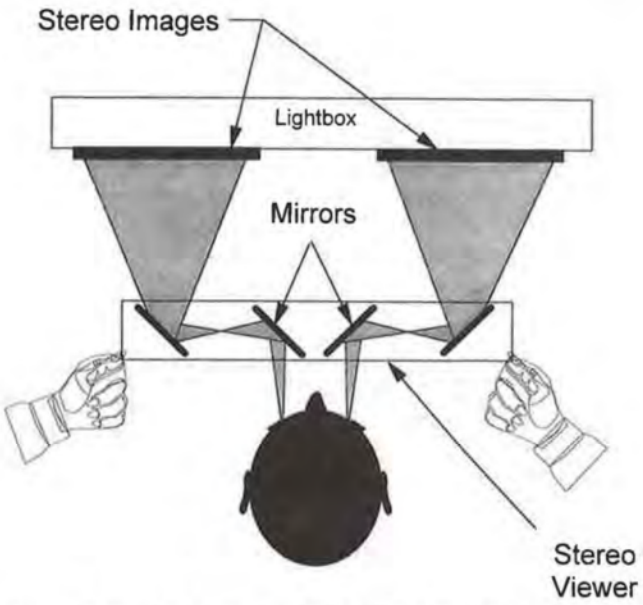



**Figure 8.1.** An example of how a hand-held stereo viewer is used. The use of mirrors allows the viewer to maintain a convergence angle consistent with the accommodation distance, so crossing one's eyes is not necessary. The films need to be mounted on the light box oriented in a position consistent with how they were acquired, for proper stereo fusion.

### Viewing Film Stereo Pairs

A stereo viewer is an apparatus designed to make reading stereo radiographs fairly easy. The stereo viewer uses mirrors to project the radiographic images to each eye (Fig. 8.1). It is possible to fuse a stereo pair without the aid of a stereo viewer; however, this requires crossing the eyes, which can be uncomfortable. The eye muscles that control focusing (accommodation) are accustomed to working in synchrony with those that control the relative alignment of the eyes (convergence). To view stereo images without a stereo viewer, accommodation and convergence need to be consciously decoupled.

### Viewing Electronic Stereo Images

With the advent of modern technological advancements, stereo has enjoyed some resurgence in popularity in certain niches of radiology. Stereo fluoroscopic systems are available that use dual focal spots (separated laterally in the x-ray tube) in pulsed operation. Stereo pairs of digital images can be shown on a video monitor quite easily. The image displayed on a monitor can be switched back and forth between the two stereo images very rapidly. Electronic eyeglasses are available that block the left eye when the right image of the stereo pair is displayed on the monitor, and then block the right eye when the left image is displayed.

The electronic shutters in the eyeglasses use liquid crystal display technology, similar to digital watches and calculator displays. The whole process occurs fast enough to avoid the perception of image flicker. To add to the three-dimensional "realism," the fluoroscopic system can be rotated around the patient while the sequence of stereo images is acquired in real time. Images stored on the computer can be played back, and, in addition to the depth perception afforded by the stereo imagery, the rotation (or a rocking motion) of the anatomy contributes to the interpretation of complex anatomy. This technology is a spin-off from other scientific fields such as molecular modeling.

### Three-Dimensional Rendering from Tomographic Data

Although not strictly stereoscopy, three-dimensional rendering of medical imagery has received much recent interest. These systems use computers to render images with computer-generated monocular clues for depth perception, including shading computed from single or multiple light sources, haze, motion clues, and others. Dedicated workstations for performing the 3-D reconstructions from tomographic image sources such as CT and MRI are available from many vendors. Some systems have 3-D joysticks, which allow the user to interact with the three-dimensional data. The computer can render pairs of images, with slightly different orientations, thereby generating stereo pairs. The stereo pairs can be displayed using electronic stereo display technology, mentioned previously. This technology has been applied primarily to bony structures, such as the cranium and the cervical spine. Although these images may not be of sufficient resolution for radiological diagnosis, they do in many instances provide useful information for referring physicians. Three-dimensionally rendered images are particularly popular among maxillofacial and orthopaedic surgeons.

## CONVENTIONAL TOMOGRAPHY

### Description of Technique

Conventional tomography, also called body tomography or geometrical tomography, makes use of the blurring effects of motion to create planar tomographic images. Conventional tomography predates computed tomography by many decades and is a cost-effective approach to tomographic imaging in some radiological applications. In *computed* tomography, the patient's anatomy outside the plane of interest is *eliminated* from the image by collimation of the x-ray beam. In *conventional* tomography, the patient's anatomy above and below the plane of interest is *not* eliminated from the images but rather is blurred. The blurring of off-axis information is achieved by moving the x-ray tube and the film during the acquisition. The motion occurs around a geometrical pivot point between the x-ray tube and the film cassette. The location of the pivot point determines the plane of focus, as shown in Figure 8.2. The concept of *slice thickness* is somewhat of a misnomer in conventional tomography. Only the thin, central plane that is precisely at the level of the fulcrum is in focus; the image information in the planes above and

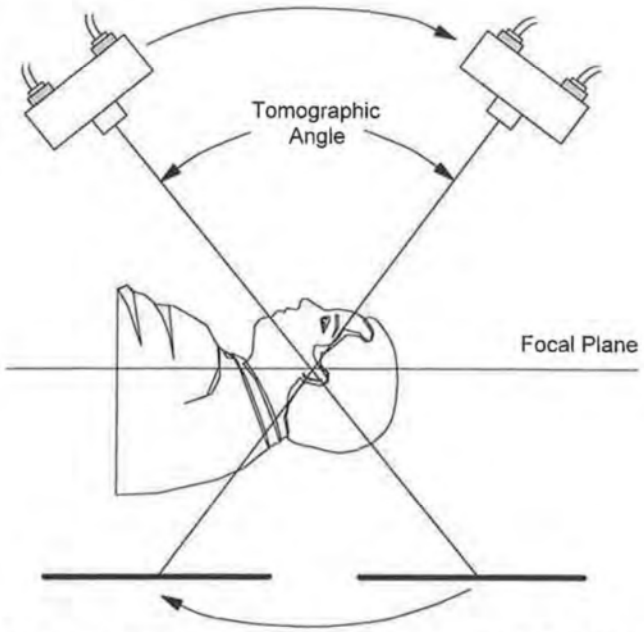



**Figure 8.2.** The acquisition technique for conventional tomography. The fulcrum point where the tube-detector axis pivots is the focal plane (or fulcrum plane) and is the plane of focus within the patient. The tomographic angle refers to the angle in which the x-ray beam is energized, and larger tomographic angles yield thinner cuts.

below the focal plane becomes increasingly more blurred with the distance away from the focal plane. Because it is common for the patient to lay supine in conventional tomography, the tomographic planes are usual coronal sections. Sagittal planes are achieved by positioning the patient on his or her side.

The only way one could discuss a slice thickness *per se* in conventional tomography is to define some (arbitrary) level of blurring that defines the slice. For example, this could be the thickness of tissue that includes the tissue volume where the loss of contrast is 25% or less. This is shown in Figure 8.3. With such a definition, a slice thickness could be assigned. One way to "sharpen" the focus of the focal plane, i.e., produce a narrower focal plane, is to use a larger tomographic angle during acquisition. As the tomographic angle increases, the area that an object is blurred over also increases. Narrow tomographic angles of 10° result in a relatively thick plane of focus, and this technique is called *zonography*. It is sometimes used to delineate suspected pathology better in a thick section of the patient.

Conventional tomography uses motion blurring to reduce the contrast of objects away from the focal plane. The type of motion used during tomographic acquisition will determine the path on the image where a particular object is blurred onto. Linear tomographic systems distribute the contrast of an object over a straight line on the image. Other more

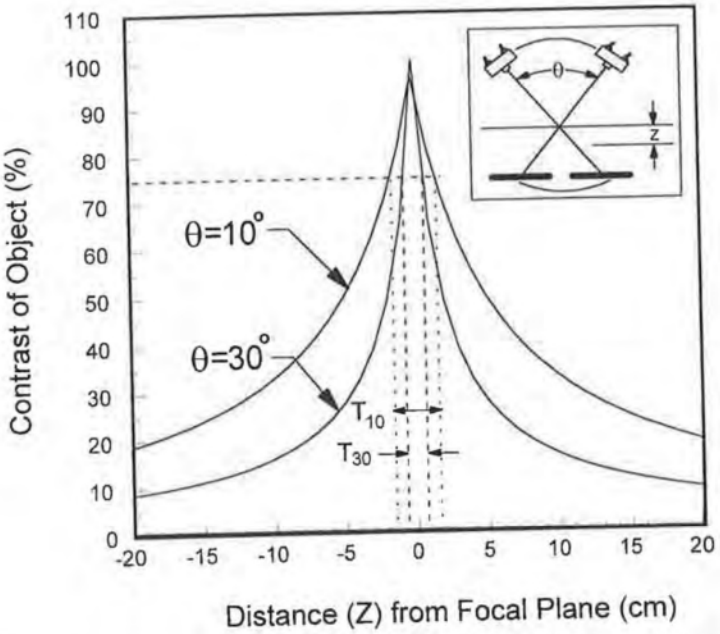



**Figure 8.3.** The concept of slice thickness in conventional tomography is different from that of computed tomography. In conventional tomography, all of the patient's anatomy is imaged onto the film. However, the anatomy becomes increasingly blurred and hence lower in contrast with distance from (above or below) the focal plane. Larger tomographic angles result in a more rapid blurring with distance away from the focal plane, and hence effectively yield a thinner plane of focus.

complex motions, such as circular, hypercycloidal, trispiral, and so on, distribute the contrast of the object over these geometric paths. The further an object is away from the focal plane, the greater the path length (linear motion) or diameter (other motions) of the blur path will be. This is why objects become more blurred with the distance away from the focal plane: As an object's contrast is distributed over a larger area (a longer blur path), it becomes more faint.

The anatomic features of the patient that are above and below the focal plane are blurred onto the image. Although off-focus anatomy is less visible because it is so blurred, it is nevertheless smeared around the image. This low-frequency background signal reduces the contrast of the patient's anatomy that is *in* the plane of focus, in a manner similar to how scattered radiation reduces contrast in the image. Consequently, conventional tomography is not an imaging modality that excels in contrast resolution, unlike its more sophisticated cousin computed tomography. This means that conventional tomography is good mostly for imaging objects that are naturally high in contrast. In most institutions, conventional tomography is used for intravenous pyelograms, where the iodinated contrast agent in the renal pelvis and ureter provides very high contrast. Also, inner ear studies are sometimes performed using conven-

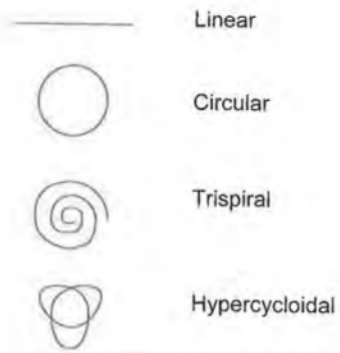



**Figure 8.4.** Some of the motions possible with dedicated tomographic systems. The linear motion can be achieved with optional attachments to a conventional radiographic/fluoroscopic system.

tional tomography, where the bony structure in the air-filled canal also provides a naturally high contrast setting.

Many standard radiographic rooms have optional attachments that allow the equipment to perform linear tomography. To use the radiographic system for tomography, the technologist attaches a metal rod that connects the x-ray tube with the bucky tray in the table. This solution is adequate for smaller institutions where the cost of a dedicated conventional tomographic system is unwarranted. The advantage of a dedicated tomographic system is that a wider range of tomographic motions is available. The specific motions that are available depend on the equipment vendor. Some examples of the motions available on dedicated units are illustrated in Figure 8.4.

Antiscatter grids are used in geometrical tomography, and because the x-ray focal spot is moving with respect to the detector, the grid alignment is critical. Tomographic systems generally use linear grids, which need to be rotated in all but linear motion techniques to ensure alignment of the grid bars with the primary radiation. This is illustrated in Figure 8.5.

### Dose Considerations

When a multislice conventional tomographic study is performed, the patient's dose should be considered. In computed tomography, the patient's anatomy that is not in the slice plane is not irradiated with the primary radiation but does receive some scattered radiation. In conventional tomography, however, the patient's off-plane anatomy is in the field of view and therefore is irradiated by the primary beam. In a series of 15 coronal slices, each taken at a different plane of focus, the entire volume of the patient is irradiated 15 times. When multiple planes are needed, the patient's radiation can add up quickly.

Consider a tomographic technique in which 100 mA is used for 6 seconds at 80 kV. At this kV, the tube emits about 8 mR/mAS at 1 meter. So at 1 meter from the tube, this technique would produce 600 mAS × 8 mR/mAS = 4800 mR = 4.8R. Because the patient's entrance surface is typ-

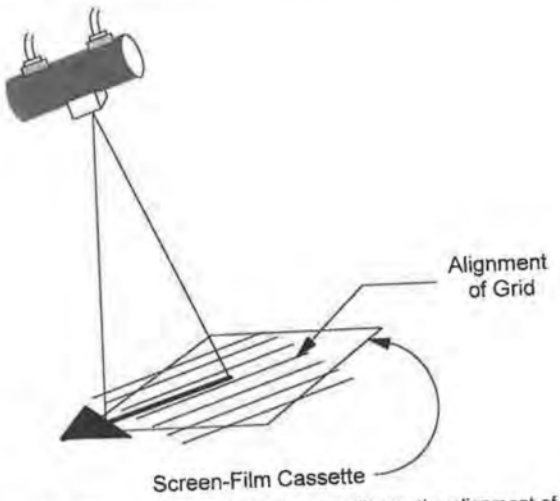



**Figure 8.5.** For tomographic motions other than linear, the alignment of the antiscatter grid needs to be maintained so that grid artifacts do not appear on the image. Only a linear grid can be used. The grid needs to be rotated on center so that the grid bars point to the position in the detector plane directly below the focal spot.

ically about 80 cm from the x-ray tube, the exposure at that location is $4.8\ \text{R} \times (100/80)^2 = 7.5\ \text{R}$. A tomographic series of 15 slices would result in about 112 Roentgens of entrance exposure to the patient.

## FILM SUBTRACTION

*Film subtraction* is used in angiography to reduce the anatomical clutter in the original cut film angiographic images, to allow the radiologist to concentrate specifically on the vascular anatomy.

### Purpose

Accurate diagnoses depend on both the skill of the radiologist and the quality of the radiographic images. One very important aspect of image quality is the signal-to-noise ratio (SNR). There are many technical details involved in the assessment of the SNR, but one that is often overlooked is simply image clutter: The complicated radiographic shadows of normal anatomy that are superimposed onto the image of the anatomy under investigation can obscure the anatomical detail crucial to an accurate diagnosis. This image clutter is referred to as *structured noise*, and does in fact reduce the image quality. It can and does interfere with the diagnosis in some cases. In angiography, the vascular anatomy is that which is of interest, and the overlying bony and soft tissue anatomy only adds structured noise. Because angiograms are acquired in a temporal sequence, the setting is ideal for subtracting the background anatomy out of the image.

### Methods

Before film subtraction, a conventional cut film angiographic sequence is acquired. From this sequence, a mask image is selected of the patient's background anatomy before the arrival of the contrast agent, and another image is selected that contains the patient's background anatomy as well as the contrast-filled vasculature (the *iodinated* image). These two images are subtracted photographically, revealing only the differences between the images. In this way, the vascular anatomy remains but the static background anatomy is subtracted out. Of course, for this procedure to work correctly, the background anatomy needs to remain perfectly still, meaning the patient and the x-ray system cannot move between the acquisition of the two images. Otherwise, the subtraction will be of poor quality.

### Photographic Subtraction

Literally, it is impossible to subtract two images photographically. Instead, one image is reversed in polarity (the dark areas are made light and the light areas are made dark), and this reversed image is superimposed over the other image. Adding the reversed polarity image is equivalent to subtracting away the information common in the two images. Once the mask image and the iodinated images are selected, the subtraction mask is made from the mask. The subtraction mask is the reversed-polarity mask image. The subtraction mask is then placed over the iodinated image, and cancellation of the static background common to the two images occurs. Once proper alignment is achieved, the two superimposed images are usually taped together with masking tape. In a perfect subtraction, the contrast media in the vasculature is all that remains. Although viewing the two superimposed images can be done, the total optical density of the two superimposed images is usually quite high, meaning that the superimposed image is very dark. This can be made lighter by making a contact print of the pair using copy film. The exposure time in making the copy is selected so that the subtraction print is lighter than the two superimposed images.

Film subtraction is a straightforward technique; however, because of the extra effort, time, and cost involved in making the subtraction films, *digital subtraction angiography* (DSA) has in many institutions replaced much of the film subtraction that was done before the development of DSA. However, because film does have better spatial resolution than digital images, film subtraction is still often used in neurovascular imaging and other areas, where the resolution of digital subtraction angiography is not always sufficient.

The only concept in film subtraction that is not straightforward has to do with making the subtraction mask from the mask image. To reverse the polarity of a radiographic image, negative film is used. Radiographic film is negative film, because regions exposed to light become dark when the film is processed. However, because of the high average gradient (about 3) typical of radiographic film, it enhances the contrast of the original light image shone on it. Thus, if regular radiographic film were

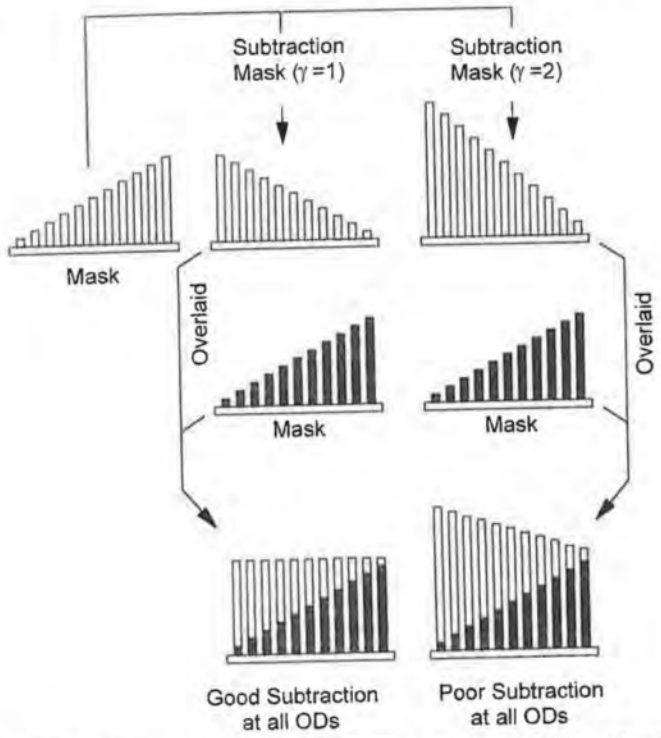



**Figure 8.6.** The consequence of using subtraction mask film with a $\gamma$ other than 1. The mask image is converted to a subtraction mask using subtraction mask film with $\gamma$'s of 1 and 2. The center column of steps illustrates the consequence of using a $\gamma$ of 1, the right column illustrates the effect with a $\gamma$ of 2. Here, the subtraction mask overlaid onto the mask itself results in complete subtraction, for all optical densities in the film. Complete *optical* subtraction implies that the resultant image is uniformly gray. When subtraction mask film with a $\gamma$ of 2 is used, the ODs do not cancel, and poor subtraction is achieved.

used to make the subtraction mask, it would be reversed in polarity but would be too high in (inverted) contrast to cancel the anatomic detail of the iodinated image properly (Fig. 8.6). Consequently, special film is used to make the subtraction mask from the mask image. It is negative film with an average gradient of one, and this film is called *subtraction film.*

## DIGITAL SUBTRACTION ANGIOGRAPHY

### Description of Technique

*Digital subtraction angiography* (DSA) became possible with the availability of digital video processors, devices that are capable of digitizing a video signal into a digital image with good spatial resolution. The central component in a digital video processor is an analog-to-digital converter (ADC), which takes the analog voltage output by a video camera and converts this to a range of digital numbers. This is done for an entire

video image in real time. Modern DSA systems are capable of producing either 512 × 512 pixel images or 1k × 1k pixel images.

The rationale for digital subtraction is identical with that for film subtraction. The subtraction process reduces the anatomical detail in the image and lets the radiologist focus attention to the vascular anatomy that is under investigation. Digital subtraction is substantially easier than film subtraction, because the images reside in a computer and the subtraction can be performed numerically, instead of photographically. During the early days of DSA development in the late 1970s, DSA was touted as primarily an intravenous (IV) procedure. Because the subtraction reduced structured noise (the background anatomical detail), the *conspicuity* of iodinated vascular in the subtracted image was improved substantially. It was originally thought that this contrast enhancement would allow the use of less invasive IV injections.

As DSA developed, the push for greater vascular contrast led to intra-arterial (IA) injections becoming more common. By injecting intra-arterially and therefore closer to the site of interest, a higher *concentration* of contrast agent can be delivered to the vascular site of interest for a given *volume* of injected contrast agent. The IV injections resulted in substantial diffusion of the contrast agent bolus before its arrival at the site of interest. Although IA injections, which are more common today, do increase the degree of invasiveness compared with IV DSA, IA DSA has several distinct advantages over conventional film and film subtraction angiography. Because DSA is capable of producing images with higher effective vascular contrast, less contrast agent has to be delivered for each angiographic run. This means that for the same number of runs, the contrast agent burden to the patient is reduced. Of course, it is the allergenic response to iodinated contrast agent that represents the greatest acute risk to the patient during angiography. Therefore, DSA can still be said to be less invasive, when lower contrast agent volumes are used. Another ramification of the reduced contrast agent volume per study is that more studies can be performed. For patients with complex disease, DSA can allow a more thorough evaluation (more studies) for the same contrast agent burden to the patient.

Another benefit of DSA is that the subtracted images are available instantaneously. This means that the image sequence can be monitored by the angiographer during the angiographic run, and the x-ray acquisition can be terminated when it is determined that the contrast bolus has passed the site of interest. This real-time monitoring capability can result in a reduction of radiation exposure to the patient, by reducing the number of images acquired during each angiographic run. A side benefit of this is that x-ray tube loading can be reduced.

### Equipment

DSA systems start with a standard angiographic suite, with an x-ray generator and tube capable of rapidly pulsed exposures. Instead of acquiring the images onto film using a film changer, the image intensifier (II) is the primary detector. The video signal from a high-quality TV camera

(coupled to the II) is digitized by the ADC to produce the raw (unsubtracted) digital images. Because the II acts as the primary detector for DSA images, the need for a high-quality II is more apparent in DSA. Also, because in some vascular studies larger fields of view are needed, large field of view IIs are often incorporated into the DSA suite.

Because the video system is a central component in producing the diagnostic images in DSA, the video system also needs to be of very high quality for the system to produce good DSA image quality. For fluoroscopy, standard video cameras have a fair amount of *lag*, which means that during the temporal sequence of images, a certain fraction of the last few images leaks into the present image. For routine fluoroscopy, lag is beneficial. Increasing lag means that the camera is integrating the image over a greater effective period of time. This means that more x-ray photons contribute to the displayed image, and that makes for lower quantum noise in the image and better image quality. Lag is a form of temporal smoothing. *Vidicons* ($Sb_2S_3$ target material) are good fluoroscopic cameras and exhibit a fair amount of lag. For angiography, however, lag is not desirable. For a rapid sequence of diagnostic images, it is important to minimize lag to reduce motion artifacts caused by the rapidly changing scene as the contrast bolus passes through the vasculature. Plumbicon cameras (PbO target material) exhibit low lag properties. The conflicting lag requirements for fluoroscopy and for DSA often results in the incorporation of two separate video cameras on the DSA system, occupying two different ports on the optical distributor. A laggy vidicon is used for fluoroscopy, and the low-lag video camera is used for image acquisition during DSA. Some systems do use the same camera but modify the internal camera electronics between fluoroscopic and DSA modes to alter the lag characteristics.

The video signal is digitized by the ADC. With some systems, a high exposure rate constant x-ray beam (non-pulsed) is used and the video signal is digitized at 30 frames per image. This type of system uses the least expensive technology and suffers from the fact that each DSA image is acquired in 1/30 of a second—33 milliseconds. This long exposure time per image results in significant motion blurring. To overcome this problem, pulsed x-ray exposure can be used. When pulsed exposure is used, certain problems can occur with standard techniques for video camera readout. In a standard 33-msec video frame, two *fields* are read out. (See Chapter 7 for more details on video cameras.) A single video frame is read odd lines first, then even lines (i.e., the odd field and then the even field). When the x-ray pulse occurs just before the readout of the first field, the readout of the first field causes a discharge of the image information stored on the target of the video camera. When the readout of the second field occurs, there is less signal on the target because of the prior readout. This situation can result in image artifacts caused by the disparity in signal intensity between the even lines and the odd lines on the digital image, unless the electronics are tuned very precisely. To overcome this and other problems that can occur when the x-ray tube is pulsed, a different strategy for TV camera readout is used, which results

in higher fidelity images. Instead of the interlaced readout where two interwoven fields are acquired in each frame, *noninterlaced* readout is used. Noninterlaced readout of the TV target is a straightforward readout of all the TV lines sequentially. Instead of reading odd lines then even ones as with interlaced scanning, the odd and even lines are read out together, producing the entire image in one sweep of the TV target. The noninterlaced scan mode is also called *progressive* scan. Noninterlaced readout of the TV camera is the preferred approach used in modern DSA systems. For standard resolution (512 × 512 pixels) images, noninterlace scanning can proceed at 30 frames per second. High resolution images of 1024 × 1024 pixels contain four times the number of pixels than the standard 512 × 512 images. To use the same bandwidth of the camera, it takes four frame times (4/30 = 133 msec) to read out 1k × 1k images. This reduces the maximal frame rate from 30 images per second to 7.5 (30/4) images per second. This frame rate is still more than adequate for most angiography studies used in radiology applications, outside of cardiac imaging.

The final major components in a DSA system are the computer, the digital-to-analog converter (DAC), and the computer display. Because DSA acquisition results in the rapid accumulation of a great deal of data in a short period of time, off-the-shelf computer systems cannot usually be used. Instead, systems with exceptionally fast disk transfer capabilities are used.

There is one important aspect of DSA that occurs during digitization that is worth understanding. For reasons that will be made apparent in the next section, the logarithm of the raw DSA images is computed before the image subtraction. Hence, in DSA, *logarithmic subtraction* is used. The computation of the logarithm requires a fair amount of time in the computer. This computational bottleneck can be reduced substantially by precalculating the logarithm for all the cases that are needed. If the ADC converts the video signal into 1024 different numbers (10 bits) ranging from 0 to 1023, then the logarithm can be computed on these 1024 values and the result for each is stored in the computer. When the logarithm of an image is to be performed, rather than performing 262,144 logarithm calculations for a 512 × 512 image, the computer is programmed to look up the logarithm for each pixel in the image from its precalculated list of values. This approach uses a so-called *look-up table* to perform the calculation, and look-up table calculations are performed routinely with digital images for many different applications. Windowing and leveling are often performed as a look-up table operation.

A logarithmic look-up table can be displayed as the (logarithmic) output as a function of (linear) input, as illustrated in Figure 8.7. The main point of all of this is that the look-up table is nonlinear. Consequently, the number of bits required in the output is less than that required in the input. Or, put the other way, for a logarithmically subtracted image with 8-bit fidelity, *a larger number of bits (e.g., 10 bits) is needed at acquisition to preserve the 8-bit resolution after the logarithmic computation.* This notion is best described diagrammatically (Fig. 8.8).

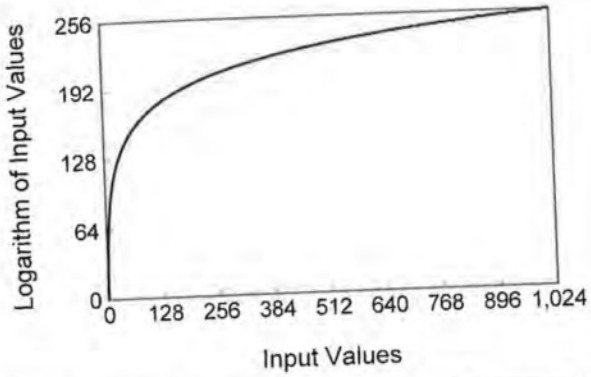



**Figure 8.7.** A logarithmic look-up table ("LUT," in computer vernacular). When the computer needs to compute the logarithm for a particular pixel value, it uses the pre-calculated values that are stored in the look-up table. It looks to the input value (along the *x* axis) associated with the pixel value, and then retrieves the output value at that memory location (the *y* axis here). This eliminates the need for the computer to have to calculate the logarithm on all the pixels in the image.

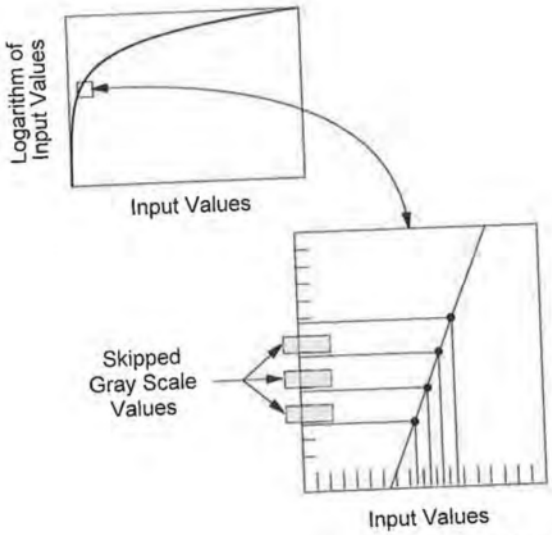



**Figure 8.8.** The nonlinear nature of the logarithmic look-up table shown in Figure 8.7 results in slopes much greater than one within the look-up table. If the same number of input and output (*x* and *y* axis) bits are used, the look-up operation will result in output gray scale values that are never used. This reduces the gray scale fidelity of the displayed image. To compensate for this, the data are digitized using a larger number of bits than the displayed image. Although the numbers can vary, typically in DSA the image data are digitized to 10 bits (1024 shades of gray), are run through the look-up table, and an 8-bit (256 shades of gray) result is kept.

where $\xi$ is the linear attenuation coefficient of the contrast agent and $z$ is the thickness of the vessel that the contrast agent is in. The logarithmic subtraction of these two images results in the subtracted image where:

$$I_{subtracted} = Log[I_{mask}] - Log[I_{contrast}]$$

$$I_{subtracted} = \{Log[I_o] - \mu x\} - \{Log[I_o] - \mu x - \xi z\} = \xi z$$

The intensity of the pixel values in DSA are related *linearly* to the thickness of the vessel, $z$. This is a consequence of the logarithmic subtraction that is performed. The linear attenuation coefficient for the iodinated contrast agent, $\xi$, is a constant of proportionality. If it is higher, the subtracted DSA image will have more contrast. The linear relationship between the pixel values (the digital number of each pixel) and the vessel thickness implies that the DSA images can be used to make certain calculations pertaining to the thickness of the imaged vessels. Because the value of $\xi$ is unknown, only the *relative thickness* of the vessels is known, the absolute thickness (in mm) is usually not known. However, because $\xi$ is usually constant along a certain segment of a vessel, relative thickness measurements can be performed along that segment of vessel. Specifically, the amount of stenosis can be calculated. This approach to quantifying vessel dimensions is called *videodensitometry,* or just *densitometry* (Fig. 8.9). It is heralded by some as the preferred technique to determine stenosis (as opposed to evaluating the shape of the stenosis visually), because in principle it is independent of the projection angle through the vessel. It is noted that *additive* errors that occur before the logarithmic operation, e.g., scattered radiation and veiling glare, as well as improper system calibration, are not totally subtracted out by the logarithmic operation. Consequently, the promise of this technique is mitigated somewhat by quantitative errors that can be caused by scattered radiation, veiling glare, or less than perfect system calibration.

# X-RAY COMPUTED TOMOGRAPHY




Computed Tomography (CT) is in its third decade of clinical use and has proven invaluable as a diagnostic tool for many clinical applications, from cancer diagnosis to trauma to osteoporosis screening. CT was the first modern imaging modality that made it possible to probe the inner depths of the body, slice by slice. Since 1972, when the first head CT scanner was introduced, CT has matured greatly and gained technological sophistication. Concomitant changes have occurred in the quality of CT images. The first CT scanner, an EMI Mark 1, produced images with $80 \times 80$ pixel resolution (3-mm pixels), and each slice required approximately 4.5 minutes of scanning time and 1.5 minutes of reconstruction time. Owing to the long acquisition times required for the early scanners, it was originally thought that CT would only be practical for head scans, because cardiac and respiratory motion in the thoracic cavity is significant over such a long time interval.

CT is one of the many technologies that was made possible by the invention of the computer. The clinical potential of CT became quite obvious during its early clinical use, and the excitement forever solidified the role of computers in medical imaging. Recent advances in acquisition geometry, detector technology, and x-ray tube design have led to scan times now measured in fractions of a second with some systems. Modern computers deliver the computational power that allows the reconstruction of the image data virtually in real time.

The invention of the CT scanner earned Godfrey Houndsfield of Britain and Allan Cormack of the United States the NOBEL prize for medicine in 1979. CT scanner technology today is not only used in medicine but in many other industrial applications such as nondestructive testing and soil core analysis.

## BASIC PRINCIPLES

The mathematical principles of computed tomography were first developed by Radon in 1917. Radon's treatise essentially proved that an image of an unknown object could be produced if one had an infinite number of projections through the object. Although the mathematical details are

beyond the scope of this text, we can understand the basic idea behind tomographic imaging with an example taken from radiography.

One of the problems of plain film imaging is that the three-dimensional anatomy of the patient is reduced to a two-dimensional projection image. The optical density at a given point on the radiograph represents the x-ray attenuation characteristics within the patient integrated along a line that extends between the x-ray focal spot and that point on the film. Consequently, with a radiograph of the patient's anatomy displayed over two dimensions (height and width), information with respect to the third dimension (depth) is lost. This limitation can be overcome, at least for obvious structures, by acquiring a PA projection *and* a lateral projection of the patient. The posteroanterior image yields information concerning height and width, integrated along the depth of the patient, and the lateral projection provides information about the height and depth of the patient, integrated over the width dimension (Fig. 10.1). For objects that can be identified in both images, such as a pulmonary nodule on posterior-anterior (PA) and lateral chest radiographs, the two films provide valuable location information. For more complex anatomy, however, the two projections do not provide a complete enough picture. Imagine that instead of two projections, i.e., the posteroanterior and lateral chest images, a series of 360 radiographs were acquired at 1° angular intervals around the patient's thoracic cavity. Such a set of images provides essen-

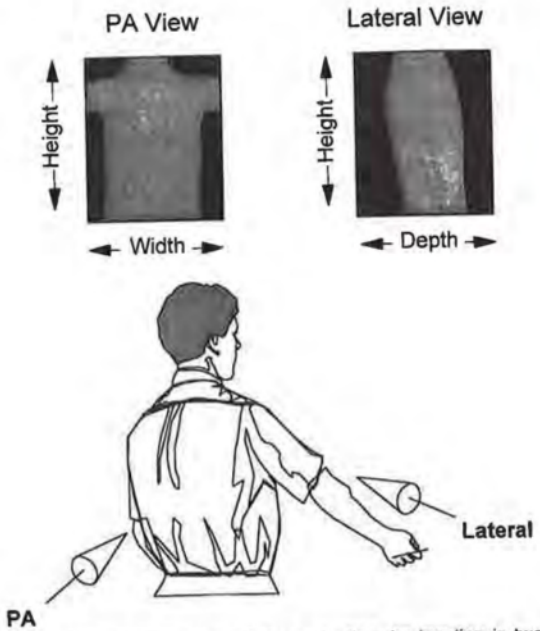



**Figure 10.1.** The conventional approach to evaluating the location in two dimensions of an object within the patient. PA and lateral views are acquired which provide the capability to locate an object when it can be seen in both views. The raw data that are acquired in a series of thoracic CT scans are comparable to acquiring 360 radiographs at one-degree intervals around the patient.

tially the same data as a series of contiguous axial CT images running from the cervical spine to the mid-diaphragm. However, the 360 radiographic images display the anatomical information in a way that would be impossible for a human to assimilate into the perception of cross-sectional information. If these 360 images were stored into a computer, the computer could reformat the data and generate a complete set of axial CT images.

## Acquisition

The purpose of the CT scanner is to acquire a large number (100–1200) of CT projections around the patient (Fig. 10.2). Unlike film, which acquires a two-dimensional image, the detector or detector array on a CT scanner only acquires data along a thin line, as shown in the figure. So for one complete set of CT projections going all the way around the patient, only a single CT image can be computed. Before the acquisition of the next slice, the table that the patient is lying on is moved slightly in the cephalic or cranial direction, which positions a different axial slice of tissue in the path of the x-ray beam for the next series of acquired projections.

The tomographic image is a representation of a slice of the patient where the x-rays were incident. The two-dimensional CT image corresponds to a three-dimensional section of the patient, meaning that even with CT, three dimensions are compressed into two. However, unlike the case with plain film imaging, the slice-thickness dimension is very thin (1–10 mm), approximately uniform, and is adjustable with modern CT scanners. The two-dimensional array of pixels (short for *pic*ture *el*ements) in the CT image correspond to an equal number of voxels (*vol*ume *el*ements) in the patient. The voxels have the same coordinates as pixels, except that they include the slice thickness. A given pixel on the CT image displays the average attenuation properties of the tissue or bone in the corresponding voxel (Fig. 10.3).

The data acquired by a CT scanner are a set of linear projections. There may be 700 or more data points per projection, and there may be

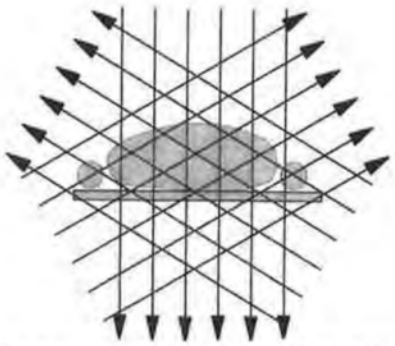


**Figure 10.2.** CT acquisition results in the collection of linear (one-dimensional) projection data at many different angles around the patient.

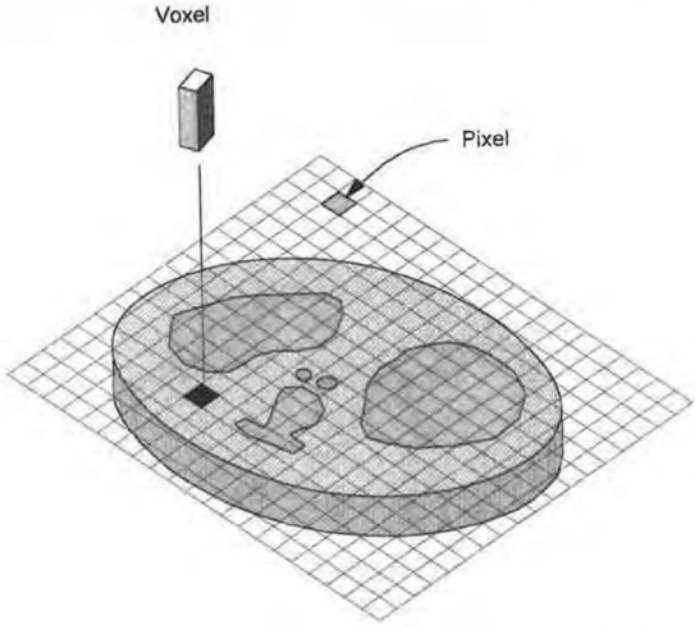



**Figure 10.3.** The CT image is composed of *pixels (pic*ture *el*ements*)*. Each pixel on the image displays brightness information concerning the patient's anatomy that is located in the corresponding *voxel* (*vol*ume *el*ement). The pixel width and height are equal to the voxel width and height, but in addition the voxel embodies a third dimension. The thickness of the voxel is determined by the slice thickness, which is governed by mechanical collimation of the x-ray beam by lead jaws. Typical values for pixel dimensions are 0.5 mm × 0.5 mm. Typical slice thicknesses run from 1.0 mm to 10 mm.

600 or more projections in the data set. The projection data can be displayed as an image, by stacking the individual projection data and creating a two-dimensional image from the set of one-dimensional data. This type of display is called a *sinogram* (Fig. 10.4). The data running in the horizontal direction are the data points in each projection, and the vertical axis in the sinogram represents each different projection angle. Sinograms are not used for clinical purposes, but the concepts that they embody are interesting and relevant to understanding tomographic principles.

Each data point that is acquired by the detector array in CT is a transmission measurement through the patient along a given line. Each data point {I(x)} therefore follows the basic equation:

$$I(x) = I_o\, e^{-\mu x}$$

The intensity of the x-ray beam is also measured without any patient in the way, and therefore $I_o$ is determined at some point during the scan (this depends on the geometry used for acquisition) for each transmission measurement, I(x). Therefore, both I(x) and $I_o$ are known. From this information, the projection data, P(x), is calculated as:

$$P(x) = \ln\{I_o/I(x)\} = \mu x$$

This preprocessing of the data before image reconstruction results in a CT image that is independent of the intensity of the x-ray beam that was used to generate the projection data. With film-based radiographic images, the appearance of the image changes appreciably depending on the exposure techniques used. For example, radiographic images can be too light or too dark. The preprocessing step in CT normalizes variations in beam intensity and provides attenuation measurements that are a *fraction* of the incident intensity. CT scans do not show up "too light" or "too dark" depending on the technique. (The CT technique *will* affect the amount of noise in the image, and this will be discussed later.) The independence of CT images from the intensity of the exposure makes them one step better with regard to the ideal notion of what an image should be. The ideal image of a patient should display information about the patient, and not contain superfluous information about the technique used to acquire the image.

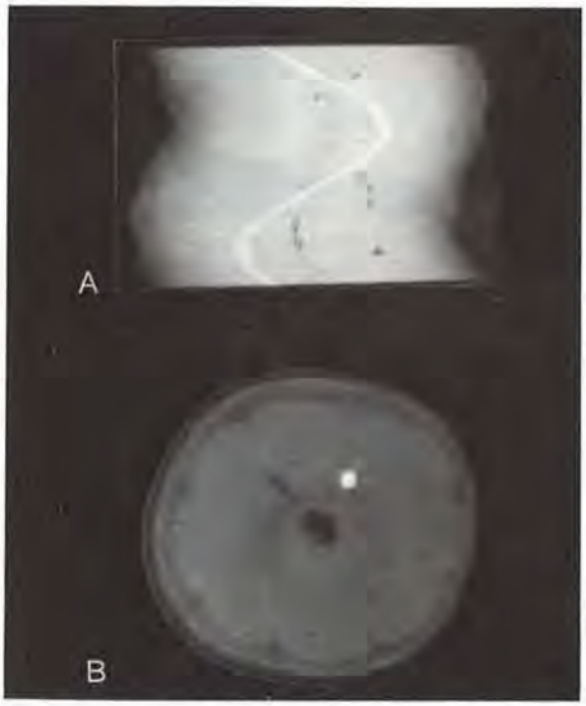



**Figure 10.4.** A *sinogram* of a lemon. The horizontal direction of the sinogram corresponds to the ray data in each projection. The vertical axis corresponds to the different projections acquired at different angles through the lemon. The CT image of the lemon is shown as well. A metal rod was inserted into the lemon before the scan. The bright region corresponding to the high attenuation of the rod shows up as an obvious sine wave in the sinogram. Because the projection data that make up the sinogram were acquired over 360°, the sine wave caused by the metal rod is one complete cycle.

## Tomographic Reconstruction

In a CT scanner, the computer orchestrates the acquisition of a large number of transmission measurements taken through the object being scanned and stores this raw data. The raw data, after some preliminary algebra, are *reconstructed* to produce the tomographic images. There are numerous reconstruction strategies; however, *filtered backprojection* reconstruction is most widely used in clinical CT scanners. The backprojection method builds up the CT image in the computer by essentially reversing the acquisition steps (Fig. 10.5). During acquisition, attenuation information along a known path of the narrow x-ray beam is *integrated* by a detector. During backprojection reconstruction, the detected value is *smeared* along this same path in the image of the patient. As the pro-

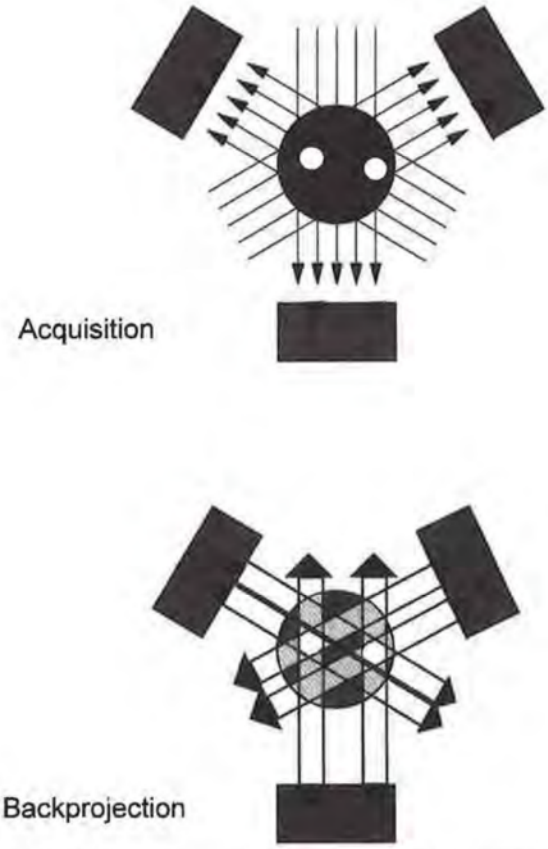



**Figure 10.5.** The CT image is computed in a process akin to reversing the CT data acquisition. During acquisition, the one-dimensional views through the object are acquired at many different angles. Computation of the CT image typically involves the smearing of the acquired projection data along a geometry corresponding to the acquisition. The smearing is called *backprojection,* and this procedure builds up the CT image by allowing bright areas to be positively reinforced and dark areas to be negatively reinforced.

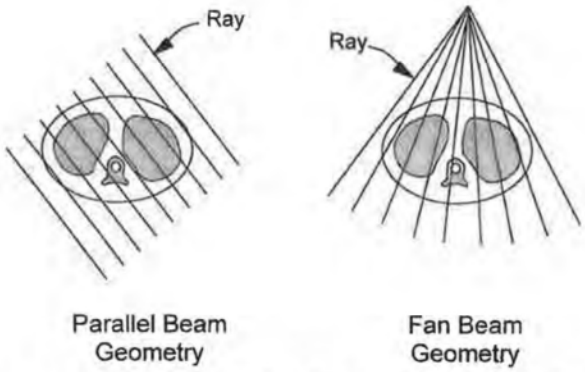



**Figure 10.6.** The two geometry's that have been used in clinical CT scanners. Parallel beam geometry was used in earlier CT scanner designs. Fan beam geometry makes use of the divergent nature of the x-ray beam as it is emitted from the x-ray tube.

jection data from a number of different angular profiles are smeared back onto the image matrix (backprojected), areas of high attenuation tend to reinforce each other, and areas of low attenuation also reinforce, thus building up the image in the computer. The precise geometry in which the data are acquired is as important as the data itself, and the angular information must be stored by the computer during the acquisition process.

A single transmission measurement through the patient made by a single detector at a given point in time is called a *ray.* A series of rays that pass through the patient at the same orientation is called a *projection,* which is also called a *view* or *profile.* There are two different geometries that have been used in CT imaging over the years (Fig. 10.6). The most basic is called *parallel beam geometry,* where all of the rays in a given projection are parallel to each other. In *fan beam geometry,* the rays that pass through the patient for a given projection angle have the appearance of a fan. This fan-like appearance is the natural consequence of the divergent beam that is emitted by the x-ray tube during CT acquisition. Most modern CT scanners incorporate fan beam geometries in the acquisition and reconstruction process.

## CT Numbers and Houndsfield Units

A CT image is a two-dimensional matrix of numbers, with each number corresponding to a spatial location in the image and in the patient. For a typical (modern) CT image, the matrix of numbers is 512 pixels wide by 512 pixels tall, with 4096 different possibilities for the value of each pixel (12 bits). Each pixel corresponds to a voxel in the patient, and the physical location of each voxel is a straightforward concept to understand. The numerical value of each pixel in the computer represents a certain level of gray on the CT image. In the earlier EMI scanners, these values were called EMI numbers. Other names for the numbers that correspond to the brightness of each pixel in a CT image are *Houndsfield*

*units,* or *CT numbers.* Other names for the brightness of each pixel in digital images (CT or otherwise) are *pixel values, gray scale values,* and *digital numbers.* Although optical density is the standard unit that brightness is measured by in film images, it is the CT number (or any of the other synonyms mentioned) that is most frequently referred to in CT images.

CT images represent rich visual information and are invaluable in radiological diagnosis. The radiologist quickly becomes familiar with the appearance of normal and abnormal CT images, based on visual patterns contained within the images. With all the visual detail in these images, it is easy to forget that CT images look like they do because of the physical interactions of x-rays within the patient. The CT number for a certain pixel actually corresponds to *physical properties* within the patient in the corresponding voxel. Because the physical properties dictate what ultimately will show up in the image, it is important to understand what the CT numbers represent. Such an understanding is fundamental to knowing what the limitations of CT images are and what they can and cannot be used for in making diagnoses.

### What is Being Measured?

The CT reconstruction process results in a two-dimensional matrix of floating point numbers in the computer which range from near 0.0 up to values equal to 1.0. These numbers correspond to the average *linear attenuation coefficient* of the tissue contained in each voxel. In conventional radiography, the optical density of the image depends on the type of screen-film system used, on the radiographic technique that was used, and some dependency on the patient's anatomy. Even under the best situations, radiography produces images that are only qualitative in nature. CT, however, actually yields a map of the linear attenuation coefficients within the patient. Thus, CT has the potential of being a *quantitative* as well as a qualitative imaging technique.

The nature of computer display hardware is such that integer numbers are required. To accommodate this, the linear attenuation values that range roughly from 0.0 to 1.0 are scaled up to an integer range that encompasses 4096 values, between −1000 and 3095 (typically). In scaling the linear attenuation values to a larger range, they are also normalized to the attenuation coefficient of water:

$$\text{CT Number} = 1000 \times (\mu_{\text{pixel}} - \mu_{\text{water}})/(\mu_{\text{water}})$$

If the linear attenuation coefficient for a given pixel ($\mu_{\text{pixel}}$) is equal to that of water, the CT number will be 0. If $\mu_{\text{pixel}}$ is less that $\mu_{\text{water}}$, the CT number will be negative, and negative CT numbers are typical for air spaces, lung tissues, and fatty tissues. Values of $\mu_{\text{pixel}}$ greater than $\mu_{\text{water}}$ will result in positive CT numbers. Dense tissues and bones have large positive numbers. Most soft tissues have CT numbers near that of water, so soft tissues will have CT numbers that are approximately in the −100 to +100 range. The earliest systems used *EMI numbers*; a multiplication constant of 500 was used (instead of 1000, as indicated in the above equation), and the numbers ran from −500 to +500.

Thus, the CT numbers are rescaled linear attenuation coefficients. The linear attenuation coefficient is a characteristic of the elemental composition of the material and its density, but it also depends on the x-ray energies used in acquiring the data. In CT, relatively high kVs are used, usually 120 kV to 140 kV. In addition, there is a large amount of x-ray beam filtration in the beam, which further increases the effective energy of the x-ray beam used in computed tomography. Chapter 2 refers to the attenuation coefficient in diagnostic radiology as a combination of the attenuation produced by the photoelectric effect, Rayleigh scattering and Compton scattering. At high energies, however, the photoelectric effect and Rayleigh scattering are only minor components of attenuation. Consequently, in CT, Compton scattering is the primary type of interaction that contributes to the subject contrast in the images.

Compton scattering depends on both the mass density ($gm/cm^3$) of the material as well as the number of electrons per unit mass (electrons/gm). The mass density dependency is straightforward to understand. As the mass density increases, the amount of matter in each voxel increases, clearly causing an increase in the attenuation (higher linear attenuation coefficients). The number of electrons per unit mass is equal to NZ/A, where N is Avagodro's number ($6.02 \times 10^{23}$), Z is the atomic number (number of protons in the nucleus), and A is the atomic mass. The predominant elements that compose tissue are carbon, oxygen, nitrogen, and hydrogen. The most common isotopes of these elements are $^{12}C$, $^{14}N$, $^{16}O$ and $^{1}H$. Because the atomic numbers of these elements are $Z_C = 6$, $Z_N = 7$, $Z_O = 8$ and $Z_H = 1$, the ratio of Z/A for C, N, and O is exactly 0.5. For hydrogen, the ratio of Z/A is 1.0. These numbers indicate that the CT number is, relatively speaking, not too dependent on the atomic number of the material in a given voxel, with the exception of hydrogen. Because adipose tissue has a high fraction of hydrogen, this suggests that CT is good at differentiating fat from other tissues, which it is.

Bone tissue has a fair amount of calcium, in addition to C, H, O, and N. The atomic number of calcium is 20, and Ca has a Z/A ratio of 0.5 also. Although Compton scattering is the predominant type of x-ray interaction in CT, the high atomic number of calcium relative to C, H, O, or N causes increased photoelectric absorption in bone, because of the $Z^3$ influence. In addition to an increase in Z, the mass density of bone is about three times that of water. For both of these reasons, bones have high linear attenuation coefficients relative to water, and consequently the CT number of bone is high. (CT numbers for bone range from $\sim +300$ to $+3000$, depending on density.)

Lung tissue is highly aerated, and because the density of air is negligible ($\rho_{air} = 0.001293$ $gm/cm^2$), the density of tissue and air mixed together in a voxel is quite low. This means that the linear attenuation coefficient of lung is often lower than that of water, and so the CT numbers in lung tissues are negative values.

## HISTORICAL DEVELOPMENT: CT "GENERATIONS"

Part of understanding an imaging modality involves the appreciation of the maturation of that modality. In addition to a historical interest, the

discussion of the evolution of CT scanners also allows the presentation and reinforcement of several key concepts in CT imaging.

### First Generation: Rotate/Translate, Pencil Beam

CT scanners represent a diverse cadre of technologies, from computers, motor control systems, x-ray detector design, and x-ray tube/generator systems. The first generation of CT scanners was a rotate/translate, pencil beam system (Fig. 10.7). Only two x-ray detectors were used, which measured the transmission of x-rays through the patient for two different slices. The acquisition of the many profiles and the many rays per profile required that the single detector (per CT image) be moved throughout all the necessary positions. This system used parallel ray geometry. Starting at a particular angle, the x-ray tube and detector system translated linearly across the field of view (FOV), acquiring 160 rays across a 24-cm FOV, for the projection at that particular angle. When the x-ray tube/detector system was finished with its translation, the whole system was rotated, and then another translation was used to acquire the next projection set. This procedure was repeated until 180 projections were acquired at 1° intervals.

There were other problems in addition to the amount of scan time that the first-generation systems posed. The NaI detector system could not accommodate the huge *dynamic range* in x-ray intensities. As the system translated and measured rays from the thickest part of the head to the area adjacent to the head, it experienced a significant change in x-ray flux. The early detector systems could not accommodate this large change in signal, and consequently the patient's head was inserted into a flexible membrane surrounded by a water bath. The water bath acted to bolus the x-rays so that the intensity of the x-ray beam outside the pa-

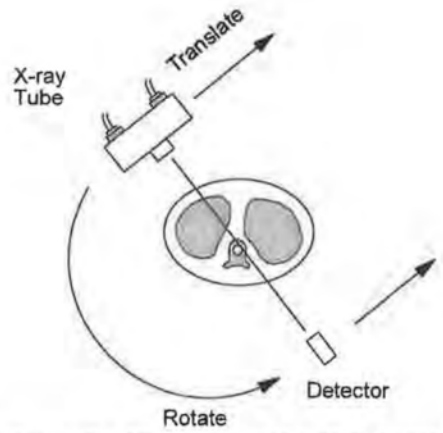



**Figure 10.7.** First-generation CT scanners used a rotate/translate motion. The x-ray tube was mechanically coupled to the detector. The whole stage was translated across the field of view, and then the stage was rotated. This procedure was repeated until 180 different transitions were made. The first-generation scanner acquired data in parallel beam geometry.

tient's head was similar in intensity to that inside the head. The NaI detector also had a significant amount of "afterglow," meaning that the signal from a measurement taken at one period of time decayed slowly and carried over into the next measurement if the measurements were made temporally too close together.

One advantage of the first-generation CT scanner was that it accepted only a very small pencil ray of x-rays, because only two detectors measured the transmission of x-rays through the patient. The pencil beam allowed very efficient scatter reduction, because scatter that was deflected away from the pencil ray was not measured by a detector. With regard to scatter rejection, the pencil beam geometry used in first-generation CT scanners was the best.

### Second Generation: Rotate/Translate, Narrow Fan Beam

The next incremental improvement to the CT scanner was the incorporation of a linear array of 30 detectors. The use of 30 detectors increased the utilization of the x-ray beam by 30 times over the single detector used per slice in first-generation systems. A relatively narrow fan angle of 10° was used. In principle, a reduction in scan time of about 30 times could be expected. However, the whole of this reduction in scan time was not realized because more data (rays and views) were acquired. The shortest scan time with a second-generation scanner was 18 seconds, 15 times faster than the first-generation system. Because there was an increase in the number of rays per view (to 600) and in the number of views (to 540), the image quality improved substantially.

On the downside of incorporating an array of detectors, instead of just two detectors, the detector array required the use of a narrow fan beam of radiation. Although a linear scanning *slit* arrangement makes for excellent scatter rejection compared to that used in plain film imaging, it does allow more scattered radiation to be detected than the pencil beam that was used in first-generation CT. The difference between pencil beam, fan beam, and open beam geometry in terms of scatter detection is illustrated in Figure 10.8.

### Third Generation: Rotate/Rotate, Wide Fan Beam

The translation motion of first- and second-generation CT scanners was a major limitation because at the end of each translation, the translational inertia of the x-ray tube/detector system had to be stopped, the whole system rotated, and then the translational motion had to be restarted. This design could never have led to fast scanning, because of the practical physical limitations that accelerating and decelerating a heavy stage and scan arm imposed. However, the success of CT as a clinical modality in its infancy gave manufacturers reason to explore more efficient, but more costly, approaches to the scanning geometry.

The number of detectors used in third-generation scanners was increased substantially (up to about 750 detectors), such that the linear detector array formed an arc wide enough to allow the x-ray beam to interrogate the entire patient (Fig. 10.9). Because detectors and the nec-

discussion of the evolution of CT scanners also allows the presentation and reinforcement of several key concepts in CT imaging.

### First Generation: Rotate/Translate, Pencil Beam

CT scanners represent a diverse cadre of technologies, from computers, motor control systems, x-ray detector design, and x-ray tube/generator systems. The first generation of CT scanners was a rotate/translate, pencil beam system (Fig. 10.7). Only two x-ray detectors were used, which measured the transmission of x-rays through the patient for two different slices. The acquisition of the many profiles and the many rays per profile required that the single detector (per CT image) be moved throughout all the necessary positions. This system used parallel ray geometry. Starting at a particular angle, the x-ray tube and detector system translated linearly across the field of view (FOV), acquiring 160 rays across a 24-cm FOV, for the projection at that particular angle. When the x-ray tube/detector system was finished with its translation, the whole system was rotated, and then another translation was used to acquire the next projection set. This procedure was repeated until 180 projections were acquired at 1° intervals.

There were other problems in addition to the amount of scan time that the first-generation systems posed. The NaI detector system could not accommodate the huge *dynamic range* in x-ray intensities. As the system translated and measured rays from the thickest part of the head to the area adjacent to the head, it experienced a significant change in x-ray flux. The early detector systems could not accommodate this large change in signal, and consequently the patient's head was inserted into a flexible membrane surrounded by a water bath. The water bath acted to bolus the x-rays so that the intensity of the x-ray beam outside the pa-

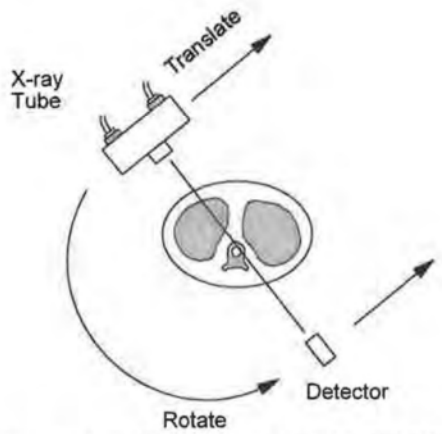



**Figure 10.7.** First-generation CT scanners used a rotate/translate motion. The x-ray tube was mechanically coupled to the detector. The whole stage was translated across the field of view, and then the stage was rotated. This procedure was repeated until 180 different transitions were made. The first-generation scanner acquired data in parallel beam geometry.

tient's head was similar in intensity to that inside the head. The NaI detector also had a significant amount of "afterglow," meaning that the signal from a measurement taken at one period of time decayed slowly and carried over into the next measurement if the measurements were made temporally too close together.

One advantage of the first-generation CT scanner was that it accepted only a very small pencil ray of x-rays, because only two detectors measured the transmission of x-rays through the patient. The pencil beam allowed very efficient scatter reduction, because scatter that was deflected away from the pencil ray was not measured by a detector. With regard to scatter rejection, the pencil beam geometry used in first-generation CT scanners was the best.

### Second Generation: Rotate/Translate, Narrow Fan Beam

The next incremental improvement to the CT scanner was the incorporation of a linear array of 30 detectors. The use of 30 detectors increased the utilization of the x-ray beam by 30 times over the single detector used per slice in first-generation systems. A relatively narrow fan angle of 10° was used. In principle, a reduction in scan time of about 30 times could be expected. However, the whole of this reduction in scan time was not realized because more data (rays and views) were acquired. The shortest scan time with a second-generation scanner was 18 seconds, 15 times faster than the first-generation system. Because there was an increase in the number of rays per view (to 600) and in the number of views (to 540), the image quality improved substantially.

On the downside of incorporating an array of detectors, instead of just two detectors, the detector array required the use of a narrow fan beam of radiation. Although a linear scanning *slit* arrangement makes for excellent scatter rejection compared to that used in plain film imaging, it does allow more scattered radiation to be detected than the pencil beam that was used in first-generation CT. The difference between pencil beam, fan beam, and open beam geometry in terms of scatter detection is illustrated in Figure 10.8.

### Third Generation: Rotate/Rotate, Wide Fan Beam

The translation motion of first- and second-generation CT scanners was a major limitation because at the end of each translation, the translational inertia of the x-ray tube/detector system had to be stopped, the whole system rotated, and then the translational motion had to be restarted. This design could never have led to fast scanning, because of the practical physical limitations that accelerating and decelerating a heavy stage and scan arm imposed. However, the success of CT as a clinical modality in its infancy gave manufacturers reason to explore more efficient, but more costly, approaches to the scanning geometry.

The number of detectors used in third-generation scanners was increased substantially (up to about 750 detectors), such that the linear detector array formed an arc wide enough to allow the x-ray beam to interrogate the entire patient (Fig. 10.9). Because detectors and the nec-

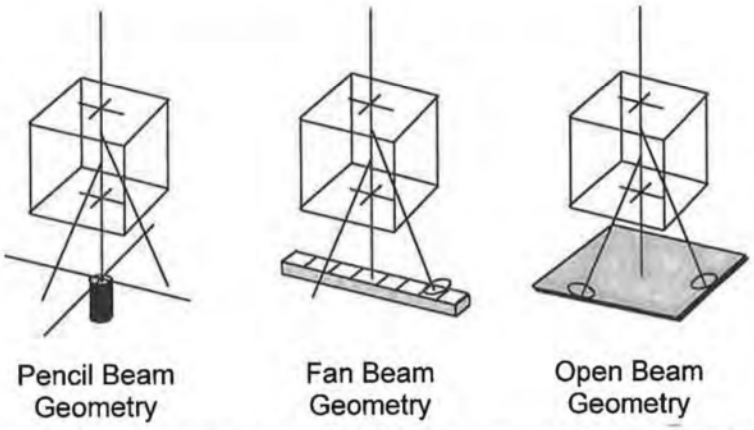



**Figure 10.8.** The pencil beam geometry used in first-generation CT was very efficient in eliminating the detection of scattered radiation (left). With fan beam geometry (center), a slit of radiation is incident on the patient. When x-rays are scattered in the same plane as the detector array, the scattered x-rays can strike adjacent detectors *(circle)*. With planar acquisition such as that used in screen-film radiography, an open beam geometry (right) is used. In this case, scattered x-rays in either direction can be detected *(circles)*.

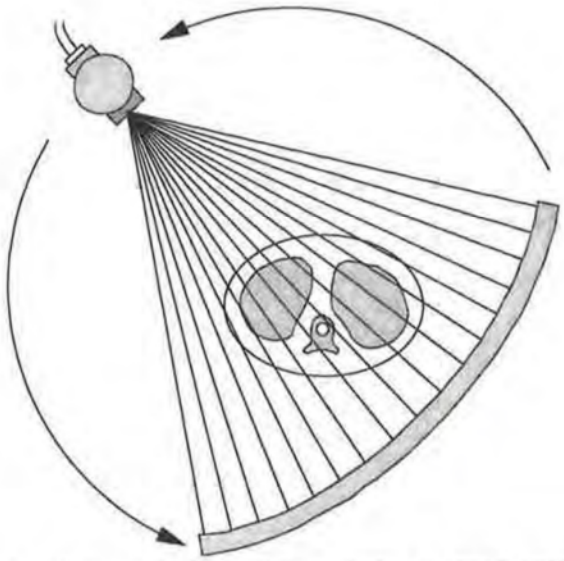


**Figure 10.9.** Third-generation CT acquisition embodies an array of detectors that is wide enough to image a complete projection across the patient. The many detectors (>700) eliminate the need for translating a single detector through a multitude of positions. The x-ray tube and the detector array are mechanically attached to each other, and rotate around the patient together. This motion is also called *rotate/rotate*.

essary electronics are expensive, this led to more expensive CT scanners. However, by replacing the single detector used in first-generation CT with an entire row of detectors, there was no need for translating an individual detector. The multiple detectors in the linear detector array capture the same number of measurements in one instant as was required by a complete translation of the first-generation scanner. Consequently, the x-ray tube and detector array, which are mechanically fastened to each other, rotate together around the patient without the need for any translation. The motion of third-generation CT is rotate/rotate, referring to the rotation of the x-ray tube and the rotation of the detector array. By eliminating the translation motion, the scan time could be reduced substantially. The early third-generation scanners could deliver scan times shorter than 5 seconds. Newer systems have scan time options of less than 1 second on some systems.

The evolution from first- to second- to third-generation scanners involved radical improvement with each step. Developments of the fourth- and fifth-generation scanners led not only to some improvements but also some compromises in clinical CT images compared to third-generation scanners. Consequently, rotate/rotate scanners are still as viable today as they were when they were introduced in 1975. The differences between third- and fourth- (as well as fifth-) generation CT should be compared by the reader, because each offers some benefit but also some trade offs. The third- and fourth-generation CT geometries have experienced a recent modification by way of an electrical slip ring, and this will be discussed in the section below about helical scanners.

### Fourth Generation: Rotate/Stationary

Although the rotate/rotate geometry of third-generation CT solved the mechanical inertia problems by removing the translational motion, practical problems remained. The signals from the large number of detectors (as many as 1000 or so detectors) in the linear detector array all needed to be conveyed via wires from the rotating gantry to the computer system sitting fixed on the floor. This means that the ribbon cable used to connect the detectors with the electronics that recorded the signal needed to be carefully rolled out from a cable spool as the gantry rotated, and then as the gantry stopped and began to rotate in the opposite direction, the ribbon cable needed to be retracted. Consequently, having the detectors on the moving part of the scanner made for pragmatic problems with cable wear, the generation of spurious signals from the moving signal wires, and so on. In addition to these problems, it is never possible to have such a large number of detectors in perfect balance with each other. Each detector and its associated electronics will have a certain amount of drift, causing the gain in the signals from the many detectors to shift over time. The rotate/rotate geometry of third-generation scanners leads to a situation where a single detector is responsible for an annular path through the image, as shown in Figure 10.10. Detectors toward the center of the linear detector array provide data in the reconstructed image in an annulus that is small in diameter. The annular re-

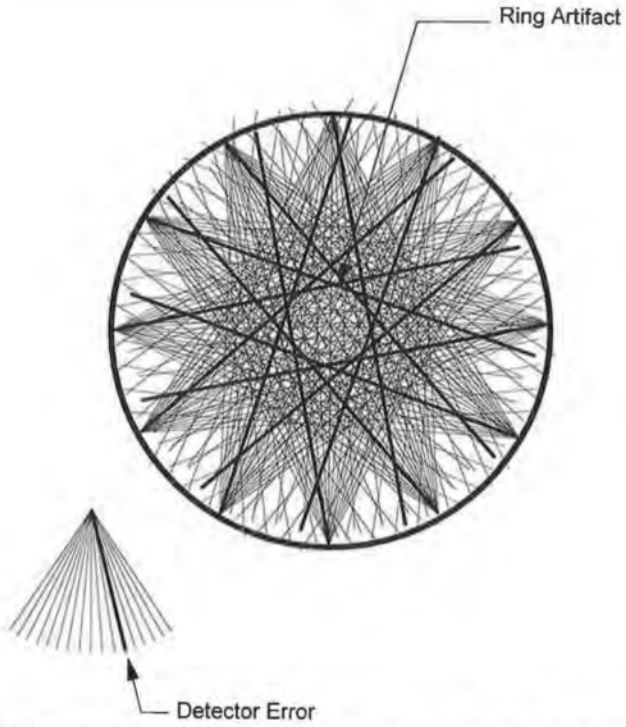



**Figure 10.10.** In third-generation CT acquisition, detector calibration is crucial. If one detector goes out of calibration, it can cause ring artifacts on the reconstructed image. This figure illustrates how one detector is responsible for an annular ring in the reconstructed image. The diameter of the ring artifact will increase as the errant detector position moves from the center of the detector array to the periphery.

gion in the image associated with each detector has a larger diameter as the associated detector is positioned toward the periphery of the detector array. Because of the dependency of an annular region on a single detector (which is a consequence of the way the images are acquired and reconstructed from the raw data), when a single detector experiences some electronic drift and goes out of calibration, ring artifacts can be seen on third-generation CT images.

Fourth-generation CT scanners were designed to overcome the problem of electronic drift between the many detectors used in the system, and therefore this design eliminates ring artifacts due to detector calibration problems. With fourth-generation design, the detectors are removed from the rotating gantry and are placed on a stationary annulus around the patient (Fig. 10.11). Because the detectors are stationary, the wires leading between them and the stationary electronics and computer system are stationary also. However, instead of needing an arc of detectors as with third-generation CT, an entire 360° ring of detectors is needed in fourth-generation CT to encircle the patient. Since detectors and their associated electronics are expensive, fourth-generation CT led to further

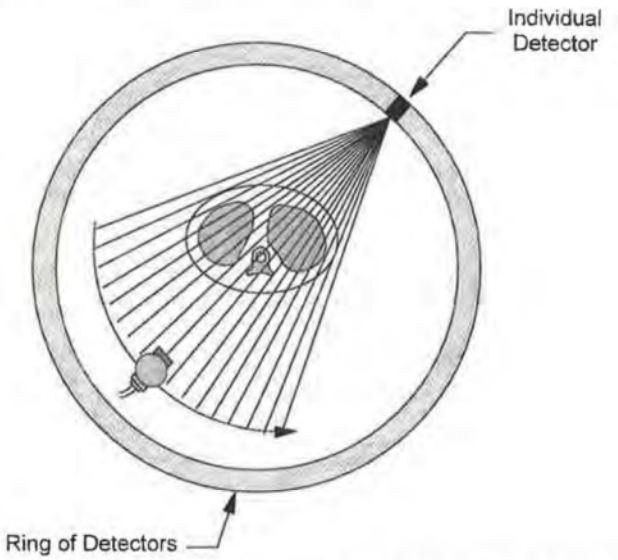



**Figure 10.11.** Fourth-generation CT scanners use a stationary ring of detectors positioned around the patient. Only the x-ray tube moves, and hence the motion of a fourth-generation scanner is rotate/stationary.

increases in cost for CT systems. Modern fourth-generation CT systems use from 1200 to 4800 individual detectors. Because the x-ray tube still rotates but the detectors are stationary, fourth-generation CT uses a rotate/stationary motion.

There is a consequence of making the detector array stationary that is not obvious but is the foundation of the fourth-generation design. The fan beam in third-generation CT uses a fan where the apex of the fan is the x-ray tube, and the rays fan out from the x-ray focal spot to the multiple detectors positioned on the detector array. The detectors toward the center of the array make the transmission measurements I(x), while a reference detector at the end of the detector array acquires the reference intensity, $I_o$. The fan beam in fourth-generation CT, however, uses a fan where each ***detector*** is the apex of the fan, and the rays acquired by each detector fan out to different positions of the x-ray source. In the vernacular of CT, third-generation design uses a *source fan,* whereas fourth-generation uses a ***detector fan.*** The third-generation fan data are acquired by the detector array simultaneously, in one instance of time. The fourth-generation fan beam data are acquired by a single detector over the period of time that is required for the x-ray tube to rotate through the arc angle of the fan. This difference is illustrated in Figure 10.12. With fourth-generation geometry, each individual detector is responsible for acquiring a fan of transmission data, I(x). Each individual detector also makes its own reference measurement of $I_o$. In third-generation systems, the $I_o$ measurement is made by a separate detector that is positioned toward the edge of the fan. Because the same detector is used for the

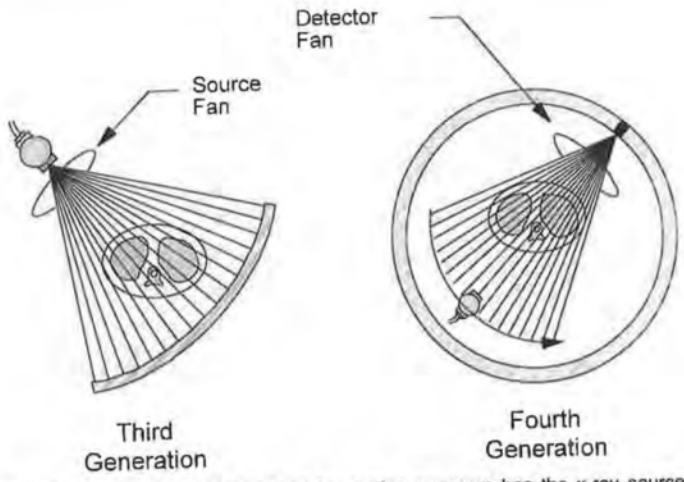



**Figure 10.12.** The fan beam in third-generation scanners has the x-ray source (the x-ray tube) as its apex, and this configuration is referred to as a *source fan.* Third-generation scanners require excellent detector calibration and stability. Fourth-generation scanners have a single detector as the apex of the fan beam, a so-called *detector fan.* Fourth-generation scanners require excellent x-ray tube output stability.

transmission measurements and the $I_o$ measurement in fourth-generation systems, any differences in detector calibration cancel out. The drift of a given detector can be described by a detector-specific gain value, g. The CT projection value, P, is calculated as:

$$P = LOG\{(g_1\ I_0)/(g_2\ I(x))\}$$

With third-generation scanners, the $I_o$ value and the I(x) value are acquired by different detectors, which may have different gains, for example $g_1$ and $g_2$. With fourth-generation scanners, $I_o$ and I(x) are acquired by the same detector, and therefore $g_1 = g_2$. When $g_1 = g_2$, the gain terms cancel out of the above equation, and therefore the projection values (P) are not sensitive to detector drift with fourth-generation design. This is the principal benefit of fourth-generation scanners. Because differences in detector calibration are automatically compensated for by the way the data are normalized, fourth-generation scanning geometry eliminates ring artifacts. Fourth-generation scanners require very stable x-ray sources (constant output over time) since the transmission measurements, I(x), and the $I_o$ measurements are acquired at different *times* during the scan.

Some fourth-generation CT scanners add an additional motion of the detector array during CT acquisition. The x-ray tube is normally constrained to rotate inside the detector ring that surrounds the patient. This causes an increase in focal spot magnification and also makes for a smaller usable bore of the scanner. If the region of the detector array that is near the x-ray tube is wobbled out of the way (Fig. 10.13), room can be made for the x-ray tube to rotate outside (or adjacent to) the detector array. This wobbling motion is called *nutation,* and scanners that use this tech-

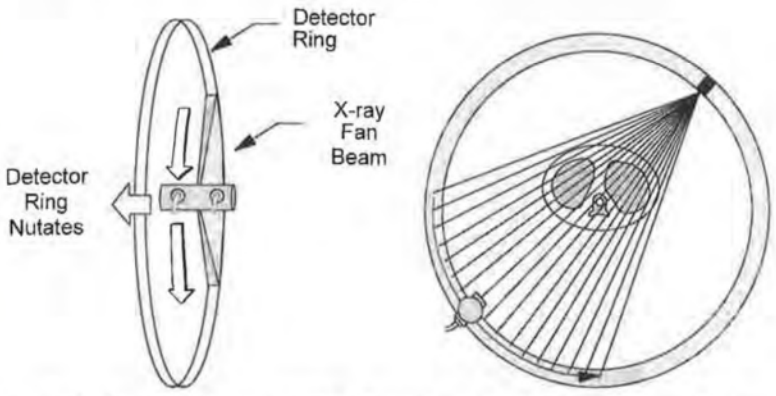



**Figure 10.13.** Some fourth-generation CT scanners use a *nutation* of the x-ray detector ring. This design permits the x-ray tube to be positioned further away from the patient, which reduces focal spot magnification and dose to the patient. As the x-ray tube rotates around the patient, the detector ring wobbles out of the way to mechanically permit the tube to pass by.

nique are called rotate-nutate/stationary or fourth-generation/nutate scanners.

The differences in fan beam geometry account for the fundamental difference between third-and fourth-generation CT; however, there are numerous other advantages and disadvantages for each scanning geometry. These are discussed in a comparative sense in the following section.

## Comparison between Third- and Fourth-Generation CT

This section contains discussion of some of the advantages and disadvantages in third- and fourth-generation scanner geometries. Table 10.1. lists of some of the commercial scanners and their geometry.

### Detector Types

Most modern CT systems use either Xenon detectors or solid-state scintillator detectors. The xenon detectors use high pressure (about 25 at-

**Table 10.1**
**The Scanning Geometries of Several Commercially Available CT Scanners**

| Vendor and Model | Scanning and Geometry |
|---|---|
| General Electric 9800 | Rotate/Rotate |
| General Electric Advantage | Rotate/Rotate (slip ring) |
| Philips T60 | Rotate/Rotate |
| Picker 1200 | Rotate/Stationary |
| Picker PQ2000 | Rotate/Stationary (slip ring) |
| Shimadzu | Rotate/Rotate |
| Siemens DRH | Rotate/Rotate |
| Toshiba 900S | Rotate/Stationary (slip ring/nutate) |
| Toshiba Xpress | Rotate/Rotate (slip ring) |

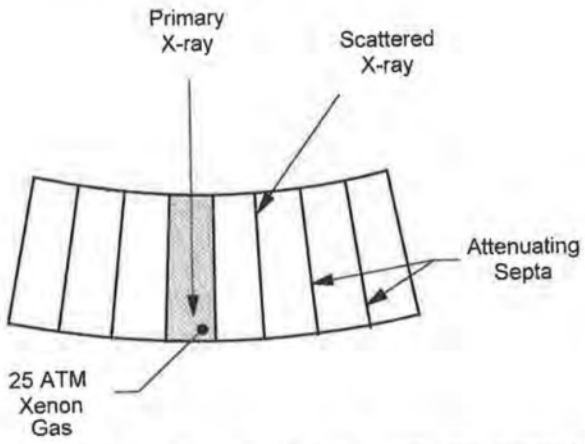



**Figure 10.14.** Xenon detectors collect the charge resulting from ionization of the gas molecules in the active volume of each detector element (ionization detectors). Because the density of gas is lower than solid detectors, the sensitive volume is made quite long in the attempt to detect as many incident x-ray photons as possible. The vanes between the individual detector cells act in a manner similar to the grid bars in an antiscatter grid. Xenon detectors, because of their strong directional dependency, need to be aligned with the x-ray source at all times. Therefore, only third-generation scanners can use xenon detectors.

mospheres) nonradioactive xenon gas, in long thin cells between two ionization plates (Fig. 10.14). Although a gaseous detector does not have the same detection efficiency as a solid one, the ability to pack xenon detectors tightly compensates to some extent for the lower absorption efficiency. The good packing density improves the geometric efficiency. By eliminating dead space between detectors, fewer x-rays are wasted.

The long, thin ionization plates of a xenon detector are highly directional. Xenon detectors need to be positioned in a fixed orientation with respect to the x-ray source, because of their high directionality. This means that xenon detectors cannot be used for fourth-generation scanners, since fourth-generation detectors have to record measurements as the x-ray tube sweeps over a wide angle. Xenon detectors are therefore only used for third-generation systems, where the orientation between the x-ray tube and the detector array is mechanically fixed.

Solid-state detectors are made of scintillator materials, which emit visible light when struck by x-rays. The light emitted by the scintillator is collected by a photodiode, an electronic device that converts light into an electrical signal. Solid-state detectors in CT are often made of $CdWO_4$, or of gadolinium-based ceramic materials. Because the density of solid, high atomic number materials is substantially higher than that of pressurized xenon gas, solid-state detectors typically have better absorption efficiency than xenon detectors. This means that fewer x-ray photons pass through the solid-state detectors and go undetected. It is sometimes argued that because solid-state detectors cannot be placed right next to each other, they have lower geometric efficiency than xenon detectors.

Spaces between adjacent detectors that allow x-ray photons to pass through undetected result in poorer geometric efficiency. Modern fabrication technology, however, has resulted in solid-state detectors that can be packed very closely next to each other, and therefore their geometric efficiency has improved substantially. Solid-state detectors are used on all fourth-generation CT scanners and are used on many third-generation systems.

**Scatter Rejection**

The long, thin plates that are used in xenon detectors also act like the vanes of a scatter grid. The high degree of directionality of the xenon detector provides a good acceptance angle for primary x-rays but rejects scattered x-rays that strike the detector at different angles. With third-generation geometry, the alignment between the detector and the x-ray tube is fixed. Indeed, the detector array and the x-ray tube are mechanically mounted on the same gantry. Therefore, scatter grids or beam collimation devices can be used, even with solid-state detectors. With fourth-generation scanners, the orientation between each detector and the x-ray beam changes as the x-ray tube rotates around, and therefore no collimation or grid-like system can be used. Consequently, third-generation scanners have better in-plane scatter rejection than do fourth-generation systems.

Third-generation scanners have another advantage with regard to scatter rejection. With some fourth-generation systems, there is no mechanical support on the post-patient side of the beam. This means that in the slice-thickness dimension, there is no post-patient collimation, which can serve to limit the detection of scattered radiation (Fig. 10.15). For systems without post-patient collimation, greater scatter acceptance will result in reduced image quality.

**Focal Spot Magnification**

With fourth-generation systems, the detector array is wrapped all the way around the patient. Clearly, the path of the x-ray tube as it rotates on the gantry cannot intersect the detectors. This means that the x-ray tube in fourth-generation systems is closer to the patient than with third-generation systems. The source-to-patient distance is shorter, whereas the patient-to-detector distance is about the same. Therefore, there is more geometric magnification with most fourth-generation systems. The magnification of the x-ray tube focal spot can cause a reduction in the resolution of the CT image. Some fourth-generation systems use x-ray tube nutation, which allows the x-ray tube to be positioned outside the circle imposed by the detector ring. This design is aimed at reducing the geometric magnification by increasing the source-to-patient distance.

**Image Reconstruction**

The fan data used in reconstruction are preprocessed by mathematical filtration (convolution). In third-generation systems, the first fan beam is acquired just moments after the x-ray acquisition starts. This means that the computer can start the necessary mathematical computations on the

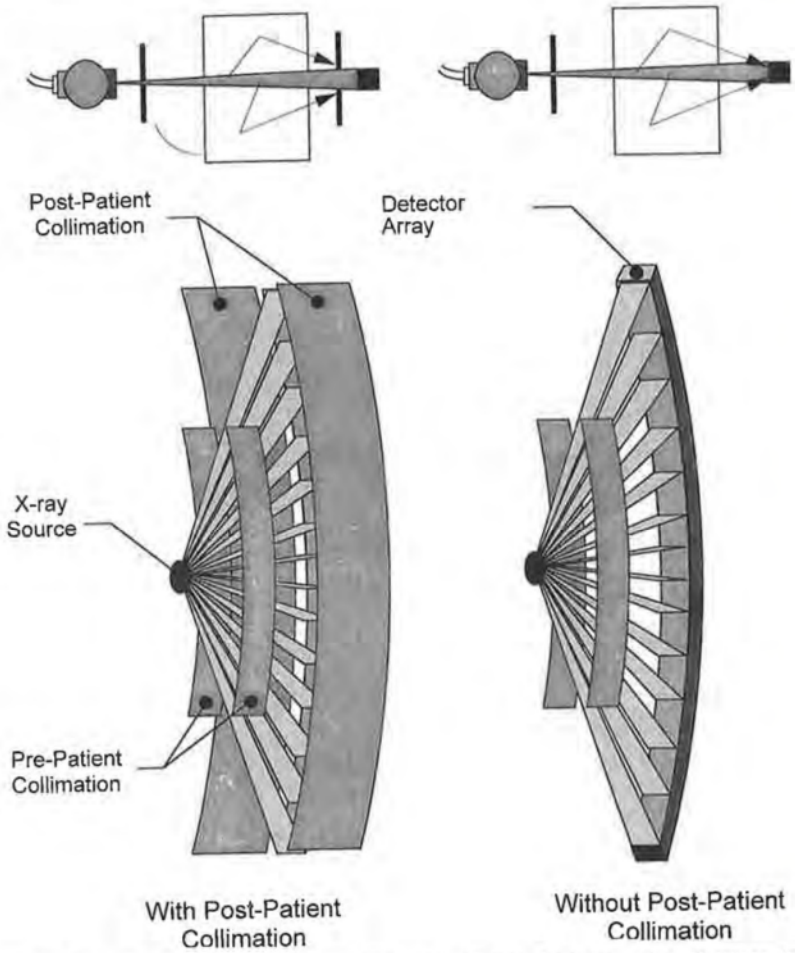



**Figure 10.15.** The slice thickness is determined by lead jaws that collimate the beam before it strikes the patient, and these are called the *pre-patient collimator*. Post-patient collimation is used to prevent multiply scattered radiation that emanates from within the patient from reaching the detector.

acquired data while it is coming from the detectors, thus speeding up the reconstruction time. With fourth-generation scanners, however, each fan of information is acquired over a sizable period of time as the x-ray tube sweeps through the arc of the fan. This does not allow for the simultaneous mathematical processing of the data, which can slow the reconstruction time and thus reduce the patient throughput of the scanner. This was more of a factor when computers were slower, but as computer technology advances this becomes less of a concern.

### Fifth Generation: Stationary/Stationary

A novel CT scanner was developed for cardiac tomographic imaging. This "cine-CT" scanner does not use a conventional x-ray tube but rather a

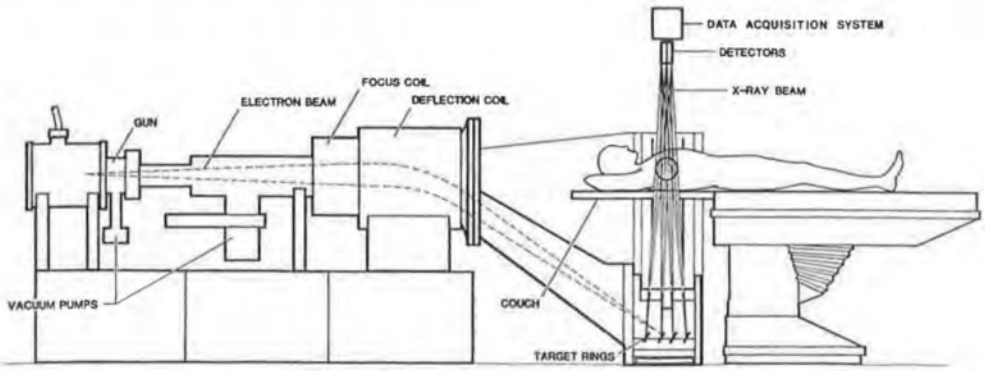



**Figure 10.16.** The fifth-generation CT scanner design uses no moving parts during the scan. The detector ring is stationary as in fourth-generation design. Instead of a rotating x-ray tube, the Imatron CT scanner uses a stationary ring of tungsten. A highly energetic focused electron beam is magnetically steered around the tungsten ring during the scan, causing x-ray emission where the electron beam strikes the tungsten ring.

large ring of tungsten that circles the patient, which lies directly opposed to the detector ring. The x-rays are produced from the focal track as a high-energy electron beam strikes the tungsten. There are no moving parts to this scanner gantry. The electron beam is produced in a cone-like structure (a vacuum enclosure) behind the gantry and is electronically steered around the patient so that it strikes the annular ring of tungsten (Fig. 10.16).

The cine-CT system is marketed primarily to cardiologists. It is capable of 50-millisecond scan times and can produce 17 CT slices each second. Although invaluable for imaging rapidly moving structures within the patient such as the heart, the nonconventional x-ray generation system has some limitations with respect to x-ray tube output in the short scan time used. Consequently, the number of x-ray photons used to generate an image is lower than most comparable third- or fourth-generation systems, unless multiple scans are added together.

### Helical CT Scanners

Recently, CT vendors have modified the design of third- and fourth-generation scanners so that no connections are directly hardwired to the x-ray tube from the generator or to the detector array from the computer electronics. Instead, the electrical supply to the x-ray tube and the electrical connections between the moving detector array and the stationary computer are achieved using *slip-ring* technology. This technology, although not new, has achieved a renewed interest by manufacturers and buyers of such slip-ring scanners. The slip ring is a circular contact with sliding brushes that allows the gantry to rotate continually. This design makes it possible to achieve greater rotational velocities than conventional systems, which allows for shorter scan time.

A recent innovation has been made possible by improvements in x-ray tube design and computer speed. *Helical scanning* uses third-generation or fourth-generation slip-ring design. While the gantry is rotating,

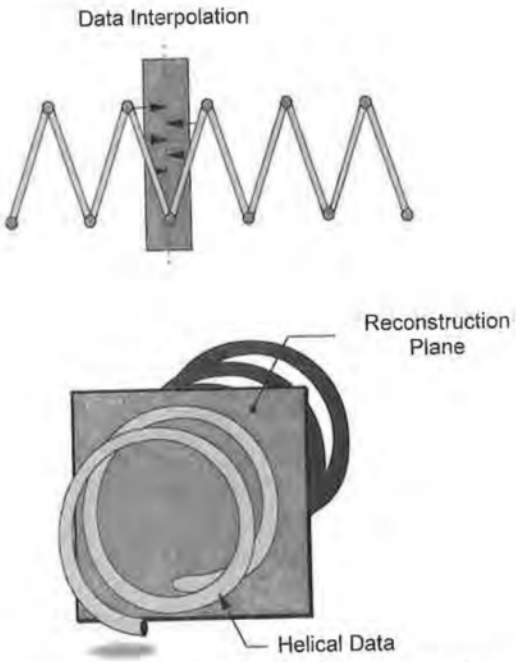



**Figure 10.17.** Helical CT scanners use either third- or fourth-generation gantry design. Electrical slip-ring contacts allow the gantry assembly to rotate continuously. By moving the table (and hence the patient) during the scan, the date are acquired in a helical geometry around the patient. To reconstruct a cross-sectional planar image, the helical data need to be interpolated into a plane before reconstruction.

the table is moved simultaneously. By avoiding the time required to index the patient table, the total scan time for imaging the entire patient can be much shorter (e.g., 30 sec/entire abdomen). Consequently, helical scanning allows the use of less contrast agent, since the total scan time is shorter, and increases the throughput of patients through the scanner. Furthermore, in some instances the entire scan can be performed within a single breath-hold of the patient, so that inconsistent levels of inhalation typical of conventional scanner acquisitions are avoided.

The advent of helical scanning has introduced many different considerations. Because the patient is advancing while the gantry rotates, a full 360° set of projections for each slice in the patient is not measured. Consequently, to produce reconstructions of *planar* sections of the patient, the raw data from the helical data set are interpolated to approximate the acquisition of planar reconstruction data (Fig. 10.17). Notice that the motion of a helical scanner is in fact helical, not spiral, despite the loose marketing terminology that is used by some vendors. A spiral has a continually decreasing diameter, a helix does not. The speed of the table motion relative to the rotation of the CT gantry is a very important consideration, and the *pitch* is the parameter that describes this relationship. The pitch is defined as:

Pitch = (table increment distance [in mm] per 360° gantry rotation) / (slice thickness [in mm])

For a 10-mm slice thickness, if a gantry makes a full revolution in 1 second, and the table is moved 10 mm per second, the pitch will be 1.0. If the table is moved 15 mm per second, there is a 1.5 pitch. A high pitch value describes a helical scan that is loose, a low pitch value is a tightly wound helix (Fig. 10.18). By increasing the pitch, a greater FOV can be imaged in a given amount of time. However, pitch values greater than 1.0 imply that some of the data in the patient have been skipped, i.e., the data acquisition is not contiguous. Pitch values less than 1.0 imply a certain amount of oversampling.

A 30-second scan with a pitch of 1.0 for a 10-mm slice thickness and a scanner rotation velocity of 1 rotation per second would yield a helical set of data with 30 revolutions covering a length of 30 cm of the patient. Conventional wisdom would suggest that 30 tomographic images, each

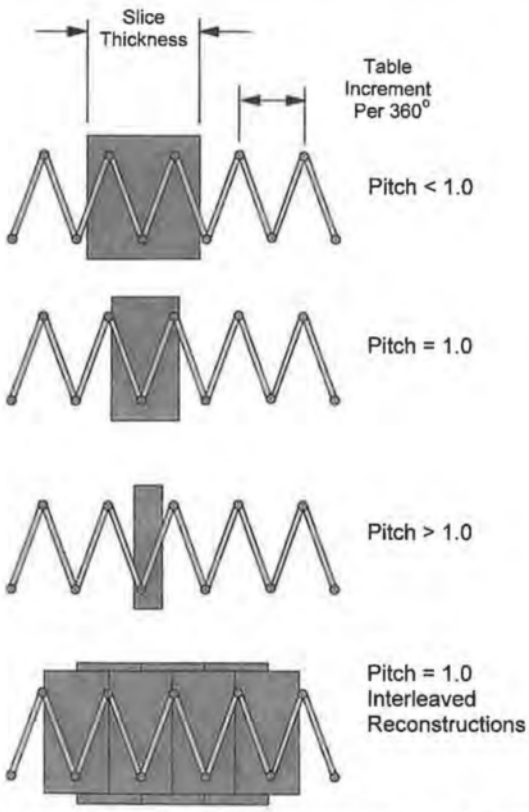



**Figure 10.18.** The *pitch* of a helical scan essentially determines how tightly the helix is wound. A pitch of 1.0 means that the table increment per 360° rotation of the x-ray tube is equal to the slice thickness. A pitch greater than 1.0 is a loosely wound helix and implies that a certain amount of the projection data is skipped. A pitch less than 1.0 is a tightly wound helix and implies that over sampling of the data occurs.

image contiguous with the next, should be computed. However, the way that the data are acquired in helical scanning allows almost an infinite variety in the reconstruction strategy. For example, this data set can be used to generate 300 images, each indexed 1 mm from the next. The slice thickness would still be 10 mm. Although 300 reconstructions would require too much computer time to be practical routinely, a large number of slices is advantageous for multiplanar reconstructions and three-dimensional rendering. It would be practical to reconstruct 60 interleaved (10-mm) slices, from the 30-cm helical data set. By interleaving the reconstructed images, partial volume effects could be reduced for anatomical regions of interest (e.g., the liver).

## DETAILS OF ACQUISITION

### Slice Thickness

The slice thickness in CT is determined by the physical collimation of the incident x-ray beam with two lead jaws. As the gap between the two lead jaws widens, the slice thickness increases. However, the width of the detectors in the detector array places a maximal limit on the slice thickness. Opening up the collimator jaws to the point where the projected slice thickness at the detector is wider than the detector will do nothing to increase the slice thickness (Fig. 10.19).

There are trade-offs with respect to slice thickness. For a scan performed at the same kV, mA and time, the number of detected photons increases linearly with the slice thickness. For example, going from a 1-mm slice thickness to a 3-mm slice will triple the number of detected

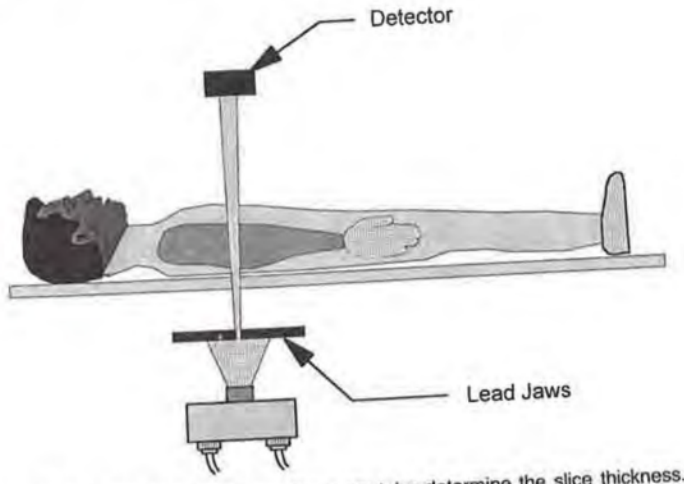



**Figure 10.19.** The lead jaws near the x-ray tube determine the slice thickness. The lead jaws are moved by small motors when different slice thicknesses are called for. The detector thickness determines the maximal slice thickness. Because of the finite focal spot and detector sizes, and the beam divergence in the slice thickness dimension, the volume of tissue that is irradiated and that contributes to the image is not completely planar.

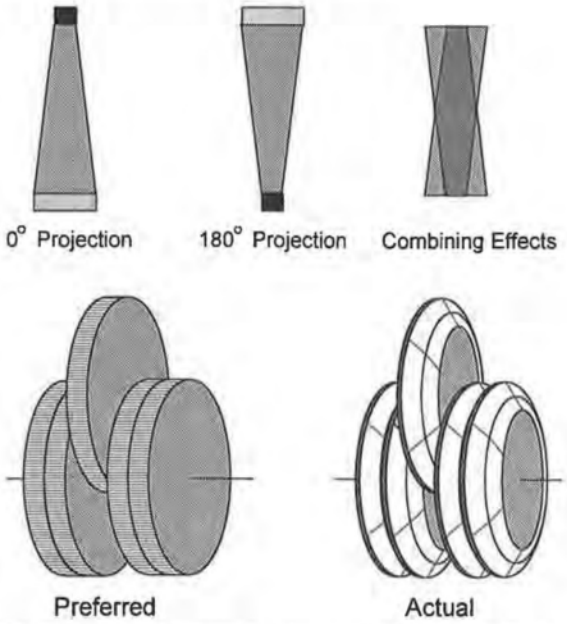



**Figure 10.20.** In modern CT scanners, data are acquired in both directions along a line. The combined influence from a projection and its 180° complementary projection make for slice sensitivity profiles that are not planar but rather are shaped like Frisbees.

x-ray photons, and going from a 5-mm slice to a 10-mm slice will double the number of detected x-ray photons. Since the noise in the reconstructed CT images is reduced (the signal to noise is increased) as the number of detected x-ray photons increases, wide slice thicknesses yield better contrast resolution of larger objects than narrow ones, at the same x-ray techniques. The benefit of narrower slice thicknesses is improved spatial resolution in the thickness dimension of the image and reduced partial volume averaging of small objects. To maintain the same statistical integrity (signal-to-noise ratio) in going from a 5-mm slice to a 1-mm slice, the tube current per slice (milliAmpere Seconds—mAS) would have to be increased by a factor of five.

Because x-rays diverge from the focal spot in any x-ray system, the *slice sensitivity profile* is not a perfectly planar section. When contiguous 10-mm slices are acquired on a CT scanner, one has the impression that the images correspond to sections in the patient similarly to how a loaf of bread is sliced into individual slices. Unlike the bread example, where each slice has parallel sides that abut evenly with the next slice, the thickness of the voxels in a CT image would look more like a stack of frisbees (Fig. 10.20). The unevenness in the apparent slice sensitivity profile is the result of the relatively large focal spots combined with the edge effects of the collimator and x-ray scatter.

### Number of Projections

The number of projections has a profound effect on the CT image quality. In principle, the x-ray projections around the patient only need to encircle 180°, since the direction of the x-ray beam does not matter in determining the attenuation along a given path. However, there are nuances in CT acquisition that make the rays acquired in opposite directions not completely redundant. Consequently, a 360° (or more) acquisition produces better image quality than partial scans. An increase in the number of projections means that more x-ray photons will contribute to the formation of the image, assuming that each projection is acquired with the same x-ray fluence. Also, the edges of the x-ray beam are not perfectly parallel with each other as the beam diverges from the collimator jaws to the detector array. This was discussed in the last section. By acquiring two rays in opposite directions, the divergence in the x-ray beam is made symmetrical, and thus the shape of the slice sensitivity profile is at least symmetrical around the central axis in the image. Also, the resolution in the image is very much related to the size and spacing of the detectors in the detector array. The central axis of rotation of a third-generation scanner is aligned precisely with a point in the central detector that is ¼ of the width of the detector. This *quarter detector shift* results in the detector array sampling with exactly a *half* detector shift from one projection to the 180° opposite projection (Fig. 10.21). This shifting of the detector array results in an oversampling in the data, which improves the spatial resolution of the image.

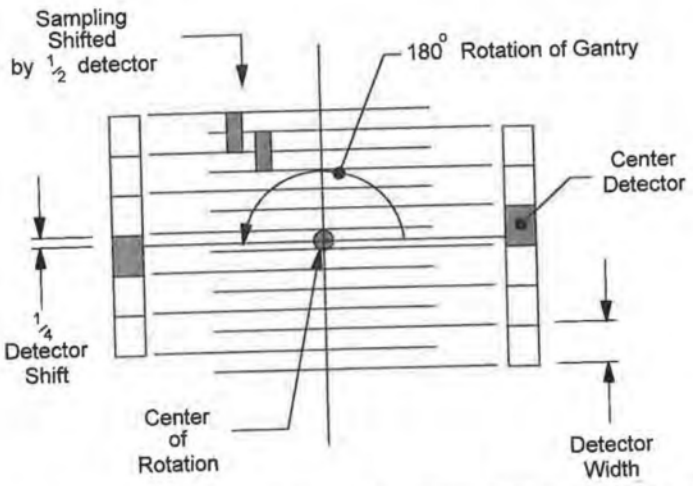



**Figure 10.21.** Many CT scanners incorporate a *quarter detector shift,* which means that the center of rotation of the gantry is aligned ¼ of the way from the edge of the center detector. With this alignment, the opposite projections at each angle will represent *half* detector shifts. By shifting the detector array by one-half detector width, the ray sampling is doubled and the possibility of aliasing is reduced.

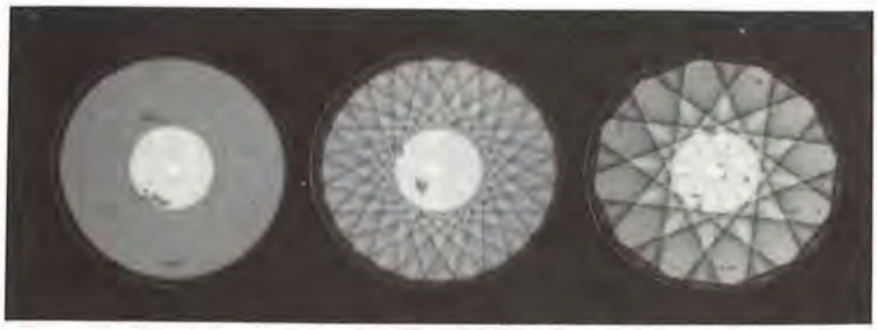


**Figure 10.22.** A series of three images showing the effect of a different number of projection data. No quantum noise is present in these images. The number of rays per view was 200, and the number of views used in the reconstruction were 96 (left), 24 (center), and 12 (right).

The theoretical minimal angle around the patient that needs to be sampled is 180° plus the fan angle. The fan angle for modern third-generation scanners is about 50°, so the minimal rotation of the gantry to acquire a CT image in this case would be 230°. The maximal angle of rotation for conventional scanners is determined by the high voltage cables connected to the x-ray tube, and is typically a 450° to 500° rotation. For slip-ring scanners, there is no maximal angle, and theoretically a large number of rotations could be acquired to enhance the statistical integrity in the image.

The number of projections also has an impact on the image quality. Fewer projections lead to a more choppy set of backprojected points, which results in poor image quality. This effect is illustrated in Figure 10.22. When the number of projections used in the image is sparse, the circumferential resolution becomes worse. The circumferential resolution (i.e., the resolution along a concentric circle in the image) is determined by the number of projections (Fig. 10.23). With third-generation scanners, the number of projections that are acquired is dependent on how frequently the detector array is sampled in time. Because this is easily adjustable with third-generation scanner geometry, the number of projections can be varied depending on the desired image quality. In fourth-generation scanners, however, the number of projections is determined by the number of detectors that are in the detector array around the patient. For a 1200 detector system, 1200 projections can be used. A fewer number of projections can be made by adding the values from two adjacent detectors, for example to get 600 projections. This would be done if reconstruction time were critical, or to trade spatial resolution for increased number of photons and therefore lower relative noise.

### Number of Rays

The number of rays in each projection is determined by the number of detectors in the detector array, for third-generation systems. With fourth-generation systems, the number of rays is determined by how frequently

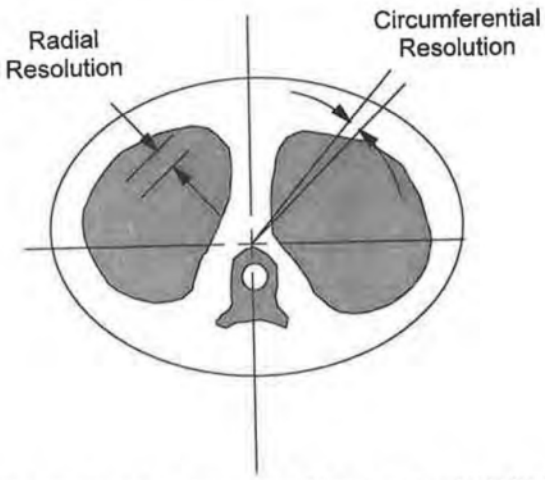



**Figure 10.23.** The resolution elements on a CT scan are peculiar to the reconstruction process. The number of views determines the *circumferential* resolution. The circumferential resolution gets worse toward the periphery of the image, because the view density is greatest in the center of the image. The *radial* resolution, which is the resolution along a line extending from the center of the image to the edge, is determined by the ray sampling.

the individual detectors are sampled as the x-ray tube sweeps around the fan angle. The more frequently the detector is sampled, the more rays that result. The number of rays in a CT scan affect the radial component of resolution. That is, the resolution along a line running from the center of the image to its periphery is determined by the number of rays per projection. A sequence of images acquired with different numbers of rays per projection is shown in Figure 10.24.

There are many parameters that influence image quality in CT. The bottom line in terms of the number of rays and projections used, is the more the merrier. The first-generation EMI scanner used 160 rays per

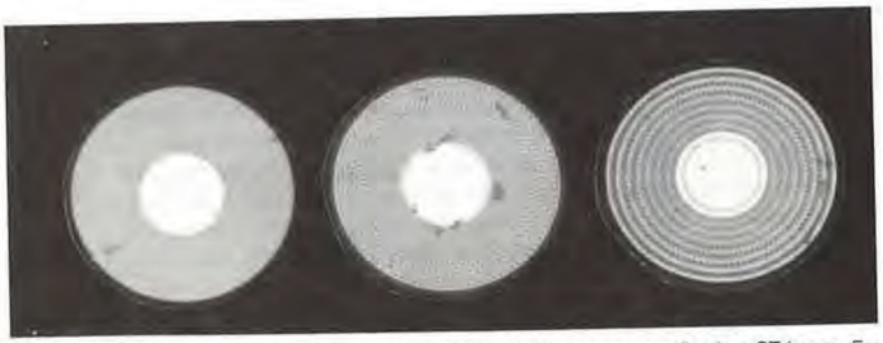


**Figure 10.24.** A series of three images that demonstrate the effect of different ray sampling in a CT image. For these images, 100 views were used in each, but the number of rays were 200 (left), 50 (center), and 25 (right). The concentric circle artifacts in the right image illustrate that ray sampling determines the radical component of resolution.

view for 180 views totaling 28,800 data points in the reconstruction. With the 80 × 80 pixel matrix, this translates to an average of 5.7 data points per pixel in the reconstruction circle. By comparison, a modern third-generation scanner may use 750 rays per projection with about 600 projections, totaling 450,000 data points. For the 512 × 512 image matrix, this corresponds to an average of 2.8 data points per pixel in the reconstruction circle.

### Signal to Noise versus Patient Dose

With pixel sizes on the order of 0.5 mm, the spatial resolution of CT is no where near that of screen-film radiography. The Nyquist limit for 0.5-mm pixels in CT is 1.0 line pair per mm, versus the 10 line pairs per mm that is possible with mammographic screen-film systems. CT, however, has excellent contrast resolution. Contrast resolution is determined essentially by the signal-to-noise ratio (SNR), which in turn is determined by the amount of quantum noise in the image. Because a CT scan requires a fair amount of dose to the patient (3–8 Rads), which is many times the dose for most screen-film images, it is reasonable to expect that CT images should have better SNRs. The gray scale values in CT range from −1000 to 3095, a total of 4096 different values. On a typical CT scan of, for example, a water phantom, the standard deviation that can be measured on the system is about 5 gray scale values. This means that the minimal amount of contrast that is detectable with CT is on the order of 0.5%. With screen-film radiography, the minimal detectable contrast level is on the order of 5%, ten times worse.

### Spatial Resolution

Although the spatial resolution of CT is much lower than that of screen-film radiography, combined with the exquisite contrast resolution of CT, the spatial resolution is quite good for many applications. There is an assortment of parameters that influence spatial resolution. Many of the same factors that influence spatial resolution in conventional radiography also affect the resolution in CT. For example, the size of the focal spot will impact CT resolution, as will patient motion during the scan. In CT, patient motion can blur diffuse edges as in radiography, but can also cause streaking artifacts if the motion is of a high-contrast object (such as a surgical clip).

In radiography, the resolution characteristics in the image are approximately the same over the entire extent of the image. For example, the blur imposed by the screen-film system will be the same over the whole FOV. In CT, however, because of the way in which the image is reconstructed, the resolution characteristics change depending on location in the image. The resolution limitations do not run strictly in the horizontal and vertical directions, but rather have radial components and circumferential components.

In any digital imaging technique, the size and spacing of the detectors will influence the resolution. Smaller detectors permit higher resolution (Fig. 10.25). The width of the backprojected rays through the im-

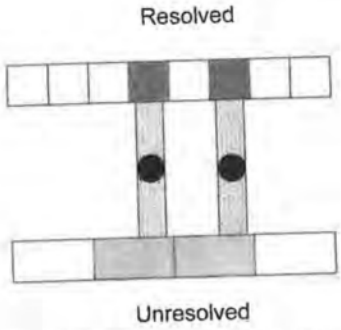



**Figure 10.25.** The spacing of the detectors in CT determines, along with other considerations, the spatial resolution that is possible with a CT scanner. In this figure, the upper detector sampling is sufficient to *resolve* the two objects that are present. The lower detector sampling is insufficient to distinguish that two objects are present instead of one.

age are essentially the width of the detector used in acquiring the data. The detector has two dimensions. The thickness of the detector, coupled with the slice thickness collimators, determine the voxel thickness of a given CT image. How does the slice thickness (along the $z$ axis) affect *spatial resolution in the (x,y)* plane of the image? If the anatomy that is being imaged does not change rapidly in the $z$ direction, then the spatial resolution of the image will be good, even for thicker slices. An example of this would be an axial slice through an arm. Because the bones, vessels, muscles, and ligaments tend to run along the long axis of the arm (parallel to the $z$ axis), their position does not change too much through the depth dimension of the voxel. Good resolution in the image would result. For anatomical sections where the anatomy changes more rapidly along the $z$ dimension, thicker slices will result in a more blurred appearance and thus a loss of resolution in the CT image (Fig. 10.26).

The FOV of a CT image is usually changeable with most CT scanner designs. With the same size image matrix (typically 512 × 512), as the FOV increases the pixel size increases. For example, for a 50-cm FOV, with 512 pixels across the diameter of the reconstruction results in pixel sizes of about 1 mm (500 mm / 512 pixels = 0.98 mm). With large fields of view, the pixel size can become the limiting factor in terms of spatial resolution. This can be overcome by using *zoom reconstruction* which entails reconstructing the data within a smaller FOV and displaying it using the same pixel matrix. For example, if a 30-cm FOV is reconstructed, the pixel size becomes 0.59 mm (i.e., 300 mm/512 pixels). At the point where the pixel size no longer limits spatial resolution, further levels of zoom will not produce better images. This limit is reached when the pixel size is about equal to the detector width.

The number of rays and projections influence the spatial resolution as discussed above. In addition, various mathematical filter algorithms applied during the reconstruction can enhance or suppress spatial resolution. Table 10.2. lists other parameters that influence the resolution in CT images.

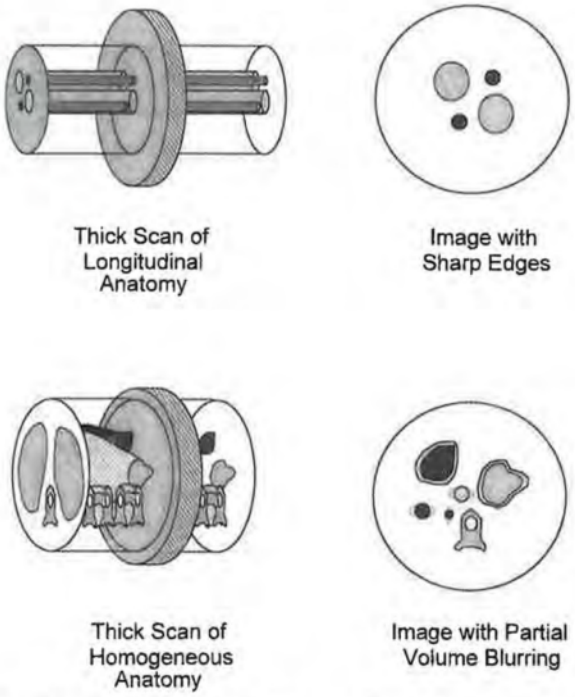



**Figure 10.26.** Because of the finite thickness of CT slices, there is a volume averaging effect that occurs in the depth dimension of the slice. If the anatomy that is imaged is longitudinally oriented (top diagrams), as the bones, ligaments and blood vessels in an extremity are, volume averaging will not have too much effect. However, in the head or abdomen (bottom diagrams), the heterogeneous anatomy will induce more volume averaging problems.

## Radiation Dose

The radiation dose in CT is decidedly higher than that of conventional screen-film radiography. Also, the dose distribution is different because the incident radiation beam rotates around the patient during the scan. Typical dose measurements in CT require a special phantom made from

**Table 10.2**
**Factors That Affect Spatial Resolution of a CT Scanner**

| |
|---|
| Focal spot size |
| Detector size and spacing |
| Number of rays per projection |
| Number of projections |
| Magnification |
| Pixel matrix |
| Reconstruction algorithm (bone versus soft tissue filter) |
| Slice thickness |
| Patient motion |
| Scanner motion (helical especially) |

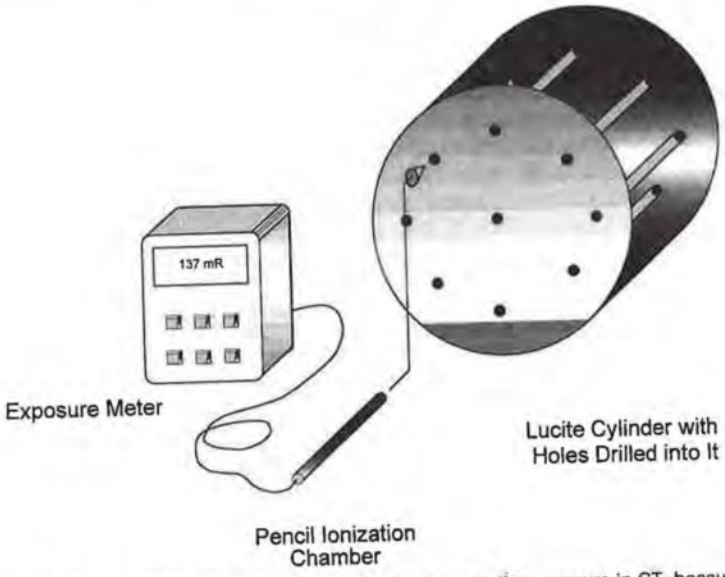



**Figure 10.27.** Special equipment is required to measure the exposure in CT, because of the rotating nature of the x-ray tube. A homogeneous Lucite or Plexiglas (tissue equivalent) phantom is used that has holes bored to accept a *pencil ionization chamber*. The pencil chamber is long enough to detect the in-plane primary and scattered rays and most of the out-of-plane scattered radiation generated in the phantom. The measurement is therefore representative of the dose resulting from a contiguous series of CT scans. The holes in the phantom that do not have the chamber in them are loaded with Lucite rods to replace the air volume with tissue equivalent material.

Lucite, and a special "pencil" chamber for the ionization meter. Figure 10.27 illustrates the way that dose is commonly measured in CT scanners. Thermoluminescent dosimeters (TLDs) are sometimes used as well. Common values for CT doses range from 30 mGy (3 Rads) to as high as 90 mGy (9 Rads) for high mAS studies. Table 10.3 lists typical CT doses measured at the center of a phantom.

The units of *absorbed dose* are the Rad (100 ergs/gram) or preferably in SI units, the Gray (1 Joule/kg). The units of radiation dose are normalized by the amount of tissue that is exposed. The Rad and the Gray measure the energy deposited *per unit mass* (of tissue, in this case) where 1 Gy = 100 Rad. This normalization (per unit mass) leads to confusion in some cases. For example, the dose for a single CT slice (1 image) of the head is about 30 mGy (3 Rads). The dose for 10 CT slices (10 different

**Table 10.3**
**Typical Doses for Computed Tomography**

| Scan Type | kV & mAS | Slice Thickness | Dose |
|---|---|---|---|
| Head (16-cm dia) | 120 kV/420 mAS | 10 mm | 65 mGy (6.5 Rads) |
| Spine (16-cm dia) | 140 kV/420 mAS | 5 mm | 23 mGy (2.3 Rads) |
| Body (32-cm dia) | 120 kV/420 mAS | 10 mm | 15–25 mGy (1.5–2.5 Rads) |

images) of the head is still 30 mGy (3 Rads). Which has more cancer risk associated with it? The 10-image study is 10 times the risk than the single image (assuming a linear, no-threshold dose-effect curve), but the *dose* in both cases is 30 mGy (3 Rads). This example illustrates the limitation of the use of *dose* as a measure of radiation risk.

Because the radiation is distributed quite homogeneously in a CT scan, and the volume of the irradiated tissue is different with each slice, a straight dose comparison between a CT scan and a radiographic procedure is misleading. Probably, the best measure of risk (of cancer) is not dose but *integral dose*. Integral dose is just a measure of the *amount of energy deposited* in tissue, regardless of its distribution. To calculate the integral dose, one just calculates the average dose (energy/mass) for a mass of tissue and then multiplies by the mass of tissue:

$$\text{Integral Dose (joules)} = \text{Dose (joules/kg)} \times \text{Mass of Irradiated Tissue (kg)}$$

To illustrate the utility of integral dose versus dose, consider this example:

A pediatric radiologist is considering replacing a 2-view radiographic sinus study with a limited-slice CT exam. The entrance dose for the AP and lateral skull radiographs are 4.8 mGy (480 mRad) and 2.8 mGy (280 mRad), respectively. The in-plane dose for one 10-mm thick CT image is 30 mGy (3.0 Rad), and 7 slices are needed for the examination. For simplicity, we assume the child's head is cylindrical and is 16 cm in diameter.

To calculate the integral dose for the CT examination, we assume that the dose throughout the CT slice is homogeneous at 30 mGy (3 Rads). For one slice, the area is $\pi(8\text{ cm})^2 = 201\text{ cm}^2$, and because the slice thickness is 1 cm, the volume is 201 $cm^3$. Since the density of tissue is roughly the same as water (1 $gm/cm^3$), the mass of the 201 $cm^3$ volume is 201 gm. Three Rads is equal to 300 ergs/gm. The integral dose (in ergs) for one slice is 300 ergs/gm × 201 gm = 60,300 ergs. For the 7 slices, the total integral dose is 7 × 60,300 ergs = 422,100 ergs.

The dose is not distributed evenly in a radiographic examination, in fact it is quite uneven. The tissue near the entrance of the x-ray beam receives the most dose (the so-called entrance dose), and the dose to the deeper tissues falls off exponentially. To calculate the integral dose, an integral equation encompassing the exponential falloff of dose within the patient can be derived. The solution of the integral equation is:

$$\text{Integral Dose} = (D_o A/\mu)(1 - e^{-\mu d})$$

where $D_o$ is the entrance dose, $d$ is the thickness of the patient, and a $\mu$ is the linear attenuation coefficient of the x-ray beam. For a skull examination, the $\mu$ is about 0.33 $cm^{-1}$. For the posteroanterior radiograph, $D_o = 0.480$ Rad, $d = 16$ cm, $A = 256\text{ cm}^2$ (16 cm × 16 cm) and $\mu = 0.33$. Putting these values into the above equation gives 370 "gram-Rads"—the unit of integral dose. One gram-Rad = 100 ergs, and so the posteroanterior film delivered about 37,000 ergs to the patient. For the lateral view,

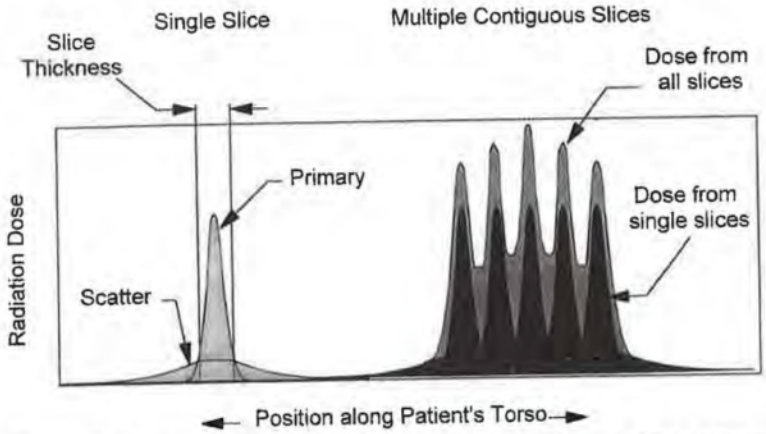



**Figure 10.28.** The dose in a CT scan is due both to the primary and the scattered radiation. The primary radiation is confined mostly to the slice thickness but is higher in the center because of the beam divergence and the penumbra effects of the collimation. The scattered radiation is more diffuse and extends laterally out in both directions away from the slice (left). Because the scattered dose contributes to the dose in adjacent slices, the dose in each slice volume is greater when contiguous slices are acquired.

the entrance dose is 0.280 Rad, resulting in 21,600 ergs (rounded). The total integral dose (in ergs) due to the two radiographs is 58,600 ergs.

In the above example, the two-view radiographic series "cost" 58,600 ergs, whereas the 7 slice CT examination resulted in 422,000 ergs (rounded) deposited in the patient's tissues. These values provide a good comparison for evaluating the relative risk between the two examination options.

The dose profile in CT is very much related to the slice sensitivity profile, previously discussed. The majority of the dose is deposited by primary radiation within the slice. There is some contribution of scattered radiation to the patient's dose (~30%), and this contribution occurs both in the CT slice volume and extends out to the adjacent tissue. The dose profiles in CT for a single view and for contiguous slice examination are shown in Figure 10.28.

### Cone Beam Acquisition

CT scanners in specialized situations may use a planar detector instead of a linear detector array. The two-dimensional acquisition of the projection data all the way around the patient allows, in principle, the reconstruction of many CT slices with only one rotation around the patient. The example given previously of the 360° acquisition of chest radiographs is such an example. Planar acquisition allows more scattered radiation to be detected and thus the image quality is reduced; however, for some applications the image quality is adequate. The planar receptor that is used for acquisition is often a large FOV image intensifier system, where the video image is digitized. Such a system is used commercially as an inexpensive alternative to CT acquisition in radiation therapy treat-

ment planning. In this application, the diagnosis has already been made. The purpose of the CT images here is to plan the delivery of radiation to specific sites. When planar images are used to acquire the CT data, a *cone beam reconstruction* algorithm is often used. The cone beam algorithm takes into consideration the beam divergence in both spatial dimensions, just like a fan beam algorithm considers the beam divergence in just one dimension.

### Quantitative Measurements: Bone Mineral Densitometry

Research has shown that the trabecular bone mineral density (mg bone tissue/ $cm^3$) measured in the vertebral bodies of a patient is related to the level of osteoporosis. *Bone mineral densitometry* is a quantitative CT technique that is useful for evaluating the density of bone mineral in a patient. CT has the ability to separate the trabecular bone (which has high turnover rates) from the compact bone (with slower bone mineral turnover rates), thus improving the sensitivity of the measurement of bone mineral. Although CT numbers are in principle quantitative, because of the numerous types of artifacts that can occur with CT images (e.g., beam hardening, scatter, partial volume, discussed later) there is a realistic limitation on the quantitative accuracy of CT numbers. To compensate for systematic fluctuations in the CT number, a bone mineral phantom that has several tubular regions with known bone mineral densities is scanned simultaneously with the patient. The CT numbers are determined from the resulting CT image in small regions of interest placed on the various levels of bone mineral. Knowing both the absolute bone mineral density and the corresponding CT numbers, a relationship between the two is determined for each CT image. The CT numbers are then measured in the patient's vertebral body, and the known relationship between absolute bone mineral density and CT numbers is used to calculate the bone mineral density in the patient's vertebral body. These numbers are compared to a "normal" population database and are useful clinically in assessing the need for therapy, such as hormone supplementation.

## RECONSTRUCTION TECHNIQUES

### Overview

The CT scan results in the acquisition of a projection set for each CT slice. The computer hardware and software convert the raw CT data into CT images, through a process called *image reconstruction*. CT reconstruction can be described in full mathematical glory; however, here we use limited mathematics and simple graphical methods to convey what is being performed. The raw data consist of the digitized transmission measurements for each ray for each projection. These data are preprocessed by using some simple algebra, before CT reconstruction. The first corrections to the data are multiplicative corrections that correct for the variation in detector gains and sensitivities. The correction factors are derived from calibration scans that the technologists or service personnel perform on regular intervals. In addition to correcting for electronic drift in

the individual detectors, corrections are required to compensate for a variety of geometrical distortions that occur during the examination. For example, in a fourth-generation scanner, the sensitivity of a single detector will change depending on the angle that the beam strikes the detector. A series of measured values that are taken at different angles are corrected by the known geometric efficiency for the known angles. Once the raw data are corrected for detector calibration and geometric effects, the projection value is calculated as:

$$p(x) = \ln(I_o/I(x))$$

Since $I(x) = I_o\, e^{-\mu x}$, the projection value P is equal to $\mu x$. In fact, P is a weighted sum of the linear attenuation coefficient of each material times its thickness along each ray. The thickness term (x) is nullified during the image reconstruction, and thus the remaining CT numbers are related to the linear attenuation coefficient, $\mu$, as previously discussed.

## Iterative Reconstruction

Iterative reconstruction techniques were used in the early days of CT. They are also used for tomographic reconstruction in specialized applications, usually in the research environment. Iterative reconstruction techniques repeat a series of updates to the reconstructed image, and each update is called an *iteration*. The set of equations that is supposed to generate the updates embodies the iterative reconstruction technique, and there are many different mathematical approaches. The way iterative reconstruction works is described in the following sequence:
Before the first iteration, the numbers representing the image matrix are set to some values. They can all be set to a uniform gray, or set randomly; it depends on the particular iterative approach that is being used. Then, CT projections *are calculated* from the present image. In this step, the computer assumes that the image is an object, and it simulates a CT scan of that object, producing a number of projections at numerous angles. In the next step, the projections that were generated from the image are compared with the actual projection data that were physically acquired. The simulated projection data and the actual projection data are subtracted from each other, and the result is an estimate of the error remaining. The error from all the projections around the reconstruction circle is used to cleverly modify the numbers in the image matrix. The particulars of how the error influences the modification of the pixel values in the image matrix depend on the specific algorithm used. In principle, the updated numbers in the image matrix will be closer to what the image of the object looks like than before the update occurred.

These steps are performed repeatedly, until the error between the simulated projection data and the actual projection data becomes acceptably small. It may require hundreds of iterations for the image to *converge* on the actual image of the object. The iterative reconstruction approach is diagrammed in Figure 10.29.

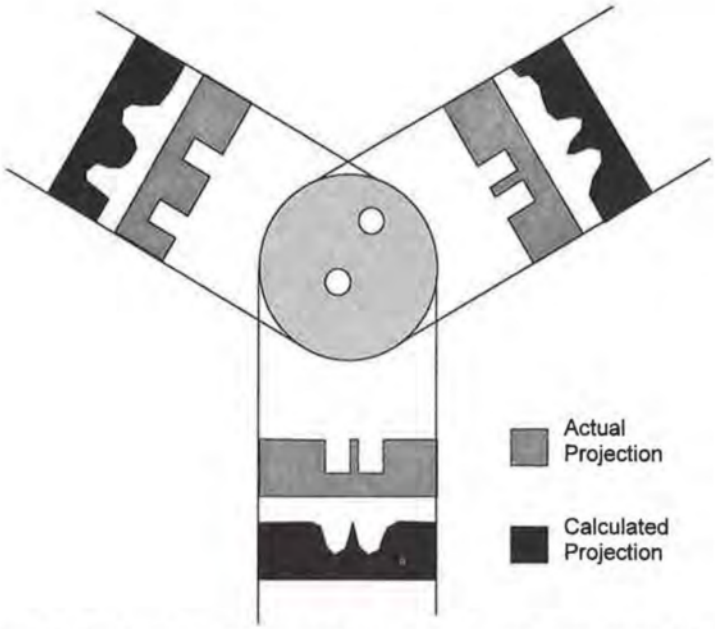



**Figure 10.29.** Iterative reconstruction techniques use a series of calculations that run repeatedly. After each run, the resulting image appears more and more like the actual object. After a certain number of iterations (the number depends on the particular algorithm), the image *converges* with the image of the actual object. During the iterative process, the present iteration image is used to calculate each projection. The calculated projections are compared with the measured projection data that were acquired during the CT scan. The errors between the measured and calculated CT projections are used to update the image for the next iteration.

## Simple Backprojection

Simple backprojection illustrates what would happen if the preprocessed projection data were smeared back onto the image matrix, without any other manipulation. Each data point in a projection is a transmission measurement through the object along a particular line. In addition to the numerical value associated with the transmission measurement, the precise path through the object is known for each data point. In simple backprojection, the image matrix is initially set to zero. For each data point in each projection, the transmission value is added to each pixel in the image that corresponds to the linear path through the object corresponding to the transmission measurement. When all the rays in each projection are smeared into the image matrix, areas of high attenuation (large projection values) tend to reinforce, and areas of lower attenuation (small projection values) also tend to reinforce each other (Fig. 10.30). This process, which is merely a geometrical construction of the image, produces an image that resembles the object being reconstructed; however, the image is very blurred. The simple backprojection technique

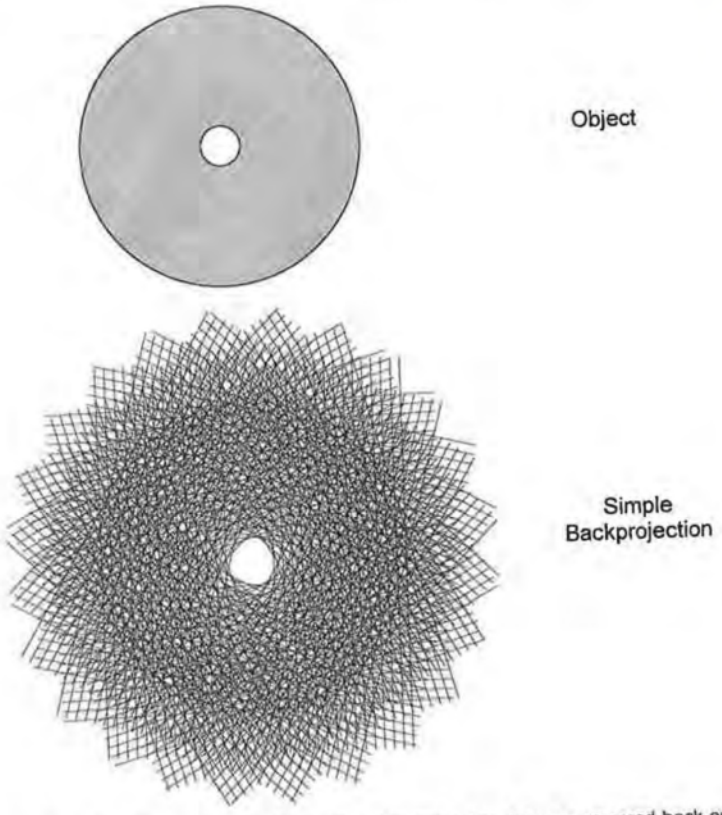



**Figure 10.30.** With simple backprojection, the projection data are smeared back onto the image matrix in the orientation that it was acquired at. When this process is completed over all of the acquired projection data, an image is built up that is a reasonable (but not identical) facsimile of the original object. The simple backprojection image is a blurred rendition of the actual one.

does not compensate for a blurring function that results as a consequence of the geometrical overlaying of the data.

## Filtered Backprojection

To compensate for the blurring that occurs in simple backprojection, the blurred reconstruction image created by simple backprojection can be mathematically filtered to eliminate the blurring effect. Thus, the "filter" in filtered backprojection refers to a mathematical operation. Although it is very feasible to take the blurred reconstructed image and apply a convolution filter to correct for the blurring, this sequence of events would require a large amount of computer time. Instead of filtering the two-dimensional reconstructed image, the one-dimensional (preprocessed) projection data are mathematically filtered before being backprojected to generate the reconstructed image. Filtering the one-dimensional projection data before backprojection is a faster operation than filtering the

two-dimensional backprojected image. As discussed in Chapter 5, the mathematical operation performed on the projection data is called *convolution*. Sometimes filtered backprojection is called *convolution backprojection*.

The blurring that is intrinsic to simple backprojection makes the true image appear as if it has been convolved with a convolution kernel that has a 1/r shape to it. A 1/r convolution kernel means that the intensity that should be assigned to a pixel at a certain point in the image (call this the parent pixel) is spread around into neighboring pixels. The spreading into adjacent pixels (ones that touch the parent pixel) is most severe, and the amount of intensity that is redistributed decreases with the distance that the recipient pixel is away from the parent pixel. In mathematical terms, the 1/(r) function means that pixels that are 2 pixel spaces away receive 1/(2) = 50% of the parent pixel intensity, pixels that are 3 pixels spaces away receive 1/(3) = 33%, 4 pixels away receive 1/(4) = 25%, and so on. Figure 10.31. illustrates the 1/r blur function.

In filtered backprojection, a convolution kernel is designed that *undoes* the 1/r blurring that is endemic to simple backprojection. The projection data is convolved with the correction kernel that compensates for the 1/r blur, and then the corrected projection data are backprojected onto the image matrix. This process results in an image that accurately reproduces the appearance of the object. In essence, the mathematical convolution operates on neighboring projection data points, takes some of the intensity it finds there and puts it back into the parent data point—thereby correcting for the 1/r blur. If the projection data are described symbolically as P(r), and the convolution kernel is k(r), the corrected projection data $P_{corr}(r)$ is computed as:

$$P_{corr}(r) = P(r) \otimes k(r)$$

where the symbol $\otimes$ signifies convolution.*

Some CT scanners actually use convolution in the *spatial domain* to perform the filtering step, as just described. Others make use of filtering techniques that are applied in the *frequency domain*. Filtering techniques that are performed in the frequency domain are mathematically *identical* to the convolution techniques that are applied in the spatial domain. They achieve the same result by using a different sequence of mathematical operations. The frequency domain is sometimes difficult to understand initially, and a fuller explanation of it is given in Chapter 5. The projection data, P(r), are converted to the frequency domain by taking the Fourier transform of P(r). The frequency domain equivalent of P(r) can be denoted **P**(f), where **P**(f) = FT{ P(r) }, and FT means the Fourier transform. The kernel, k(r), can also be converted to its frequency domain equivalent by using the Fourier transform: **k**(f) = FT { k(r) }. Convolution in the spatial domain is equivalent to multiplication in the frequency domain, and so the frequency domain equivalent of

*The actual convolution integral equation is:

$$P_{corr}(r) = \int P(r - r') \, k(r') \, dr'.$$

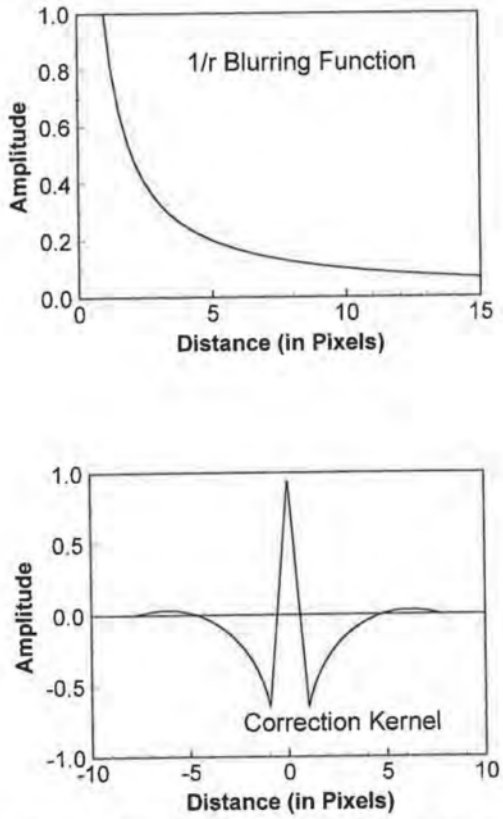



**Figure 10.31.** Simple backprojection results in an image blurred with a 1/r blurring function (top). To correct for this, the projection data is mathematically filtered using a convolution kernel that corrects for the 1/r blurring function. The filtered projection data are then backprojected ("filtered backprojection") and result in an undistorted image of the object.

$P_{corr}(r)$, which can be denoted as $\boldsymbol{P}_{corr}(f)$, is calculated by multiplication in the frequency domain:

$$\boldsymbol{P}_{corr}(f) = \mathbf{P}(f)\,\mathbf{K}(f)$$

The corrected projection data in the spatial domain are computed from $\mathbf{P}_{corr}(f)$ by taking the inverse Fourier transform, $P_{corr}(r) = FT^{-1}\{\mathbf{P}_{corr}(f)\}$. All of this can be expressed in the equation:

$$P_{corr}(r) = FT^{-1}[FT\{P(r)\}\,FT\{k(r)\}]$$

In practice, the Fourier transform of the correction kernel, $FT\{k(r)\}$, is precalculated and is stored in the computer. The reason the convolution operation is performed in the frequency domain in some CT scanners is that, depending on the shape of the kernel, the frequency domain calculation may be performed faster than its spatial domain equivalent. The main reason for introducing the frequency domain operation in so

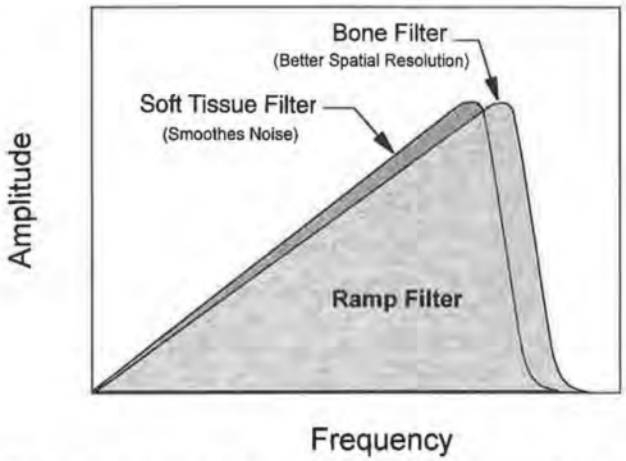



**Figure 10.32.** The mathematical filtering that is applied to the projection data before backprojection can be done in either the spatial domain or in the frequency domain. The 1/r blurring in the spatial domain corresponds to a 1/f blurring in the frequency domain. Because $(1/f) \times f = 1$, the correction function is linear with f and therefore looks like a *ramp*. The projection data are multiplied by a ramp function in the frequency domain and then are converted to the spatial domain by using the inverse Fourier transform. The filtering operation performed in the frequency domain is mathematically equivalent to the convolution filter performed in the spatial domain, but in some instances can be performed in less time by the computer. Nuances in the shape of the ramp (how far it extends and how it "rolls off") will influence the apperance of the image.

much detail is that for most clinical CT scanners, there are several different filters that one can select. For example, often there is a "bone" reconstruction filter, a "soft tissue" reconstruction filter, and several others. The differences between the various filter functions ultimately boil down to a slightly different shape of the correction kernel, k(r). The 1/r degradation that results from simple backprojection is reflected in the frequency domain by a 1/f blurring (i.e., 1/frequency). To correct for the 1/f problem, the frequency domain filter function should be a function that increases its amplitude with increasing frequency. Figure 10.32. illustrates frequency domain filters, which are essentially the shape of $\mathbf{k}(f)$ described above. As is shown, the filter function has the appearance of a ramp. The top of the ramp, however, has a rounded shape, which is put there intentionally to reduce ringing artifacts in the image. This rounded edge to the ramp filter can have different shapes, and sometimes these are described in terms of a "high frequency roll-off." If the ramp filter rolls off at lower frequencies, this will de-emphasize the higher frequencies in the reconstructed CT image. This reduces the noise in the image, but spatial resolution is compromised in the process. This would be a "soft tissue" reconstruction filter. A ramp filter with a roll-off at higher frequencies is used for producing higher resolution CT images (this is the "bone filter" or "bone algorithm"), albeit with higher noise as well (Fig. 10.32). The numerous filters often supplied by CT manufacturers are variations on a theme, with each filter having a slightly different shape.

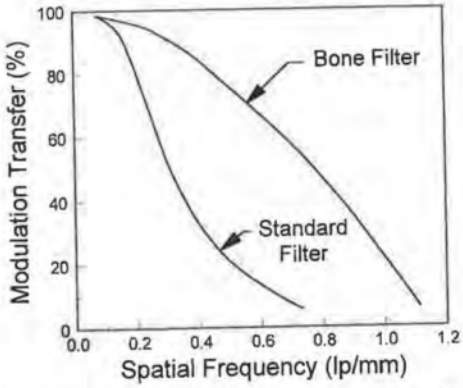



**Figure 10.33.** The spatial resolution of the CT image depends on the reconstruction filter that is used. Filters are available that smooth noise but reduce spatial resolution, or that enhance spatial resolution at the cost of some additional noise. Notice that the MTF values for CT extend to around 1 lp/mm, as opposed to screen-film systems that can extend to 10 lp/mm. CT manufacturers often use the units of lp/cm, where 1.0 lp/mm = 10 lp/cm.

The influence that the filter has on the modulation transfer function (MTF) for the CT scanner is shown in Figure 10.33.

## ARTIFACTS IN X-RAY COMPUTED TOMOGRAPHY

### Beam Hardening

The x-rays generated by the x-ray tube of the CT scanner have a wide spectrum of energies. Even after the substantial thickness of filtration that most CT systems use, the x-ray beam is *polyenergetic*. The polyenergetic nature of x-ray production is usually not a problem in radiographic imaging. However, in CT, the linear attenuation coefficients are actually being calculated on a per-pixel basis. The polyenergetic spectrum causes a problem in CT, because the linear attenuation coefficient is quite dependent on the energy of the x-ray beam. This energy dependency in $\mu$ is denoted by $\mu(E)$. As the x-ray beam is transmitted through a thickness of tissue and bone, the lower energy photons in the spectrum are attenuated more rapidly than the higher energy ones, and therefore the shape of the x-ray spectrum as the x-ray beam penetrates the depths of an object actually changes (Fig. 10.34). The lower energy photons are attenuated more rapidly than the higher energy ones, because the values of $\mu(E)$, are higher at lower energies. Therefore, the effective energy of the x-ray beam increases as it passes through tissue. This increase in effective energy as a function of the transmission path of the x-ray beam is called *beam hardening*. The effective linear attenuation coefficient, $\mu_{eff}$, is an indicator of the attenuation for the whole spectrum of x-rays, as measured by the CT scanner. When beam hardening occurs appreciably, the higher effective energy of the x-ray beam is reflected by a lower $\mu_{eff}$. The value of $\mu_{eff}$ is dependent on the specific path that the measured ray has taken through the object. When beam hardening (a change in $\mu$)

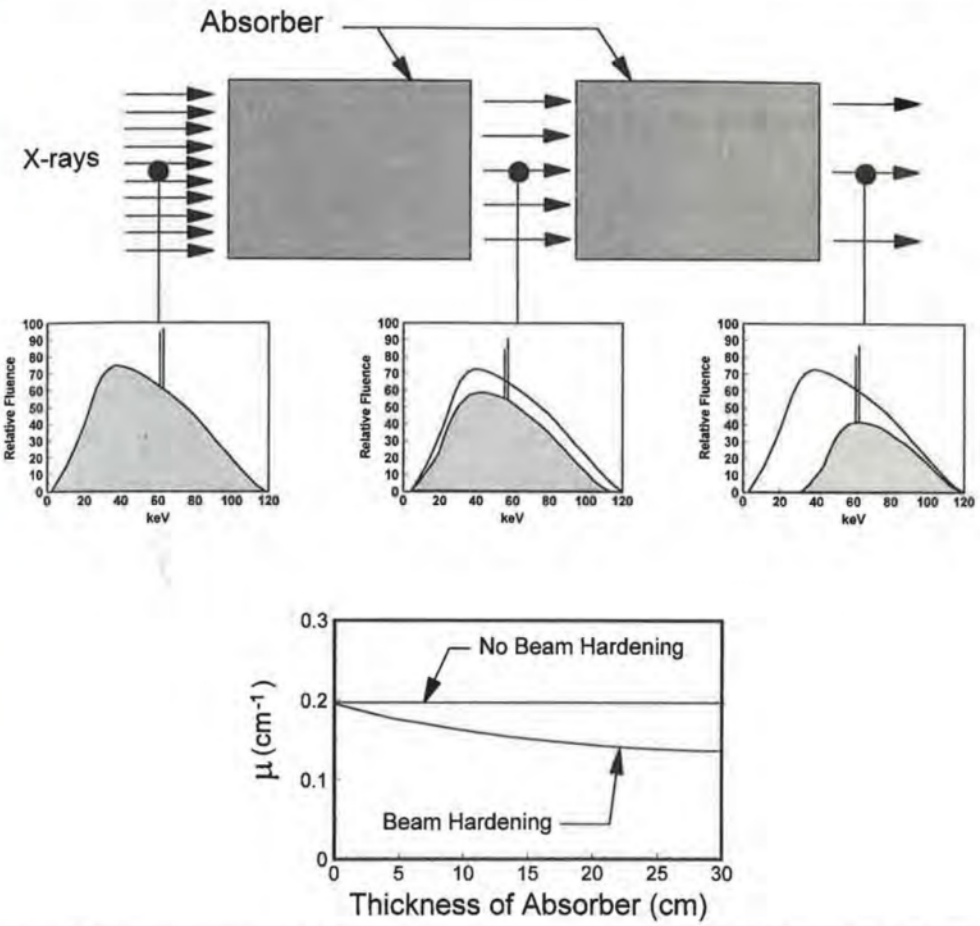



**Figure 10.34.** Beam hardening. As the x-ray beam penetrates different thicknesses of the object (top), the lower energy x-rays are preferentially removed from the beam. This is because $\mu(E)$ is higher at lower energies. Because of this, the effective energy of the x-ray beam increases with increasing tissue thickness, and this increase in effective energy is called *beam hardening*. Higher energy x-ray beams have lower attenuation coefficients. Because a CT image is a map of attenuation coefficients, when beam hardening occurs there is a lowering in the attenuation values and consequently a reduction in the image brightness.

occurs, it causes a violation of the linear superposition of attenuation values that is required by backprojection reconstruction. This violation, which is essentially an error in the assumptions that are used during backprojection, results in beam hardening artifacts.

A *cupping artifact* is a classic example of beam hardening. If a homogeneous water phantom is scanned, a profile across the CT image should be flat, with some overriding noise. Beam hardening causes a reduction in the CT numbers toward the center of the water phantom, and this produces a cupping appearance in the CT number profile across the phantom. CT rays that pass through large thicknesses of bone can be




**Figure 10.35.** A CT image illustrating beam hardening artifacts. The x-ray beam projections that run through the petris bone are hardened by the thick bones, and the CT projection values are therefore lower than they should be. During backprojection, the rays that go through the thickest amount of bone suffer the worst beam hardening. Because of this, beam hardening often appears as web-like extensions between bony regions in the image.

significantly hardened. Beam hardening artifacts usually occur in the soft tissue regions between large bony structures and result in a decreased image intensity not representative of the tissues. Figure 10.35. is an image demonstrating classic beam hardening artifacts.

Beam hardening is reduced when the x-ray beam is pre-hardened by the insertion of copper or some other attenuator in the beam near the x-ray tube. There are limits to pre-hardening the beam, however, because filtration also reduces the intensity emitted from the x-ray tube, and therefore results in increased x-ray tube heat loading. Mathematical techniques can also be used during reconstruction to reduce the effect of beam hardening. One obvious technique is to perform an initial CT reconstruction, which results in the generation of a good map of attenuation coefficients (i.e., a standard CT image). From this first image, the path of each ray used in the backprojection can be followed on the image to determine the thickness of tissue and of bone that each ray traversed. The projection data (i.e., the transmission data represented by each ray) can then be corrected to account for beam hardening, and a second, beam hardening corrected image can be reconstructed from the set of corrected projection values. Although such measures are possible, the necessary computation time for such corrections is prohibitive. They are implemented in a research environment, and await the day when faster computers become available for clinical implementation.

### Partial Volume

Partial volume artifacts are the result of a variety of different tissue types being contained within a single voxel. When the linear attenuation coefficient is different for the two or more tissue types contained within a voxel, the attenuation that occurs (and therefore that which is measured) is averaged. This partial volume averaging results in the calculation of a CT number that is not necessarily representative of either tissue type. For example, when bone and soft tissue are contained within a single voxel, depending on the ratio of the two constituents, the CT number of that pixel will be higher than for the surrounding tissue but lower than that for bone. When a bone is just partially grazed by the slice volume for a CT image, it can generate hyperattenuating regions (lighter areas) that may be confused with abnormal tissue. The same effect can occur for fatty regions, except that fat has a lower CT number than soft tissue and therefore the partial volume artifact will be hypoattenuating (dark on the image). Figure 10.36. is an image demonstrating partial volume artifacts.

Partial volume averaging can be kept to a minimum by using thinner slices; however, thinner CT slices require more tube current per slice (milliAmpere Seconds—mAS) per slice (to achieve the same signal-to-noise performance) and require more slices to cover the same volume of tissue. A solid knowledge of cross-sectional anatomy is the best defense against partial volume artifacts leading to incorrect diagnosis. With the advent of helical CT scanners, if the raw helical projection data are saved until the cases are read, the radiologist can call for more reconstructions at finer intervals. This may help to resolve suspected partial volume artifacts.

### Motion

Motion artifacts are a problem in all imaging systems that require a relatively long time to generate the data necessary for the image. Even with the comparatively short scan time for modern CT scanners (down to 1 sec), motion, especially cardiac and respiratory motion, can still be a problem. Motion due to uncooperative patients, especially in the pediatric population, is a significant problem as well. Motion artifacts occur because the backprojection algorithm assumes a stationary object geometry. If motion occurs half way through the CT scan acquisition, the first half of the projection data will backproject the anatomy in one orientation, and the second half of the data will backproject the anatomy in a different orientation. When mostly soft tissue is involved in the slice, significant motion can give rise to image ghosting; i.e., the appearance of two superimposed images. When subtle motion occurs in soft tissue regions, motion artifact will result in the apparent reduction in resolution in that region. The image will appear blurred in the area where the motion occurred. When very high contrast objects move during the CT scan, each backprojected ray can contribute a large signal to the image. When motion occurs, the strong signals from each ray do not smoothly intersect in the image, and a very obvious streaking can occur. This type of

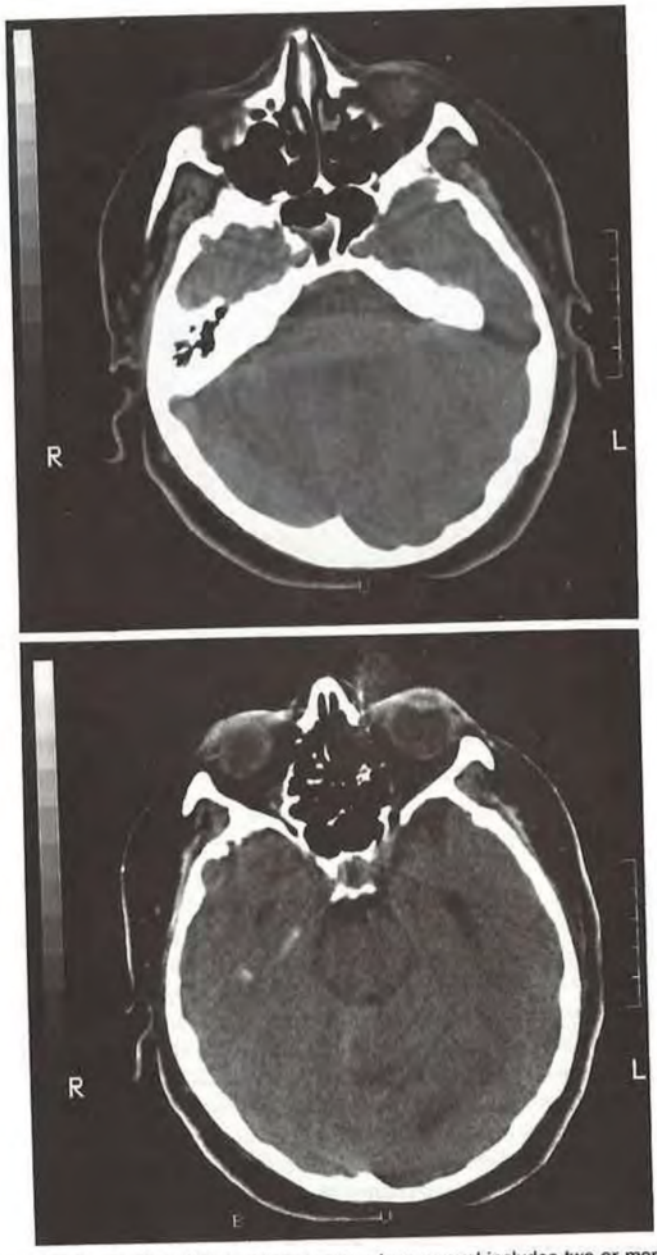



**Figure 10.36.** Partial volume artifacts occur when a voxel includes two or more types of tissue, for instance bone and tissue together or air and tissue together. The top figure illustrates a head scan with suspicious hyper attenuating areas. These areas are the result of volume averaging with the petris bones, as apparent by viewing the adjacent slice (bottom).

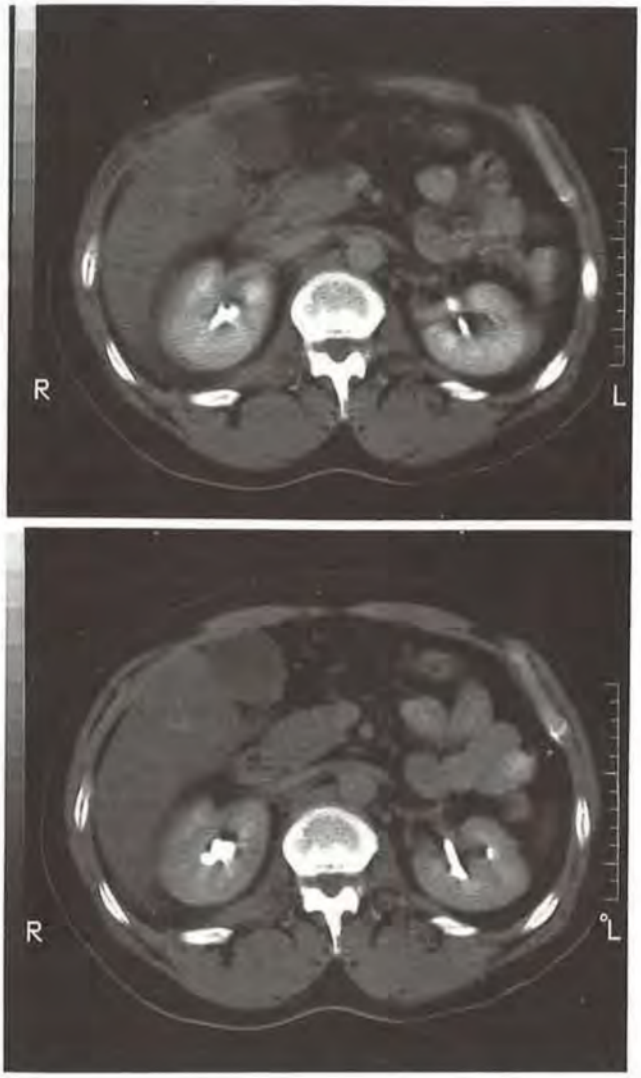



**Figure 10.37.** Motion artifacts appear as a general blurring or ghosting of structures in the image. The top image shows motion blurring of the renal pelvis and ghosting of the edges of the gallbladder. The slice was rescanned, and the image without motion blurring is shown at the bottom.

motion artifact can destroy the diagnostic integrity of the whole image. Figure 10.37 is an image showing motion artifacts.

The techniques to reduce motion artifacts incorporate common sense. Rapid scan times are the best defense against motion artifacts. For some cases, immobilizing the patient with appropriate restraints (tape) can help reduce inadvertent motion by the patient. Bolusing, such as cradling the head in foam rubber, is another good technique. In many cases, the pe-

diatric patient will need to be sedated for the study. The CT technologist can reduce patient motion by educating and enlisting the patient as a cooperative participant, before the examination.

### Scattered Radiation

Scattered radiation *adds* scattered x-ray energy to the detected measurement, increasing the value of I(x). This *decreases* the calculated projection value, P(x), since $P(x) = LOG\{I_o/I(x)\}$. Since $P(x) = \mu_{eff}x$, the reduction in projection values results in a similar reduction in the attenuation coefficients that comprise the CT image. This means that scattered radiation causes artifacts that are dark. Artifacts caused by scattered radiation appear in many of the same instances as beam hardening artifacts. They appear as dark streaks between highly attenuating objects. Scatter is a fairly diffuse (blurry, low frequency) contribution to the detected values in a CT projection, meaning that the amount of scattered energy detected by adjacent detectors will be approximately the same and will vary only slowly across the detector array. The streaking that scatter can cause is strongly related to the ratio of scattered energy to primary energy that is detected. This ratio is called the *scatter-to-primary ratio*. Although the scattered energy that reaches the detector changes slowly from detector to detector, the primary energy that is being detected simultaneously can change very abruptly. Indeed, for a detector that is under the x-ray shadow of a thick bone, the primary energy contribution to the detector can be very small. This means that in areas of high attenuation of the primary beam, the scatter-to-primary ratio can become quite high. This explains why streaking caused by scattered radiation can occur in the same areas that beam hardening artifacts occur.

Artifacts caused by scattered radiation can be minimized by the correct design of a CT scanner, such as those that embody maximal measures to prohibit the detection of scattered photons. The use of post-patient collimation is effective in reducing multiple scatter from reaching a detector. The septa used to form the ionization chambers for xenon detectors used in third-generation CT scanners is very effective at reducing the scattered radiation that does reach the detector plane. Another measure that is commonly used to reduce the impact of artifacts produced by scatter is to use a secondary, sparse array of scatter detectors, alongside the primary detector array but outside the reach of the primary radiation. These detectors measure the scatter levels adjacent to the main detector array, which measures the scattered and primary radiation combined. The signal derived from the scattered radiation detectors is subtracted from the main detector array, thus removing the contribution of the scattered radiation. In addition to hardware measures to sense and correct for scattered radiation, software techniques can and are commonly used in clinical CT scanners to help correct for the degrading influence of scattered radiation in the CT reconstruction process.

## DISPLAY

The final phase of a CT scan is the display of the image. Although the technologists often view the image on the monitor associated with the

CT scan control room, or from a satellite console, the radiologist usually first sees the case on film.

### Digital Images

Compared to analog radiographic images, digital images have display flexibility. The digital image is an array of numbers that reside in the computer. This image data can be manipulated to enhance the appearance of the image. A television monitor is capable of displaying about 256 different shades of gray (8 bits of information). CT images usually have 12 bits per pixel, representing 4096 shades of gray. Consequently, the image data have to be transformed (truncated) for display. This is performed by use of an output transform, or more commonly referred to as *windowing and leveling.*

### Window and Level Controls

To display image data stored in a CT scanner, the data are loaded from the computer disk into a special kind of computer memory called a video display RAM (RAM = random access memory). The video RAM has associated electronics that continually scan its memory buffers and to generate a real time video signal. As the display buffer is scanned by the computer, it reads the digital value associated with each pixel and converts this to a corresponding analog signal voltage for display, using a digital-to-analog converter (DAC). To manipulate the appearance of the image, a *look-up table* is used in the DAC just before the conversion of the data to an analog signal voltage. A look-up table is an expedient way to convert the 12 bit/pixel (4096 different CT numbers) image data to a range spanning 256 shades of gray. A look-up table (called a LUT in computer jargon) can be thought of as a plot of the output gray scale value (0–255) as a function of the input pixel value ($-1000$ to 3095).

There are $2^{192}$ different ways (a lot) to display the image data using the 12-bit to 8-bit LUT; however, in CT and for most medical imaging the display LUT is loaded with a simple ramp-shaped function (Fig. 10.38). The width of the ramp is called the *window,* and the midpoint value of the ramp is called the *level* setting. When the window is made narrow, the slope of the ramp increases. The slope of the ramp represents the contrast in the image, and therefore decreasing the width of the window (lower window settings) increases the contrast in the displayed image. As the window width is made more narrow, the number of pixel values (0–4096) that can be displayed simultaneously decreases. In fact, the window setting is the equal to the number of pixel values that can be displayed. The left edge of the ramp will start at the pixel value $L-(W/2)$, where $L$ is the level setting and $W$ is the window setting. The right edge of the ramp will be at the pixel value $L+(W/2)$. For image display with normal polarity, where higher pixel values are displayed brighter, pixel values below $L-(W/2)$ are truncated to 0 (displayed as black), and pixel values above $L+(W/2)$ are saturated to white.

Using the appropriate window and level settings, the soft tissue (for example) in the CT image can be displayed with very high contrast. However, high CT values, such as bone tissue, will all be displayed as white.

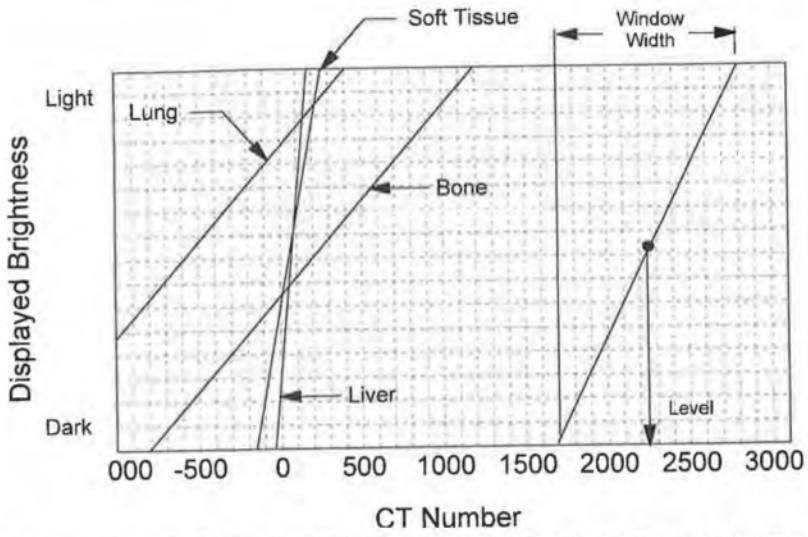



**Figure 10.38.** "Windowing and Leveling" refers to changing the way the image data that resides in the computer are displayed. The pixel data (CT numbers) are mapped to image brightness using an *output transform.* The *level* is the CT number at the center of the window. The *window* is the width (in CT numbers) of the ramp that is used to map CT number to brightness. Values to the left of the ramp are black and to the right of the ramp are white. As the window width decreases, the contrast in the image is enhanced. Typical window and level settings for lung, soft tissue, bone and liver are illustrated.

Many areas in the lung field will be displayed as black. So, although the settings may optimize the contrast in some areas of the image, other areas may be totally saturated as a result. To compensate for this problem, most CT images are displayed at two or three different window and level settings, with each display setting optimized for a specific area in the image. For instance, a thoracic CT image may be displayed with a *lung window,* a *liver window,* and a *bone window.*

### Monitors versus Film

In CT, the technologists use the display monitor(s) with the scan control console or with a satellite console to check the images and then photograph them onto film. The *multiformat camera* is a device with a film magazine and film transport system, a series of lenses, and a TV monitor. When the "expose" signal is sent to the multiformat camera (by a push of a button, for example), the image from the internal monitor is focused onto a small section of the film. CT images are usually "imaged" onto sheets of film that are 35 cm × 43 cm (14 inches × 17 inches), in formats ranging from 6 images (2 × 3) to 15 images (3 × 5).

A more expensive solution for converting the digital image data to film is to use a *laser imager,* also called a *laser camera.* Instead of exposing the film to an image displayed on an internal television monitor, a laser camera uses the digital image data directly and scans the film line by line, building up the image gradually. A laser beam is scanned over the film, and the intensity of the laser beam is determined by the pixel

value at that point in the image data. The narrow beam geometry of the laser beam creates less scattered light in the system, and therefore laser cameras produce film images with substantially more contrast than do multiformat cameras. In general, they do not suffer from focusing problems that multiformat cameras can occasionally experience. Of course, they are more expensive than multiformat cameras.

Although laser cameras use digital image data to produce the film image, either an analog or a digital interface is possible. With an analog interface, the analog video display signal is (re)digitized by the laser camera by using an analog-to-digital converter (ADC). With a digital interface, the digital data from the CT scanner is sent directly to the computer memory of the laser camera over a parallel digital interface. Because the digital interface approach does not result in the digital image being converted to analog and then being converted back to digital, less degradation in the image data will occur. Although a digital interface to the laser camera is preferred, the analog interface allows for maximal compatibility, since it emulates a multiformat camera.

## SUMMARY

The development of the CT scanner has lead to a significant improvement in the diagnosis and management of patients. The ability to literally see inside the patient has opened new horizons for medical diagnosis. Although no longer the only modality capable of tomographic imaging, CT has established itself as a tried-and-true imaging modality for a broad cross-section of clinical manifestations. The development of CT technology and its clinical success serves as an example of the contributions of scientists and engineers who work behind the scenes to provide better health care. Continuing advancements in CT technology and image quality will keep CT competitive with MRI and ultrasound well into the 21st century.

value at that point in the image data. The narrow beam geometry of the laser beam creates less scattered light in the system, and therefore laser cameras produce film images with substantially more contrast than do multiformat cameras. In general, they do not suffer from focusing problems that multiformat cameras can occasionally experience. Of course, they are more expensive than multiformat cameras.

Although laser cameras use digital image data to produce the film image, either an analog or a digital interface is possible. With an analog interface, the analog video display signal is (re)digitized by the laser camera by using an analog-to-digital converter (ADC). With a digital interface, the digital data from the CT scanner is sent directly to the computer memory of the laser camera over a parallel digital interface. Because the digital interface approach does not result in the digital image being converted to analog and then being converted back to digital, less degradation in the image data will occur. Although a digital interface to the laser camera is preferred, the analog interface allows for maximal compatibility, since it emulates a multiformat camera.

## SUMMARY

The development of the CT scanner has lead to a significant improvement in the diagnosis and management of patients. The ability to literally see inside the patient has opened new horizons for medical diagnosis. Although no longer the only modality capable of tomographic imaging, CT has established itself as a tried-and-true imaging modality for a broad cross-section of clinical manifestations. The development of CT technology and its clinical success serves as an example of the contributions of scientists and engineers who work behind the scenes to provide better health care. Continuing advancements in CT technology and image quality will keep CT competitive with MRI and ultrasound well into the 21st century.